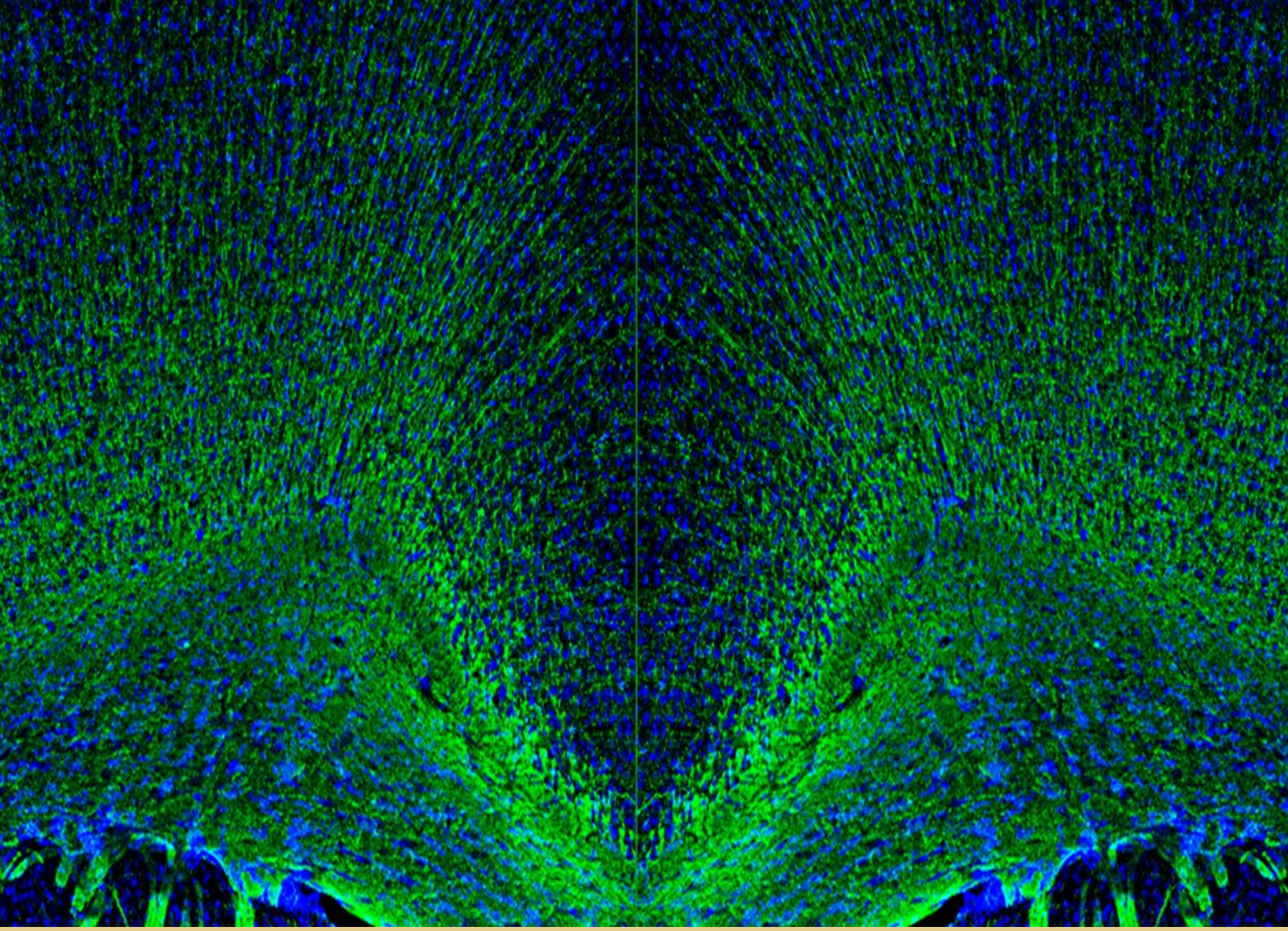

Mafalda Maria Salvador Campeão

Methylenedioxypyrovalerone (MDPV) and methamphetamine (METH) play with central innate immune system: focusing on RAGE and glial cells

Master Thesis in Biochemistry, under supervision of
Professor Frederico Guilherme Costa Pereira and Professor Ângelo José Ribeiro Tomé and presented to the Life Sciences Department of the University of Coimbra.

August 2017

· U C ·

UNIVERSIDADE DE COIMBRA

Front Cover:

Image showing the structurally diverse immunolabeling between frontal cortex and the bottom regions of corpus callosum and striatum, respectively, from C57BL/6 mice expressing myelin basic protein, MBP, (green) and DAPI (blue).

Mafalda Maria Salvador Campeão

Methylenedioxypyrovalerone (MDPV) and methamphetamine (METH) play with central innate immune system: focusing on RAGE and glial cells

A accção da Methilenedioxipirovalerona (MDPV) e da metamfetamina (METH) no sistema imunitário inato central: com especial foco no RAGE e nas células da glia

Master Thesis in Biochemistry, under supervision of Professor Frederico Guilherme Costa Pereira and Professor Ângelo José Ribeiro Tomé and presented to the Life Sciences Department of the University of Coimbra.

August 2017

UNIVERSIDADE DE COIMBRA

This work was conducted at the Laboratory of Pharmacology and Experimental Therapeutics, Institute for Biomedical Imaging and Life Sciences (IBILI), Faculty of Medicine, University of Coimbra, Portugal, under the supervision of Professor Frederico Guilherme Costa Pereira and Professor Ângelo José Ribeiro Tomé.

Also, part of this work was performed at Center for Neuroscience and Cell biology (CNC) in Institute of Immunology, Faculty of Medicine, University of Coimbra, Portugal, under guidance of Dr. Paulo Santos.

"Na altura aquilo solta-te como um pássaro, mas depois ficas dentro daquela gaiola durante meses, anos." (*In Público online*, a 17 de Fevereiro de 2013)

Nas páginas que se seguirão teremos a perspectiva científica sobre algumas substâncias de abuso. Nesta página, fica o testemunho, multiplicado por muitos, muitos daqueles que se deixaram aprisionar pelo labirintico trilho da adição. Este é um testemunho de alguém que sentiu estar provido de asas, asas na verdade ilusórias, mas que fizeram com que se deixasse abraçar por um vertiginoso e profundamente destruidor labirinto claustrofóbico….

Agradecimentos

Seria injusto da minha parte começar a deslindar os capítulos deste trabalho sem nomear aqueles que, de uma forma ou outra, contribuíram para a realização deste trabalho, pois como alguém dizia:…"se quiseres ir a algum lado, vai acompanhado…", pois bem, e assim foi.

Pensando em quem esteve directamente envolvido no trabalho gostaria muito e muito de agradecer à sempre divertida, correcta e viajada Inês Pita, pela sua prontidão e paciência em me ter passado os seus conhecimentos, e pelo facto de me ter acolhido tão bem no laboratório. Á Sofia Viana, pela infinita cordialidade, disponibilidade e generosidade por me ter permitido adquirir novos conhecimentos durante este último ano ano.

Nesta linha, tenho que agradecer às amigas do IBILI, Diana, Teresa, Luciana (muito obrigada pelas boleias estes meses todos!) e à Johanna, pelos épicos jantares até de madrugada (☺) e momentos ao sol, pelas partilhas de horas longas a fazer blots e a partilhar alguns momentos de "vais revelar?" ou "já vos aconteceu isto? Acho tão estranho!"…. Ah, e é claro pelas várias, e gradualmente retribuídas, cedências de material que aquelas paredes ouviram, como "Diana posso usar a acrilamida?" ou "Teresa emprestas-me um suporte ou posso usar a tua fonte?". Claro que por esta lógica, também tenho que agradecer ao Ricardo Leitão pela disponibilidade em ajudar e à Vanessa Coelho por ter gentilmente emprestado um ou outro reagente.

Gostaria também de agradecer ao Professor Félix Carvalho por ter, tão simpaticamente cedido o MDPV, a substância de abuso, a novidade neste estudo. Ao Professor Ângelo Tomé pela simpatia e prontidão, e claro, à minha coordenadora de mestrado, a Professora Paula Veríssimo, os meus mais sinceros, gigantes e honrosos agradecimentos. Tiro-lhe o chapéu pelo seu jogo de cintura, ampla disponibilidade e por ter salvo, nas últimas semanas, a honra deste convento, o título deste "romance"! Assim, e fechando o ciclo de agradecimentos no meio intimamente ligado ao dia-a-dia no laboratório, agradeço ainda ao Professor Frederico Pereira por me ter aceite no laboratório, pela sua disponibilidade e boa disposição.

Agora sim, aos mais chegados. Aos meus amigos da licenciature e do mestrado, Mariana, Inês, Márcia, Diana, muito obrigada pela amizada, pelos desafabafos e conversas e "vem tomar cafézinho!". E a ti, minha grande e assaz louvada AMGA, Maria Inês. Que faria eu sem ti? Mil obrigada pela amizade, pela confiança que me fazes sentir, pelas horas que passamos ao telefone comigo por vezes declamando aventuras ou soluçando desventuras, e por nunca me deixares

desligar sem antes me fazeres sentir zen (também é para isso que fazes ioga, certo?) ☺ És o meu confessonário na modalidade *call-center*!

E agora, sim, à minha família, aos meus pais, essas adoráveis e magnificos seres humanos que me aturaram as neuras e alegrias, para o bem e para o mal, obrigada por tudo. Obrigada Tuquinha por seres a companheira das horas de sofrimento, trabalho e momentos de felicidade que sabem tão bem!

Table of Contents

Index of Tables

Index of Figures

Abbreviations

A

ADAM10 Metalloprotease 10

Aβ Amyloid-beta peptide

ALR Aim2 like receptors

AGE's Advanced glycation end products

ATS Amphetamine-Type Stimulant

B

BBB Blood brain barrier

bp base pairs

C

3,4-catechol-PV 3,4-dihydroxypyrovalerone

Ca^{2+} Calcium

CCL2 Chemokine (C-C motif) ligand 2

cDNA Complementary deoxyribonucleic acid

CNS Central nervous system

ctRAGE C-terminal cytoplasmic tail

CXCL1 Chemokine (C-X-C motif) ligand 1

CXCL10 Chemokine (C-X-C motif) ligand 10

CXCL12 Chemokine (C-X-C motif) ligand 12

CPu Caudate-putamen

D

DA Dopamine

DAergic Dopaminergic

DAMP's Damage-associated molecular patterns

DAT Dopamine transporter

DCs Dendritic cells

DOPAC 3,4-dihydroxyphenylacetic acid

E

EMCDDAE European Monitoring Centre for Drugs and Drug Addiction European

ERK-1/2 Extracellular signal–regulated kinase–1 and –2

esRAGE Endogenous secretory RAGE isoforms

F

FDA Food and Drug Administration

flRAGE Full-length RAGE isoform, also denominated mRAGE

FOB Functional Observational Bactery

G

GABA γ-aminobutyric acid

GFAP Glial fibrillary acidic protein

H

HIV Human immunodeficiency virus

HMGB-1 Amphoterin protein or high mobility group box-1

I

Iba-1 Ionized calcium-binding adapter molecule 1

IL-1β Interleukine - 1β

IL-6 Interleukine - 6

IL-10 Interleukine – 10

i.p. Intraperitoneally

L

L-DOPA Levodopa

LSD (+)-lysergide

M

MAPK Mitogen-activated protein kinase

MBP Myelin Basic Protein

mDia-1 Mammalian Diaphanous-1

MDMA 3,4-methylenedioxymethamphetamine

MDPV 3,4-Metilenedioxipirovalerone

METH Methamphetamine

MHC Major histocompatibility complex

MPTP 1-methyl-4-phenyl-1,2,3,6-tetrahydropyridine

mRNA Messenger Ribonucleic acid **MMP9** Metalloprotease 9

N

NAc Nucleus accumbens

NET Norepinephrine transporter

NF-κB Nuclear factor kappa B

NLR Nod-like receptors

NO Nitric oxide

NPS New psychoactive substances

NSC Neural stem cell

O

4-OH-3-MeO-PV 4-hydroxy-3- methoxypyrovalerone

P

PAMP's Pathogen-associated molecular patterns

PBS Phosphate-buffered saline

PD Parkinson's disease

PRR's Pattern recognition receptors

R

RAGE Receptors for advanced glycation end products

RLR Rig like receptors

ROS Reactive oxygen species

RT-qPCR Real Time quantitative Polymerase chain reaction

S

SDS-PAGE Sodium dodecyl sulphate polyacrylamide gel electrophoresis

S.E.M. Standard error of the mean

SERT serotonin transporter

SN*pc* Substantia nigra *pars compacta*

sRAGE Soluble RAGE isoforms

s. c. subcutaneously

T

TH Tyrosine hydroxylase

TLR's Toll-like receptors

TNF-α Tumor necrosis factor α

U

UNODOC United Nations Office on Drugs and Crime

V

VMAT-2 Vesicular monoamine transporter

VTA Ventral tegmental area

W

WB Western blot

WDS World Drugs Survey

Abstract

Innate immunity is the first effective line of defense of all organisms, comprising cellular and molecular mechanisms for immediate action, recognizing exogenous pathogen associated molecular patterns (PAMPs), as well as, endogenous danger associated molecular patterns (DAMPs). Such detection is possible through diverse pattern recognition receptors (PRRs), thereby orchestrating the activation of innate responses. One of these receptors is the receptor for advanced glycation end-products (RAGE, also known as AGER), which is a cell-surface receptor belonging to the superfamily of immunoglobulin proteins, thus playing a central role in the inflammatory response mediating events of innate immunity. Moreover, RAGE has been implicated in the sustainment of glial activation and neurotoxicity. Noteworthy, RAGE receptor exhibits broad expression on many different cells including CNS cells, such as neurons, microglia and astrocytes. Also, as a multiligand receptor, RAGE recognizes a broad repertoire of structurally different ligand families, including S100β, belonging to the S100 protein family.

Nowadays, drug misuse, including amphetamine-type stimulants (ATS) addiction, is a major worldwide issue with an undeniable impact on public health, human rights and security. In parallel, the rapid emergence and abuse of new psychoactive substances (NPS), also termed as "research chemicals" or "design drugs", including the synthetic cathinone, Methylenedioxypyrovalerone (MDPV), known as "bath salt", clearly seems to worsen this scenario, as it acts as a substitute for illegal stimulant drugs such as cocaine. The incredibly easy access to these cathinones, including the newly synthesized MDPV, in the global drug market, through smart shops, internet ("darknet"), and the aspect of "fake legallyness" of such substances, as well as the relative affordability and better quality compared with traditional drugs, are on the basis of some of the reasons underlying their increasing popularity.

In the last decades, a great deal of attention has been drawn to the aspects underlying methamphetamine (METH; an ATS)-induced neurotoxicity, in many brain regions. Nevertheless, little is known regarding MDPV neurotoxicity, including in frontal cortex, which is known to be affected by drugs of abuse. Additionally, the behavioral profile of rodents after drug administration is poorly documented for MDPV, in comparison with METH.

Additionally, novel avenues in drug addiction sciences are being explored. As an example, there is a growing body of evidence regarding the impact of drugs of abuse including METH to both peripheral and central innate immunity. However, the effects of new cathinones (including MDPV) in the central innate immunity remain unknown. Therefore, this thesis aimed to characterize, for the first time, the impact of MDPV on frontal cortex glial cells and innate immune players including receptor for advanced glycation end-products (RAGE) and its ligand

S100β, within first 24 hours following a binge MDPV regimen. In addition, emotional behavior was assessed. A binge neurotoxic regimen of METH was also employed to deepen current knowledge on METH neurotoxicity.

Concerning the behavioral profile, we offer a first evidence that a single binge MDPV regimen did not come with any changes in both emotional and locomotor parameters, but curiously enhanced exploratory activity in mice. Secondly, we concluded that neither drug impose any changes in innate immunity as well as in neurotoxicity parameters including microglial, astrocytic, myelin and dopaminergic markers, as seen by the unaltered levels of RAGE, S100β, Iba-1, GFAP and, MBP and TH, respectively.

One cannot exclude the hypothesis whereby this is a premature time-window to observe significative molecular changes in frontal cortices following both stimulants. In this context, future studies are required to further characterize neuronal and glial effects of MDPV by using other time-points, dosing regimens and brain regions.

Keywords: Central Innate Immunity; Methilenedioxypyrovalerone; Methamphetamine; Receptors for advanced glycation end products; glial cells.

Resumo

A imunidade inata é a primeira linha de defesa efectiva de todos os organismos, englobando mecanismos moleculares e celulares com vista a uma acção imediata, reconhecendo padrões moleculares associados a patogénios de origem externa (PAMPs), bem como, padrões moleculares associados a uma ameaça de origem interna (DAMPs). Esse reconhecimento é possível através de diversos receptors de reconhecimento padrão (PRRs), orquestrando, assim, a activação de respostas imunes. Um destes receptores é o receptor dos produtos de glicação avançada (RAGE, também conhecido por AGER), que é um receptor, localizado à superfície das células, pertencendo à superfamília de proteinas imunoglobulinas, tendo um papel central na resposta inflamatória, mediando acções na imunidade inata. Para além do mais, o receptor RAGE tem sido implicado na neurotoxicidade e activação das células da glia. É de salientar que este recptor é expresso em muitos tipos de células incluíndo as células do sistema nervoso central (CNS) como os neurónios, microglia, astrócitos. De notar também que, sendo um receptor que interage com multiplos ligandos, RAGE é capaz de reconhecer um largo espectro de diferentes famílias de ligandos estruturalmente diversos, incluíndo o ligando S100β, pertencente à família de proteínas S100.

Nos dias de hoje, o consumo inadequado e a adição de drogas de abuso, incluíndo a dição dos estimulantes do tipo das anfetaminas (ATS), é um problema sério e verificado em todo o mundo, com inegável impacto na saúde pública, direitos humanos e na segurança. A par destes aspectos, a rápida difusão e abuso de novas substâncias psicoactivas *(new psychoactive substances, NPS)*, também conhecidas como "substâncias químicas de pesquisa" ou "drogas desenhadas", engloba a catinonas sintética, Methylenedioxypyrovalerone (MDPV), designada por "sais de banho", claramente parece piorar a actual situação, já que é usada como um substituto de estimulantes ilegais, como a cocaína. O acesso incrivelmente facilitado a estas catinonas, como o MDPV, no mercado de drogas global, através das *"smart shops", internet* ("*darknet"),* e o aspecto da "falsa legalidade" destas substâncias, assim como, o relativo baixo custo e a sua qualidade, comparativamente a outras drogas tradicionais, são factores que têm contribuído para a sua crescente popularidade.

Ultimamente, têm sido investigados novos aspectos dentro do tema das drogas de abuso. A título de exemplo, existem cada vez mais evidências no que diz respeito à methanphetamina na imunidade inata central e periférica. Contudo, os efeitos de catinonas (como o MDPV) na imunidade inata central ainda estão por investigar. Neste sentido, este trabalho tem como principal foco, caraterizar, pela primeira vez o impacto do MDPV nas células da glia, no cortéx frontal e nos intervenientes da imunidade inata, incluíndo o receptor dos productos de glicação avançada (RAGE) e o sei ligando S100 β, 24 houras após a um regime *binge* de MDPV.

Para além disso, o perfil comportamental dos roedores após a administração do MDPV está pouco documentado, em comparação com a METH. Assim sendo, o nosso objectivo com este trabalho foi caraterizar, pela primeira vez, o impacto do MDPV no cortéx frontal, nomeadamente nas células da glia e nos intervenientes da imunidade inata, incluíndo o receptor dos produtos de glicação avançada (RAGE) e o seu ligando S100β, nas 24 horas após um regime de "binging". Em paralelo à administração de MDPV, também foi administrada uma dosagem igualmente aguda de METH, no sentido de aumentar os actuais conhecimentos sobre a neurotoxicidade da METH.

Assim, em primeiro lugar, e no que diz respeito ao perfil comportamental, o nosso estudo oferece a primeira evidência de que um episódio de administração aguda de MDPV não acarretou perturbações emocionais nem locomoras, aumentando, no entanto, e curiosamente, a actividade exploratória nos ratinhos. Em segundo lugar, ficou demonstrado que nem o MDPV nem a METH influenciaram os parametros de neurotoxicidade relacionados com as células da microglia, células astrocíticas, fibras de mielina, bem como, com marcadores dopaminergicos. Tal foi comprovado pelos níveis inalterados de Iba-1, GFAP, S100β, MBP e TH, respectivamente. Para além do mais, concluímos que nenhuma droga influenciou marcadamente os níveis de expressão ou os níveis de proteína total correspondentes ao receptor RAGE.

Finalmente, não podemos descartar a hipótese de esta janela temporal de 24 horas corresponder a uma fase prematura para observar quaisquer alterações moleculares e celulares significativas, induzidas por ambos os psicoestimulantes, no cortéx frontal. Neste contexto, estudos posteriores serão necessários para caraterizar os efeitos, neuronais e ao nível das células da glia, do MDPV, que podem passar, quer pela adopção de outras janelas temporais, quer por outros regimes de administração, ou ainda quer pela avaliação numa outra área cerebral.

Palavras-chave: Imunidade inata central; Methilenedioxypyrovalerone; Methamphetamine; Receptores dos produtos de glicação avançada; células da glia.

Chapter 1

Introduction

1.1. Innate Immunity

Innate immunity is the first effective line of defense of all organisms, comprising cellular and molecular mechanisms for immediate action, upon a potential external or internal threat (Kovach & Standiford, 2011; Lester & Li, 2014). Therefore, innate immune system is capable of recognizing exogenous pathogen associated molecular patterns (PAMPs), from bacteria, virus and others, as well as, endogenous danger associated molecular patterns (DAMPs), which can be released from damaged tissues, healthy cells and apoptotic or necrotic cells (Janeway, 1989; Newton and Dixit, 2012;).

Such detection is possible through diverse pattern recognition receptors (PRRs) such as RAGE (receptors for advanced glycation end-products), thereby orchestrating activation of innate responses, ultimately leading to elimination of pathogens and restoration of homeostasis (Lotze &Tracey, 2005; Kawasaki & Kawai, 2014; Lester & Li, 2014). Other pattern recognition receptors include toll-like receptors (TLRs), Rig like (RLR), Nod-like (NLR) and Aim2 like receptors (ALR) (Unterholzner et al., 2010; Takeuchi et al., 2010).

1.1.1. Leading actors in Central Innate Immunity

1.1.1.1. Immune role of Glial Cells, the housekeepers

Infection, injury, toxic agents, or stress are few examples of insults that can be modulated, in the first place, by glial cells, on behalf of central immune system, thus removing or inactivating potentially harmful agents or damaged tissue. (Ransohoff et al., 2012) However, an over-reaction or activation by this system, levered by the elevated levels of immunological markers, such as pro-inflammatory cytokines and chemokines, may result in central nervous system (CNS) infiltration by peripheral immune cells including macrophages, and T lymphocytes. (Hayley et al., 2005; Leonard, 2007) This may result in the mounting of a neuroinflammatory response, with consequent alterations in brain structure and function, and ultimately leading to neurodegeneration (Hayley et al., 2005; Leonard, 2007) (**Figure 1.1).** It is also relevant to highlight that neurons and glia work side-by-side forming an intimate interconnection to support brain activity and development (Ransohoff et al., 2012).

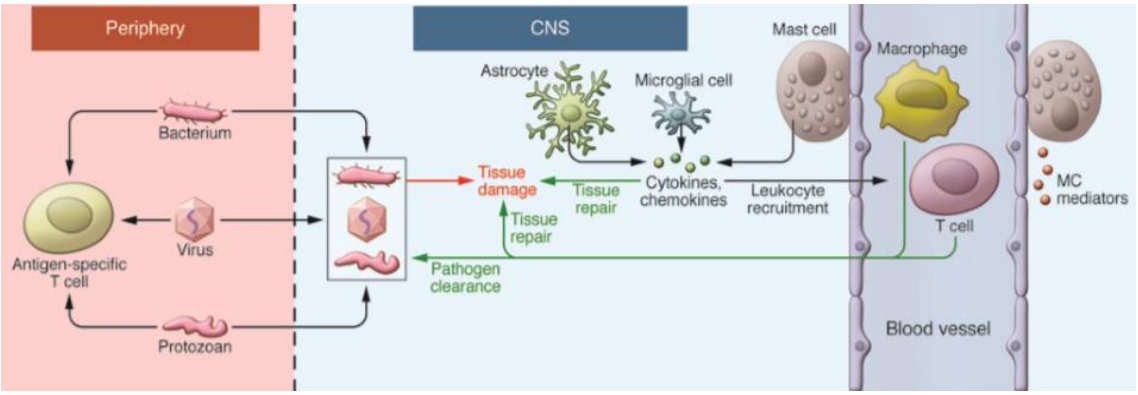

Figure 1.1 Ilustration of the immunitary response exerted by microglia and astrocytes in response of foreign pathogens or local injuries. In central innate immunity, microglia and astrocytes are the leading immune players, mitigating foreign invasors and local damage. The cytoquines and chemoquines released by those cells will consequently attract macrophages, and T lymphocytes from peripheral innate system, which are able to reach the affected brain area afterwards, because of the lesions in the Blood Brain Barrier (BBB). (*Taken from* Ransohoff et al., 2012)

1.1.1.1.1. Microglia

Microglia cells belong to a myeloid cell population and was derived from the yolk sac, originated in hematopoietic cells in the embryonary stage (Ginhoux et al., 2010). When settled in the CNS parenchyma, microglia are sustained by proliferation of resident progenitors (Ajami et al., 2007), being commonly referred as the macrophages of the CNS due to their phagocytic activity (Geissmann et al., 2010). Microglia are the primary modulators of CNS innate immunity (Stoll et al., 1998) as they constantly surveil the environment, and when they detect a potential threat, they become activated, showing morphological changes (del Rio-Hortega et al., 1892) (**Figure 1.2).** Therefore, it is through the constitutive/inducible expression of PRRs at their surface (including RAGE) that glial cells exert or amplify immune effects in response to a given insult including PAMPs or endogenous damage-associated molecular patterns (DAMPs) (Kagan, 2012).

This glial activation evokes the production of pro-inflammatory and anti-inflammatory cytokines/mediators such as IL-1β, IL-6, TNF-α, CCL2, ROS, NO and IL-10, being the ultimate effect dependent on the balance between these opposing responses (Kettenmann et al. 2011).

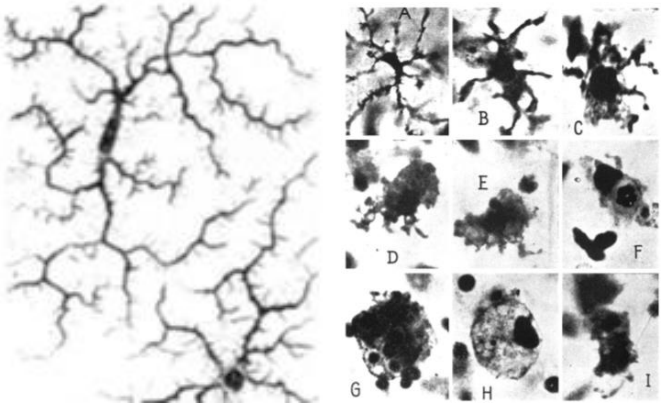

Figure 1.2. Images of ramified microglial cells. Microglial cells drawn by Pio del Rio-Hortega (1882-1945) (Left panel). Hortega. Morphological transformation of microglia to phagocytic macrophage are shown in lettered panels (Right lettered panels) (Ransohoff et al. 2012).

1.1.1.1.2. Astrocytes

Astrocytes, on the other hand, are glial cells that differentiate from a neural stem cell (NSC) pool during embryogenesis—around 16–18 weeks in human gestation (E17 in rodents)—with the peak of astrogliogenesis occurring during late prenatal/early postnatal development (P1 to P10 in rodents) (Rowitch and Kriegstein, 2010). Astrocytes are the best-characterized innate immune neuroglia (Ransohoff et al. 2012). These glial cells have a crucial role in terms of buffering CNS potassium, removing and recycling potentially toxic glutamate, brain water homeostasis, modulating the synaptic activity, blood flow, blood brain barrier (BBB) permeability and neurogenesis (Abbott *et al.*, 2006; Kim *et al.*, 2006; Allaman *et al.*, 2011). Astrocytes are also endowed with trophic, metabolic and antioxidant effects (Nash et al., 2011; Ares-Santos et al., 2013). Astrocyte dysfunction, termed "reactive astrogliosis," is a common response to all CNS injuries/diseases encompassing a spectrum of changes ranging from hypertrophy to chronic scar-forming proliferating and migrating astrocytes (Sofroniew and Vinters, 2010). Villareal et al. (2014) argued that DAMPs/RAGE interaction is essential to expand reactive gliosis in the injured brain being a tempting target for limiting reactive gliosis to prevent the glial conversion into the neurodegenerative profile (Villareal et al. 2014). Additionally, upon activation of PRRs, astrocytes participate in innate immune reactions and are the principal CNS sources of innate inflammatory mediators, including several complement components, IL-1β, IL-6, and chemokines such as CCL2, CXCL1, CXCL10, and CXCL12 (Ransohoff et al., 1993; Vesce et al., 2007; McKimmie et al., 2010) **(Figure 1.3).**

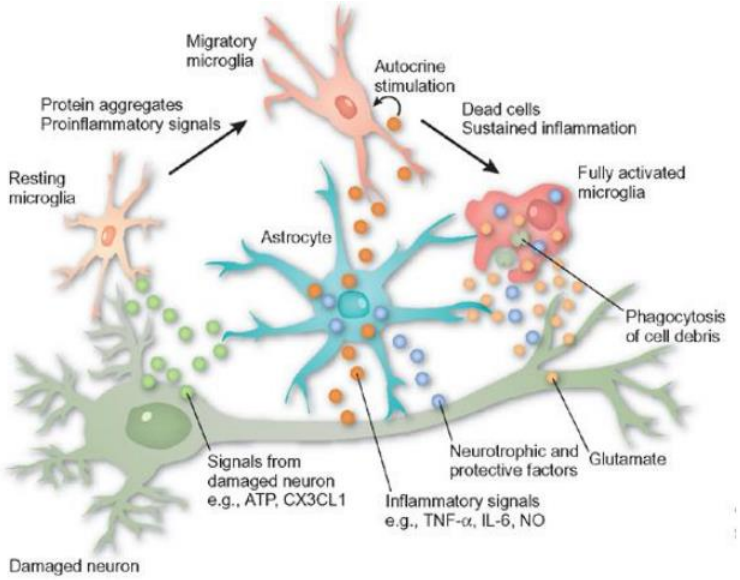

Figure 1.3 Depiction of an innate immune reaction of an activated astrocyte. Upon astrocytes activation through its PRR, an innate response played by astrocytes is triggered and, thus inflammatory mediators are released. (Taken from Monk *et al.*, 2006).

1.1.1.2. RAGE Receptors

The receptor for advanced glycation end-products (RAGE, also known as AGER), plays a central role in the inflammatory response mediating aspects of innate immunity (Tian et al., 2007). In fact, RAGE has been implicated in the sustainment of glial activation and neurotoxicity (Koch et al., 2010)

RAGE, which was described from mouse lung by Neeper and colleagues in 1992, is a cell-surface receptor belonging to the superfamily of immunoglobulin proteins (Neeper et al., 1992). It is encoded on the short arm of chromosome 6 (6p21.3), in the major histocompatibility complex III (MHC), a region containing numerous genes with an inflammatory function, that includes components of the complement system and various cytokines, such as TNF-α (Sugaya et al., 1994; Vissing et al., 1994; Traherne et al., 2008). Since then, increasing attention has been drawn to the molecular nature of RAGE signaling and its role in cellular physiology (Koch et al., 2010) due to its involvement in different pathologies (Leclerc et al., 2010) associated with inflammatory response (Hofmann et al., 1999). For example, increased expression of RAGE was reported in patients with Parkinson´s disease (PD) as well as in PD animal models (Dálfo et al. 2005; Viana et al, 2016). Studies in the postmortem human alcoholic brain and in preclinical models of adolescent binge ethanol treatment find increased expression of RAGE in the adult prefrontal cortex (Vetreno et al. 2013).

1.1.1.2.1. RAGE Structure and diversity

It has been proven that this receptor is highly conserved across species, for instance, bovine and human RAGE share 90% of homology (Neeper et al., 1992; Brett et al., 1993). Human cDNA comprises 1406 base pairs (bp) encoding an entire mature protein of 404 amino acids. This human form includes an extracellular domain of 321 amino acids, a single transmenbranar domain of 19 amino acids and an intracellular domain of 41 amino acids. (Neeper et al., 1992). Thus, the resulting transcribed mRNA is translated into a canonical full-length protein (commonly denominated flRAGE or mRAGE) of 404 amino acids with a molecular mass of ≈55kDa and comprising five domains: three extracellular ligand-binding domains, a membrane-spanning helix, and an intracellular domain as shown in **Figure 1.4** (Neeper et al., 1992).

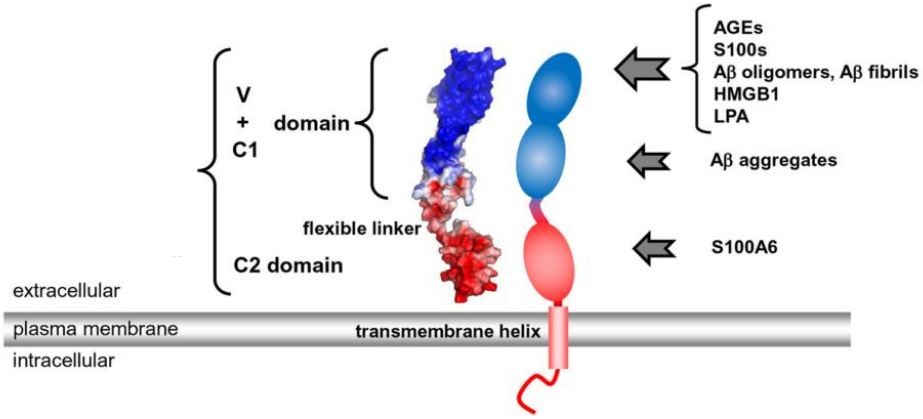

Figure 1.4 Schematic illustration of the domains of RAGE receptor. The areas in blue (V and C1 regions) stand for positive charge whereas areas in red (C2 region) represent negative charge. Several RAGE ligands are also depicted at the right-hand side (Figure extracted from Koch et al., 2010)

The ectodomain of RAGE comprises three immunoglobulin domains, one V-type and two C-type (C1 and C2) (Schmidt et al., 1992), depicted in the **Figure 1.4.** At the N-terminal, V and C1 domains form an integrated structural unit, independent from C2 domain, known as VC1, to which most of the reported RAGE ligands bind (Dattilo et al., 2007; Koch et al., 2010). Lastly, C2 is the third C-type domain and is attached to VC1 unit through a flexible linker (Dattilo et al., 2007). C2 domain is followed by the transmembrane helix which is anchored in the plasma membrane (Schmidt et al., 1992; Dattilo et al., 2007). Other splice variants of RAGE result in changes that might affect the extracellular ligand-binding domain (typically denominated as N-terminal truncated) and the removal of the sequence encoding the transmembrane/cytosolic

region, thus generating C-terminally truncated isoforms (Hudson et al., 2008; Kalea et al., 2011; Lopez-Diez et al., 2013). One C-truncated isoform is an endogenous secretory variant of RAGE (esRAGE), which is soluble (Hudson et al., 2008). Formation of secreted isoforms variants is a common phenomenon amongst membrane receptors, often acting as antagonist versions of their membrane bound version (Muda et al. 2005; Fry &Toker 2010). In fact, sRAGE may prevent RAGE signaling by acting as a "decoy" receptor. Soluble RAGE isoforms can also be produced by constitutive or induced ectodomain shedding of flRAGE by metalloprotease 10 (ADAM10) metalloprotease 9 (MMP9) and/or γ-secretase (Galichet et al., 2008; Braley et al., 2016; Metz et al., 2012) (**Figure 1.5**). Both soluble RAGE isoforms (esRAGE and cleaved RAGE) circulate in human plasma. In addition, RAGE variants, who exhibit decreased ligand binding ability (N-terminally truncated) or lack cytosolic region (C-terminally truncated), may also contribute to the overall regulation of flRAGE cellular function (Chuah et al., 2013)

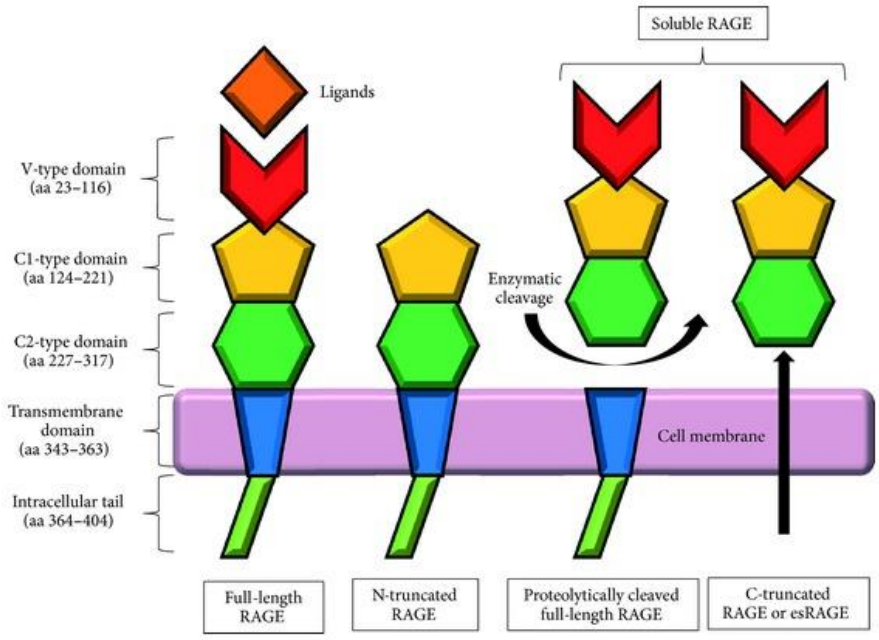

Figure 1.5 Representation of full-length RAGE and its splice variants. RAGE is composed of an intracellular tail, a transmembrane domain, and an extracellular domain consisting of three immunoglobulin-like domains, one V-type followed by two C-type (C1 and C2) domains. C stands for constant whereas V stands for variable. (Picture taken from Chuah et al., 2013)

The V-type domain is essential for ligand binding, and so the elimination of this domain gives rise to the N-truncated form. On the contrary, the C-truncated, circulating soluble RAGE form, comprises the extracellular domain of RAGE, without the intracellular tail or transmembrane domains. This truncated form may be described to be a consequence of the proteolytic cleavage of full-length RAGE, from the cell surface (cRAGE) or via alternative splicing of RAGE mRNA (esRAGE). (Chuah et al., 2013)

RAGE is constitutively expressed during embryonic development, contributing positively to cellular migration and differentiation of the neuronal tissue and neurite outgrowth (Wang et al., 2008; Saleh et al., 2013), yet it is expressed at lower levels in adulthood (Brett et al., 1993). Whereas, in pathological scenarios, such as neuroinflammation, RAGE tends to be strongly overexpressed, (Fang et al., 2010).

Noteworthy, RAGE receptor exhibits broad expression on many different cells including non-immune cells such as smooth muscle cells, hepatocytes and cardiac myocytes (Brett et al., 1993) and immune cells like mononuclear phagocytes, T and B lymphocytes and dendritic cells (DCs) (Dumitriu et al., 2007; Chen et al., 2008; Manfredi et al., 2008; Akirav et al., 2012). Importantly RAGE is also expressed by CNS cells, including neurons, microglia and astrocytes and endothelial cells (Brett et al., 1993; Schmidt et al., 2001).

1.1.1.2.2. The nature of RAGE ligands

RAGE physiological and pathological effects strongly depend on the cell type and their signaling pathways, the surface concentration of RAGE and adaptor molecules, not to mention the concentration and ligand nature (Leclerc et al., 2008; Hans et al., 2011). As a multiligand receptor, RAGE recognizes a broad repertoire of structurally different ligand families (Hori et al., 1996; Yan et al., 1996; Hofmann et al., 1999).

The first RAGE ligands to be identified were nonenzymatically modified proteins, lipids, and nucleic acids, also known as, advanced glycation end-products (AGEs) (Neeper et al., 1992). These RAGE-AGEs interactions were described in endothelial cells, smooth muscle cells, and mononuclear phagocytes (Basta et al., 2002). AGEs increase concentration as a consequence of aging and inflammatory events. (Cipollone et al., 2003). AGEs cause perturbation in a diverse group of diseases, such as diabetes, inflammation, neurodegeneration, and aging. (Ramasamy et al., 2005)

S100 calgranulins, a family of Ca^{2+}-binding proteins, are among the best characterized ligands to RAGE. Particularly, S100β is widely expressed in astrocytes and is involved in a large number of cellular functions such as calcium homeostasis, cell growth and differentiation, dynamic of cytoskeleton or energy metabolism (Donato et al., 2003). These intracellular molecules may achieve extracellular space at low concentrations, triggering trophic effects and repair after injury: nanomolar concentrations of S100β stimulates neurite outgrowth and enhanced neuronal survival during development or after injury (Winningham-Major et al., 1989; Saleh et al., 2013). However, submicromolar-microamolar concentrations of S100β may engage in neurotoxic/neurodegenerative processes (Donato et al., 2009).

Other ligands include amphoterin protein or high mobility group box-1 (HMGB-1), and amyloid-beta peptide (Aβ**)** in the form of soluble oligomers, beta sheets containing fibrils, and insoluble aggregates as well (Hori et al., 1995; Yan et al., 1996; Schmidt et al., 2001; Bucciarelli et al., 2002).

1.1.1.2.3. Intracellular pathways

Upon RAGE ectodomain-ligands interaction, intracellular factors, such as mammalian Diaphanous-1 (mDia-1), are recruited to the site of cytoplasmic domain, triggering a molecular wave propagation of intracellular signals (Hudson et al., 2008). Moreover, activated RAGE is known to recruit extracellular signal–regulated kinase–1 and –2 (ERK-1/2) resulting in downstream activation of NF-kB via the mitogen-activated protein kinase (MAP kinase) pathway (Ishihara et al., 2003). This transcription factor, NF-kB, illicit the production of pro-inflammatory molecules and enhances RAGE expression, initiating a positive feedback loop in RAGE signaling, fueling the inflammatory response and further RAGE expression, thereby perpetuating another wave of cellular activation (Schmidt et al., 1999). **(Figure 1.6**).

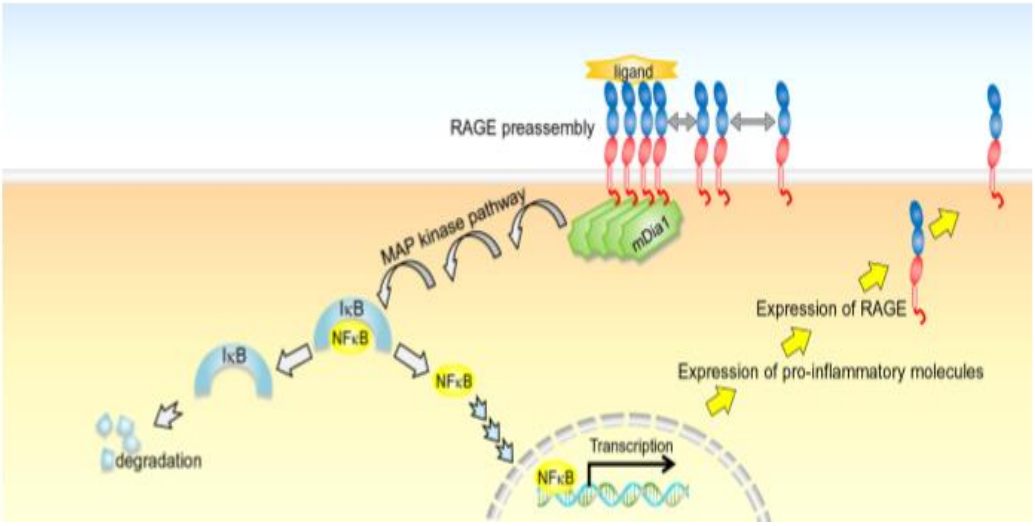

Figure 1.6 Schematic representation of the putative mechanism for regulation and activation of RAGE receptors. After RAGE-ligands binding intracellular signaling pathways are triggered, leading to NF-kB inflammatory regulator molecule activation with consequent production of pro-inflammatory molecules, as well as increased RAGE expression (This image was taken from Kierdorf et al., 2013).

.

Additionally, intracellular multiple and complex signaling pathways, upon RAGE-ligands binding, occur, as mentioned before, in endothelial cells, microglia, and neurons, with several effector events occurring downstream, as seen in **Figure 1.7.** (Donato and Heizmann, 2010)

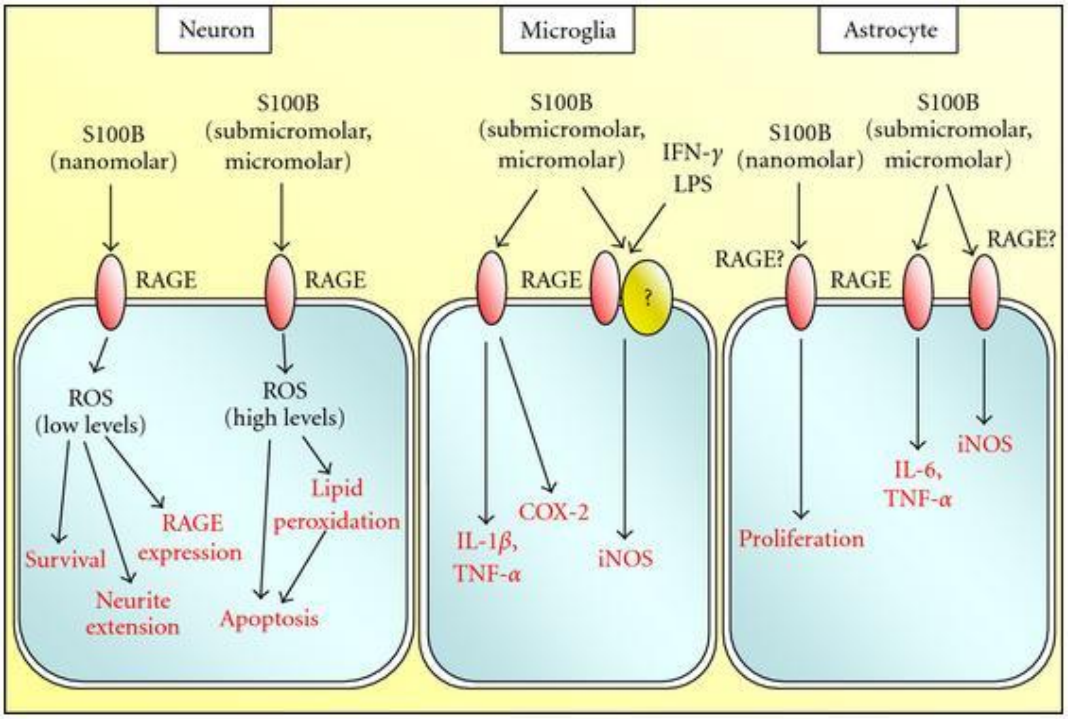

Figure 1.7 Schematic illustration of the impact of RAGE-S100β binding on neurons, microglia, and astrocytes. (Image taken from Donato and Heizmann, 2010).

Several authors have suggested that RAGE oligomerization assembly enables ligand binding, at the same time that this assembling is stabilized by those binding ligands (S100B, S100A12, or polymeric glycated proteins for instance), which might explain why and how RAGE activation, through multimeric ligands binding, leads and sustains the exerted positive feedback loop. (Koch et al. 2010). **Figure 1.8** In addition, increased RAGE levels will promote preassembly, which possibly explains the consequent hyperactivation of the RAGE pathway in long-term tissues disfunction (Bierhaus and Nawroth 2009; Rojas et al. 2010) chronic inflammatory or neurodegenerative disorders (Koch et al. 2010).

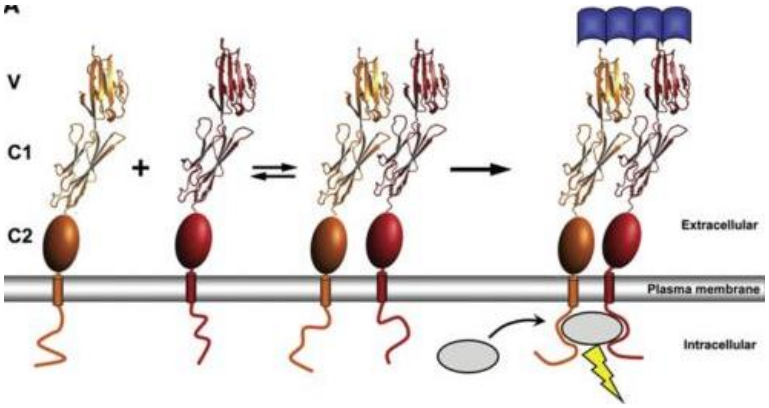

Figure 1.8 Depiction of RAGE oligomerization assembly and subsequent multimeric ligands binding. (Koch et al., 2010)

1.2. Challenging the Innate Immunity:

1.2.1. Drugs of Abuse: the other side of the coin

Drugs of abuse are a global issue with an undeniable expression on public health, development, peace and human rights, not to mention security, with approximately 190,000 people dying every year due to illicit drugs consumption. (UNODOC, 2017). Novel avenues in drug addiction sciences are being explored. As an example, there is a growing body of evidence regarding the impact of drugs of abuse including opioids, cannabinoids, alcohol and the psychostimulants cocaine and amphetamine-type stimulants (ATS) to both peripheral and central innate immunity (Szabo et al., 2015).

1.2.1.1. Amphetamine-Type Stimulant (ATS), as the origin of a season

Psychostimulants are a group of psychoactive substances which are capable of enhancing physical and cognitive activity, being associated with a high potential of addition (Aghajanian et al., 1999; Greyer et al., 2009). According to a report published by UNODC (2011), ATS such as "ecstasy" and methamphetamine were considered the world's second most widely abused drug type after cannabis, becoming one of the major public health issue worldwide, since the 1990´s (UNODOC, 2011) (**Figure 1.9).**

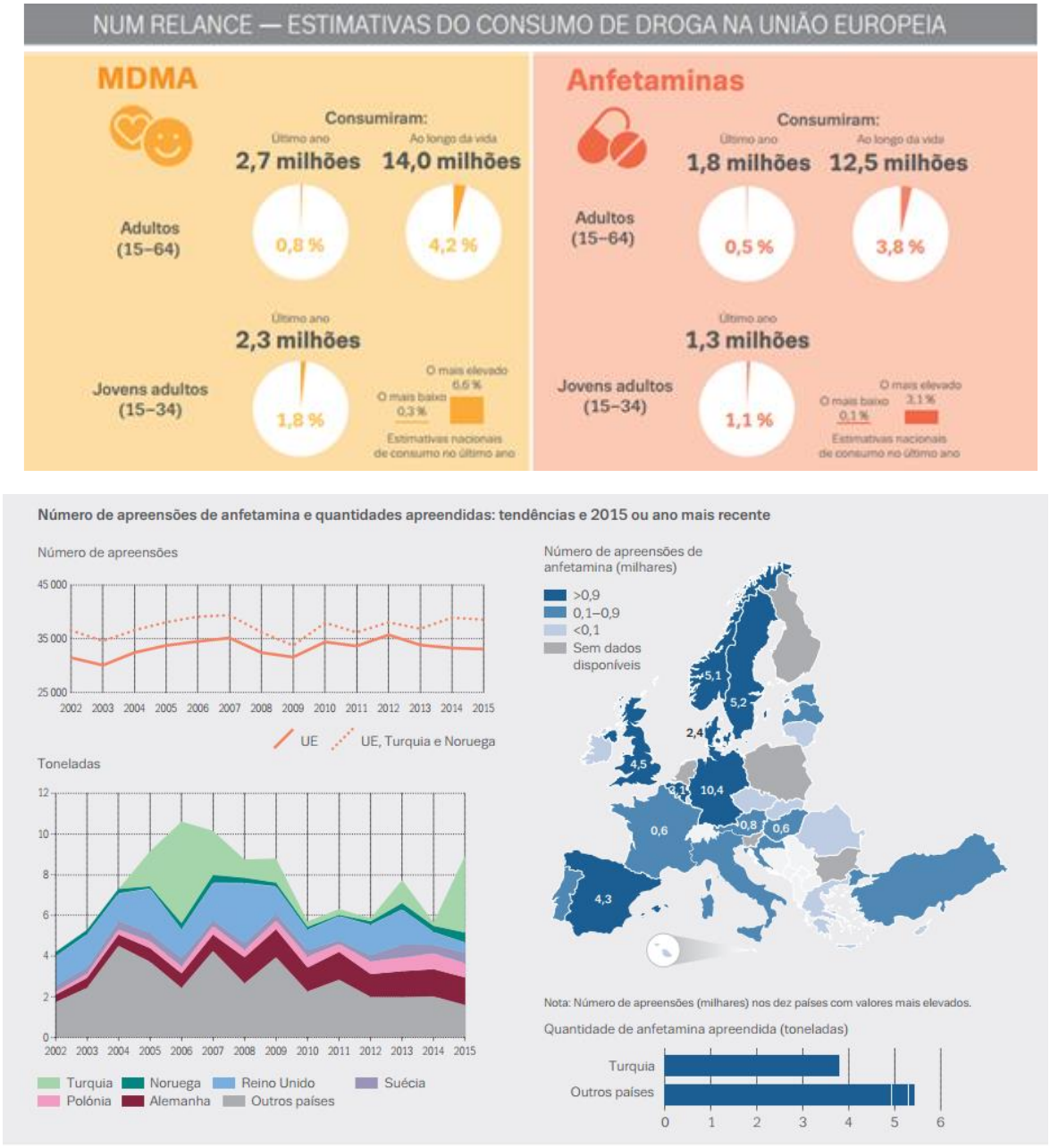

Figure 1.9 Schematization of some statistics concerning ATS in Europe as well as in Portugal. In the upper picture, quantitative expression of MDMA and anfetamines consumption, in Portugal as well in European Union. In the bottom picture, statistics on the quantity of anfetamines reported in the last couple of years, in several countries in Europe. (European Observatory on Drugs and Toxic dependence, 2017).

In 2011, UNODOC Executive Director, Yury Fedotov, mentioned that: "*The ATS market has evolved from a cottage-type industry typified by small-scale manufacturing operations to more of a cocaine or heroin-type market with a higher level of integration and organized crime groups involved throughout the production and supply chain. We are seeing manufacturing shifting to new markets and trafficking routes diversifying into areas previously unaffected by ATS*." (UNODOC, 2011)

The recently released World Drug Report 2017 highlights that old drugs of abuse including heroin still continue to be a threat, while, at the same time, methamphetamine and new psychoactive substances (NPS) spread. Moreover, it is highlighted that business models are evolving under the influence of the ever-increasing cybercrime and "darknet" (UNODOC, 2017).

Amphetamine-type stimulants (ATS) are widely used and abused these days and involve chemically-related substances such as methamphetamine (METH), 3,4-metilenedioxi-N-metanfetamina (also known as MDMA or Ecstasy) and metilenedioxipirovalerone (MDPV) **Figure 1.10** (Aghajanian et al., 1999; Greyer et al., 2009). Pharmacologically, these are categorized as indirectly-acting sympathomimetics as they enhance the levels of catecholamines (noradrenaline, dopamine and adrenaline) in the synaptic cleft, both in central and peripheral nervous system (Szabo et al., 2015). Serotonin levels are also increased (Szabo et al., 2015).

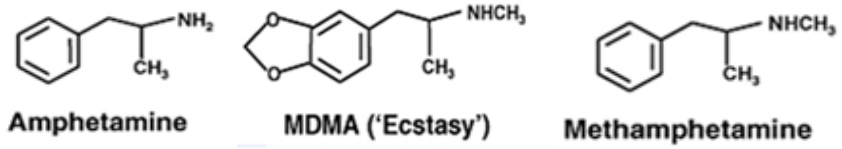

Figure 1.10 Representation of some of the Amphetamine-type stimulants (ATS) (Boyle et al., 2010).

1.2.1.1.1. Methamphetamine (METH), a case still open to debate

1.2.1.1.1.1. Methamphetamine (METH): the one and only

Methamphetamine (METH), as depicted in **Figure 1.11,** is as a highly addictive amphetamine-type stimulant (ATS) which promotes the release of neurotransmitters such as

noradrenalin and dopamine (or mentioned as an indirect agonist of dopamine), and its effects are very similar to the ones produced by cocaine, but tend to be more long-lasting. (Downes et al., 2005; Collins et al., 2014). It is well known that this drug accounts for many major psychiatric disturbances, including mood impairment, severe public health issues and socioeconomic problems (Courtney et al., 2014).

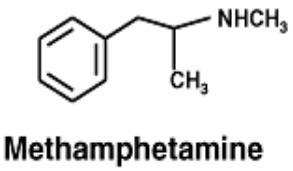

Figure 1.11 Chemical structures of methamphetamine. (Boyle et al., 2010).

1.2.1.1.1.2. Math behind METH: a queen with a solid throne

Since the last couple of years, METH is one of the most popular illicit drugs consumed worldwide, (Kaushal et al., 2011), as seen in **Figure 1.12,** and in particular, the second most commonly used illegal substance worldwide, after cannabis (UNODC, 2014), dominating the global ATS market (UNODOC, 2017), as seen in **Figure 1.13.**

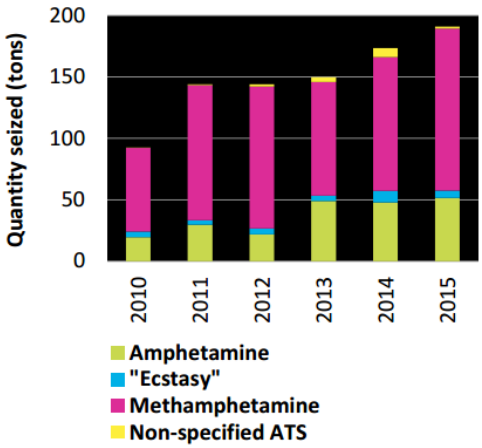

Figure 1.12 Quantities of amphetamine-type stimulants seized worldwide between 2010 and 2015. (UNODOC, 2017)

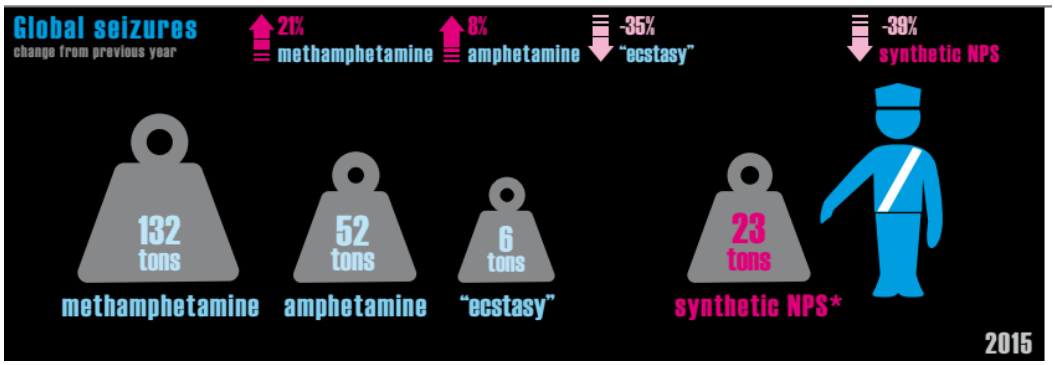

Figure 1.13 Schematic depiction on alterations of methamphetamine seizures from 2014 to 2015. (UNODOC, 2017)

Methamphetamine consumption is still spreading, embodying a major global health issue, consistent with the increasing number of methamphetamine users seeking treatment (World Drugs Survey, 2017) (**Figure 1.14)**.

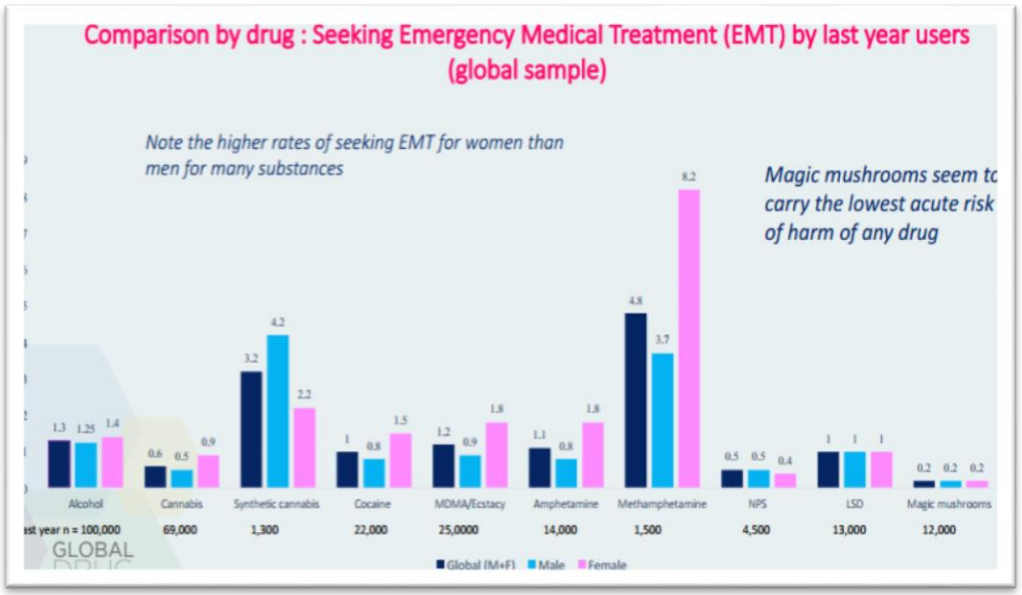

Figure 1.14 Global comparision of emergency medical treatment seeking, in the last 5 years. (World Drugs Survey, 2017)

1.2.1.1.1.3. "Biography" of a "Crystal" star: some historical facts

Literature claims that the Japanese researcher Nagayoshi Nagaiwas was the first to synthesize METH from the precursor ephedrine (Nagai and Kamiyama, 1988).

Historic facts also suggest that METH consumption became to be prominent during World War II, (1945-1948), when it was currently recommended by the governments to the military army to mitigate fatigue, to enhance endurance and alertness (Meredith et al., 2005; McGuinness, 2006). Although amphetamine-type stimulants were banned by the Food and Drug Administration (FDA) in late 1950s due to its high abuse potential (Roll et al., 2006), amphetamine and some derivatives were medically use in cases of hyperactivity, obesity, narcolepsy, and depression (Wolkoff, 1997). In the later 1980s, the consumption of METH increased, as the number of clandestine laboratories boomed (Cunningham and Thielemeir, 1996).

Currently, METH misuse and addition is a worldwide problem and governments and international organizations have begun to tackle this major global epidemic (UNODC, 2014). So far, the most common designations or "street-names" for METH are: crystal, crank, ice, glass, go, speed, and zoom. (UNODC, 2014)

1.2.1.1.1.4. Overall perspective on stimulant & neurotoxic effects

As a psychostimulant substance, METH, **at lower doses**, induces pharmacological effects associated with euphoria and enhanced mood, self-confidence, sociability alertness, concentration and energy boost (Kaushal et al., 2011; FDA, 2014). However, **higher dose**s of methamphetamine may induce neurotoxic effects which translate into complex psychiatric symptoms, including depression, anxiety, psychosis, irritability, obsessive behaviors, suicide behavior as well as cognitive impairments (Kaushal et al., 2011; FDA, 2014). On the other hand, **METH overdosing** may be responsible for cardiogenic shock, cerebrovascular accidents, high body temperature, pulmonary hypertension and kidney failure, to name a few (FDA, 2014). Acute as well as long-term neurotoxic effects underlying effects on psychomotor behaviors reflect neurochemical as well as brain structural alterations (Robinson and Becker, 1986; Ernst et al. 2000; Srisurapanont et al., 2003; Chang et al. 2007). Overall, METH abuse may result in addiction, weight loss and in neuropsychological impairments (Scott et al., 2007). Moreover, METH withdrawal may be related to anxiety, drug cravings, fatigue, increased or decreased movement, depression, lack of motivation, sleeplessness or sleepiness, for instance (Shoptaw et al., 2009). Other effects of

METH include excessive sweating, high body temperature, blurred vision, tremors, dry skin, and "meth mouth", which is characterized by abnormal teeth loss (FDA, 2014).

To our knowledge, there is no effective treatment for METH addition. This may reflect a particularly unsatisfying knowledge of the molecular and cellular mechanisms of METH. For this purpose, scientists have proposed repeated administration of METH in rodents as a model to uncover the nature of METH action (Krasnova et al., 2011; McCoy et al., 2011).

1.2.1.1.1.5. Dopamine, it is never enough

Dopamine (DA) regulates important physiological brain's functions, including locomotion, emotion, motivation, reward and cognition through different DAergic pathways, mainly originating in two mesencephalic nuclei, the ventral tegmental area (VTA) and the substantia nigra *pars compacta* (SNpc) (Calabresi *et al.* 2007; Ledonne and Mercuri, 2017; Everitt and Robbins, 2013). DAergic neurons of the VTA project to limbic areas (nucleus accumbens, NAc), hippocampus and amygdala) and cortical regions, including frontal cortex, thus composing the mesolimbic- and mesocortical pathways, respectively, (Wise, 2004; 2005) those of the SNpc constitute the nigrostriatal pathway mainly projecting to the dorsal striatum. (Barbeau, 1974; Smith, Y. & Villalba, R., 2008)

DA is a neuromodulator synthesized in the cytoplasm of dopaminergic neurons and depends on the enzymatic role of tyrosine hydroxylase (TH), which is responsible for the production of L-dihydrophenylalanine (L-DOPA) from tyrosine. (Meiser et al., 2013). This is the rate limiting step of DA synthesis (Meiser et al., 2013). Afterwards, DA is either sequestered into vesicles by vesicular monoamine transporter (VMAT-2) or is metabolically degraded (as reviewed in Pereira et al., 2012) (**Figure 1.15).**

DA receptors are coupled to heterotrimeric G proteins and are grouped according two distinct families: D1-like receptors, including D1 and D5 receptors, and D2-like, including D2, D3 and D4 receptors (Beaulieu and Gainetdinov, 2011). D1-like receptors are found post-synaptically, whereas D2-like receptors are expressed not only pre-synaptically, but also post-synaptically (Beaulieu and Gainetdinov, 2011). DA receptors are expressed in several brain regions, including frontal cortex, striatum, NAc, olfactory bulb, amygdala and also, but in lower concentrations, hippocampus and VTA (Moratalla et al., 1996; Beaulieu and Gainetdinov, 2011; Gangarossa et al., 2012).

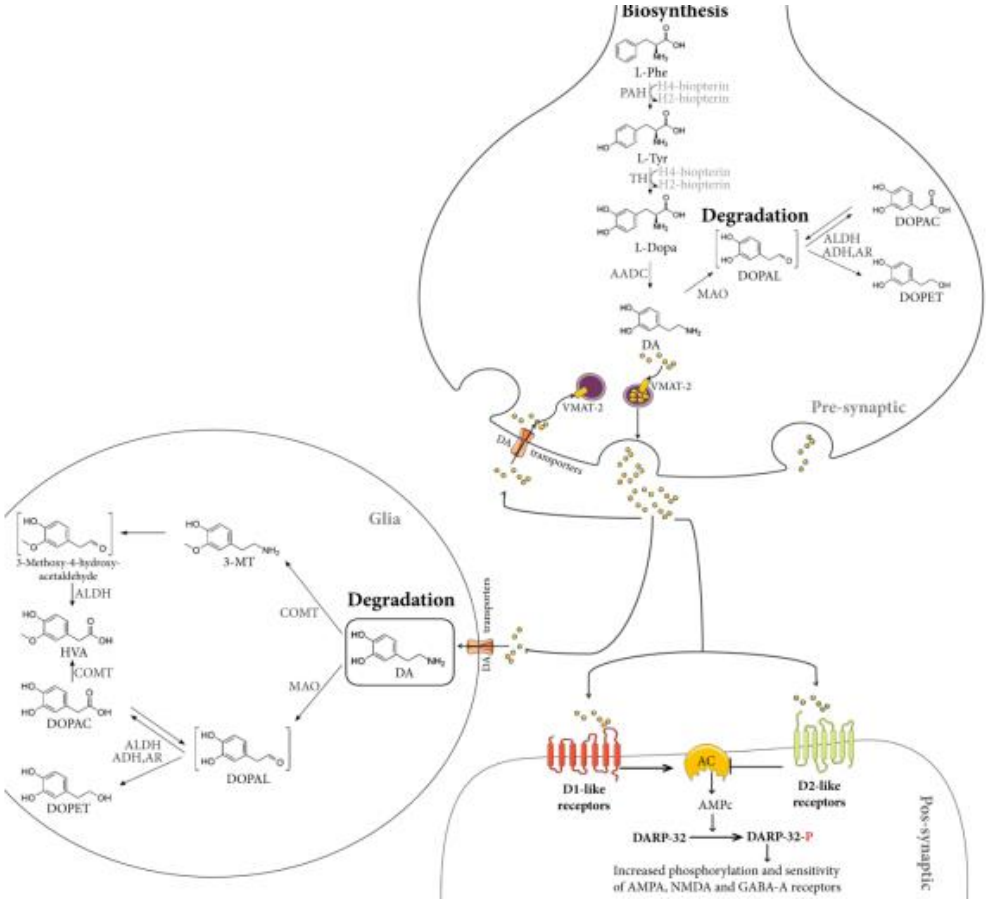

Figure 1.15 Dopamine life-cycle. (*Taken from* Viana, 2016)

1.2.1.1.1.6. METH reinforcing effects

An acute exposure to METH leads to the activation of the mesocorticolimbic dopaminergic systems, thereby producing rewarding effects (Kalivas and Stewart, 1991; Koob 1992; Brown et al., 2002; Rose & Grant 2008). In fact, reverse transport of dopamine via DAT and inhibition of VMAT-2 are primary mechanisms of action of METH, resulting in the massive outflow of dopamine from the presynaptic terminal into the synaptic cleft (Pereira et al. 2002; 2004; 2011; Fleckenstein et al. 2007; Volkow et al. 2007).

1.2.1.1.1.7. METH neurotoxic effects: dopamine system as the selected target

METH causes neurotoxicity in a dose-dependent manner (Seiden and Sabol, 1996), similarly to other amphetamine-type stimulants such as MDMA (Granado et al., 2008a; 2008b).

A large body of evidence supports that exposure to high doses or repeated doses (chronic exposure) of METH lead to long-lasting striatal dopaminergic axon terminals degeneration in animal models as well as in humans, as evaluated by a decrease in the following dopaminergic markers: DA, TH and VMAT-2 (Kogan et al.,1976; Wagner et al., 1980; Volkow et al., 2001a; Volkow et al., 2001b; Kita et al. 2003; Krasnova and Cadet 2009; McCann et al., 2008). Dopaminergic deficits were also evaluated in other brain regions including frontal cortex (Silva et al. 2014).

That is why some authors coined dopaminergic system as the ultimate target for the neurotoxic effects of METH **(**Krasnova and Cadet 2009)

Moreover, several lines of evidence suggest that individuals with a history of METH abuse have an increased risk for developing Parkinson's Disease, when compared to healthy people and individuals with a history of cocaine consumption (Callaghan et al., 2010; Callaghan et al., 2012).

1.2.1.1.1.8. Central toxicity beyond the dopaminergic system

In addition to dopaminergic neurons, METH is known to cause disruption to other neurochemical systems: serotonergic pathways - associated with mood - (Krasnova and Cadet, 2009; Silva et al., 2014), glutamatergic pathways – crucial in addiction, memory dysfunctions and psychotic episodes - (Simões et al., 2007; Miyazaki et al., 2013; Zhang et al., 2014), GABAergic pathways – influential on cognitive impairments and anxiety during withdrawal (Zhang et al., 2006; Mizoguchi and Yamada, 2011; Shen et al., 2013) and cholinergic pathways - related with locomotor abnormalies as well (Lim et al., 2014).

Therefore, degenerative brain alterations, from chronic administration, could be verified primarily in terminals of dopamine and serotonin neurons (Seiden and Sabol, 1996; Ricaurte et al., 1980).

It is noteworthy, that final neuronal and behavioral are related with the structural and functional connections between these neurotransmitter and dopaminergic systems (Miyazaki et al., 2013).

1.2.1.1.1.9. Neuroinflammation & METH

It is known that METH treatment induces neuroinflammatory processes in the rodent brain, with glial reactivity, production of pro-inflammatory cytokines (eg. TNF-β and IL-1β) peripheral immune cells infiltration and BBB disruption (Thomas et al, 2004; Gonçalves et al., 2010; Martins et al., 2011; Silva et al., 2014;). This is highly suggestive that METH impacts both innate as well as adaptative immunity.

Increasing body of evidence highlights the likelihood of the acquisition of human immunodeficiency virus (HIV) and other infectious diseases by METH abusers (Ellis et al., 2003; Urbina et al., 2004; Mansergh et al., 2006; Nakamura et al., 2011). However, there are limited studies about the effects of METH on DAMPs and PRRs that are known to activate glial responses. For example, Frank et al. (2016) suggested that HMGB1 mediates, in part, striatal neuroinflammatory effects of METH. (Frank et al., 2016) However, these authors failed to characterize its cognate receptors including RAGE. However, we previously showed that levels of striatal flRAGE were not altered 3 days post a neurotoxic METH dose (Pereira et al. 2012). Also, DAMPs originated from astrocytes (eg. S100β) were also never tested. Therefore, more research on the impact of METH on central immune innate players is warranted.

1.2.1.2. New Psychoactive Substance (NPS): the novelty in the field

United Nations Office on Drugs and Crime (UNODOC) filed new synthetic cathinones as new psychoactive substance (NPS) (UNODOC, 2011). UNODOC supports filing substances under NPS according to different categories which include chemical structure (for example, phenethylamines, tryptamines) and/or pharmacological effects (for example, cannabinoid receptor agonists) (**Figure 1.16**). Yet, it is also relevant to note that similar chemical structures do not mean identical pharmacological effects, and vice-versa, similar pharmacological effects might not reflect same chemical structures (UNODOC, 2017).

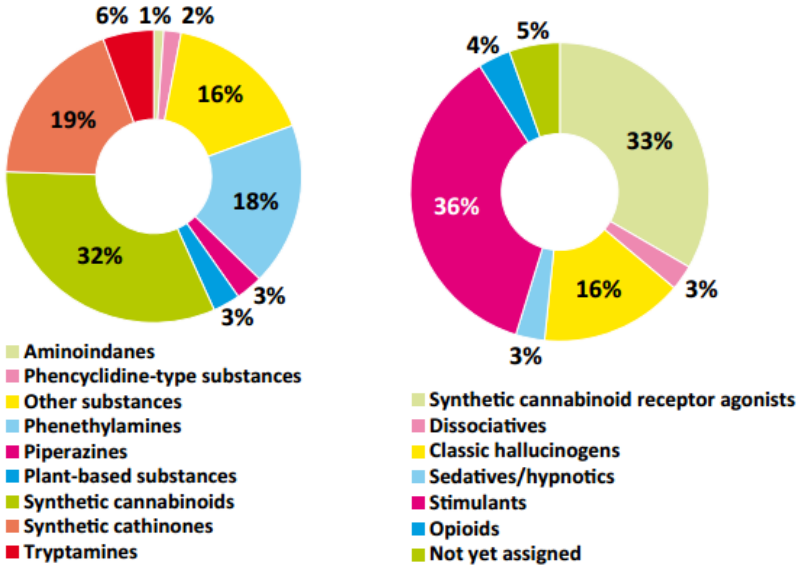

Figure 1.16 Proportion of new psychoactive substance category, in December 2016 (left-hand side); and proportion of new psychoactive substance, by pharmacological effect, in December 2016 (right-hand side). (UNODOC, 2017)

NPS have similar effects to classical drugs such as cannabis, cocaine, heroin, (+)-lysergide (LSD), MDMA ("ecstasy") and methamphetamine (UNODOC, 2017). Moreover, NPS can be termed as "legal highs" and "research chemicals" or "design drugs"; their increased intake trends are associated with the use of pills, liquids and powders rather than herbal smoking mixtures. (Global Drug Survey, 2017). Synthetic cathinones are sympathomimetic drugs that act on serotonin, dopamine and noradrenaline pathways. It came with little surprise that vertigo, paranoia, convulsions, agitation and restlessness were associated with their intake (Schifano et al., 2012; Loi et al., 2015).

These cathinones as well as synthetic cannabinoids represent nearly more than 50% of the NPS available in the market, being China or Oriental East the countries with the largest production worldwide (López-Arnau et al., 2012). The incredibly easy access to these cathinones, gauged by the ages of NPS users (**Figure 1.17)** including the newly synthesized MDPV, in the global drug market, through smart shops, internet ("darknet"), and the aspect of "fake legallyness of such substances, as well as the relative affordability and better quality compared with traditional drugs, contribute to their increasing popularity (DEA, 2011;UNODOC, 2017) (**Figure 1.18**).

Figure 1.17 Schematic representation of NPS consumption statistics in Europe. (European Observatory on Drugs and Toxic dependence, 2017).

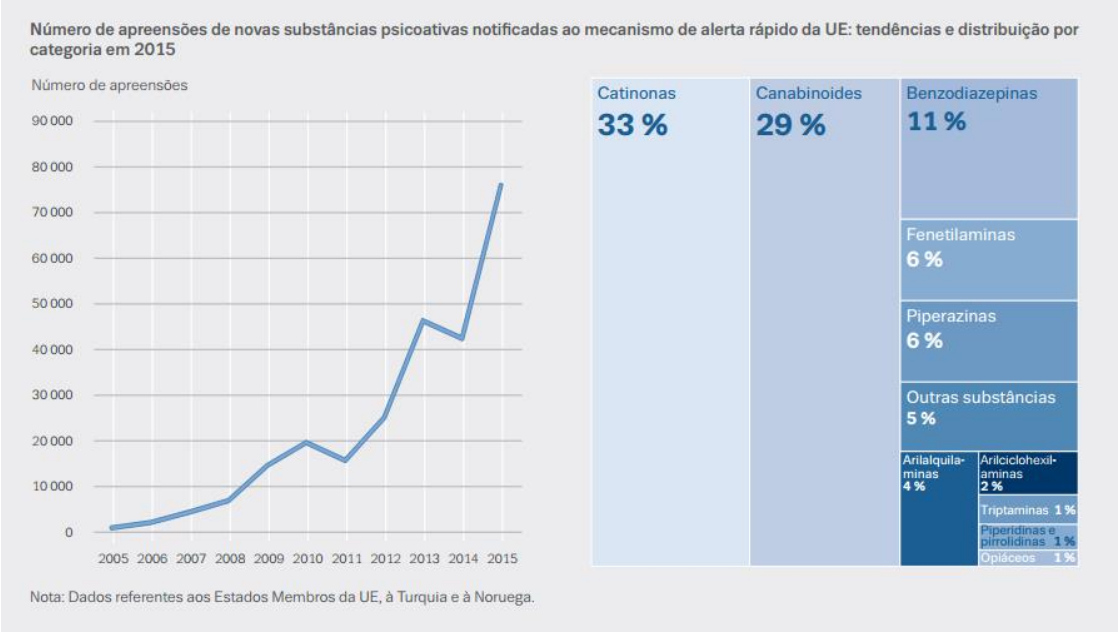

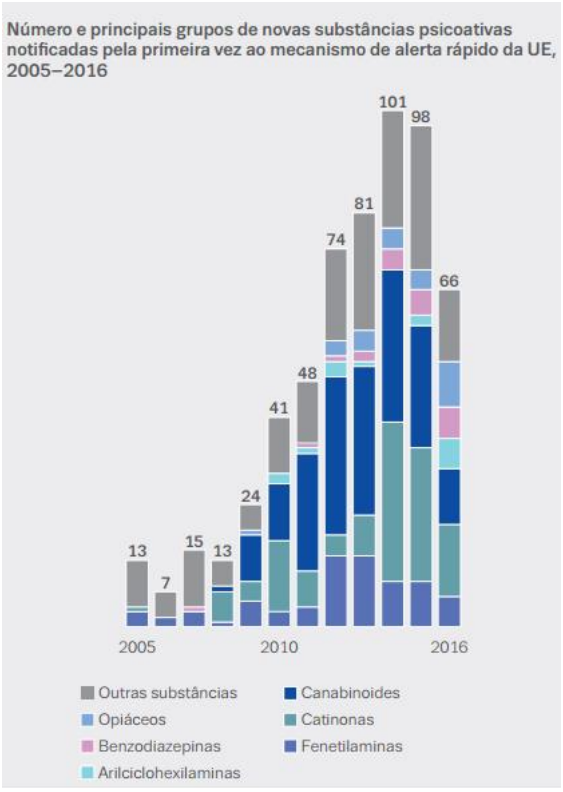

Figure 1.18 Annual amounts of synthetic new psychoactive substances seized in Europe, 2005-2015, illustrated in upper and bottom pictures. (UNODOC, 2017)

Concerning the first aspect, the drug report of European Monitoring Centre for Drugs and Drug Addiction European (EMCDDAE) claimed that, in 2013, the number of sites online selling MDPV was approximately 651, meaning that the internet has emerged as the prominent market, the so-called "darknet" (**Figure 1.19**) (EMCDAE, 2013). It also gives open access to ways of synthetizing and consuming details. In what respects to the aspect of the "fake legallyness", it is closely related to the fact that structure of NPSs can easily undergo chemical changes in functional groups, thus being converted into new molecules with brand new chemical designations not being covered by the ongoing legislation (Schifano et al., 2016).

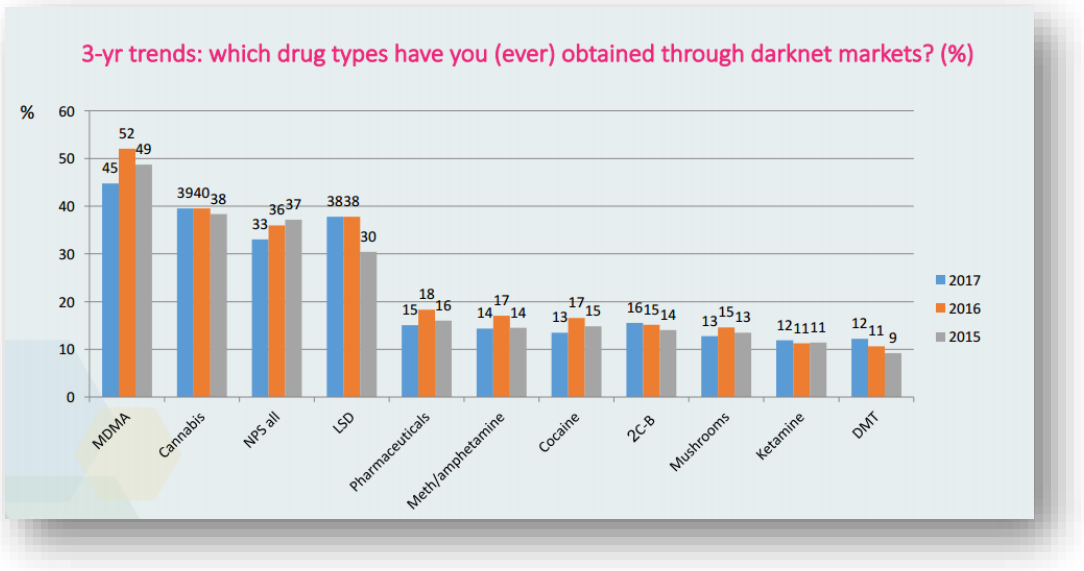

Figure 1.19 Percentages of types of drugs purchased through the so-called "darkmarkets". (Global Drug Survey, 2017)

1.2.1.2.1. Methylenedioxypyrovalerone (MDPV) phramacodinamics and pharmacokinetics: modern ways of bathing

Methylenedioxypyrovalerone (MDPV) is a synthetic cathinone and therefore is a psychoactive substance. It is commonly and commercially known as "bath salts" or "plant food", acting as a substitute for illegal stimulant drugs such as cocaine (Karila et al., 2015; UNODOC, 2011).

Bath salts forensic analysis, in 2010 and 2011, identified, among others, three main synthetic compounds: 4-methyl-N-methylcathinone (mephedrone), 3,4-methylenedioxy-N-methylcathinone (methylone), and 3,4-methylenedioxypyrovalerone (MDPV), (Shanks et al., 2012; Spiller et al., 2011) (**Figure 1.20**). Importantly, these compounds are chemically similar to cathinones, which is naturally originated from the *khat* plant, *Catha edulis*, grown in eastern Africa and southern Arabia East, and consumed for its amphetamine-like effects (Karila et al., 2015). Bath salts were banned in US (in 2013) (Drug Enforcement Administration, 2013) and in Portugal in the 2nd March of the present year (Regulation n. º 7/2017, 2nd March concerning *Decreto-Lei* n.º 15/93, 22th January, *in Diário da República*.)

Figura 1.20 Chemical representation of some synthetic cathinones that constitute bath salt as and Mephedrone, Methylone and MDPV (Baumann et al., 2016).

Bath salts can be sold as powder or crystals and can be administered through insufflation, orally, intra-nasally, smoking, rectal and intravenous methods to produce their psychoactive effects (Psychonaut, 2009; Winstock et al., 2011) At low doses of, bath salts can evoke enhanced energy, mood and psychomotor capacity, whereas at high doses or upon a binge-like regimen it might induce hallucinations, psychotic episodes, increased heart rate, high blood pressure, hyperthermia and violent behaviors (Prosser et al., 2012; Ross et al., 2012). Additionally, "excited delirium" has also been described and includes higher body temperature, delirium, agitation, breakdown of muscle tissue, and kidney failure and even death (Kesha et al., 2013; Penders et al., 2012).

Growing body of evidence supports that neurochemical effects of synthetic cathinones are dependent upon on two different mechanisms: the first one is the inhibition of monoamines reuptake through blockade of monoamine transporters (blockers), such as cocaine, whereas the second one is based on monoamines release by transporter-mediated exchange reverse transport (substrates), such as methamphetamine. (Rothman et al., 2001). Compounds reported in bath salts can act either as cocaine-like monoamine reuptake inhibitors, methamphetamine-like releasers, or a hybrid of both mechanisms (Nagai et al., 2007; Baumann et al., 2012; Martinez-Clemente et al., 2012)

MDPV displays a novel pharmacological profile when compared to other synthetic cathinones as it is a potent uptake blocker at DAT and NET with no measurable substrate activity (Angoa-Pérez et al., 2017; Baumann et al., 2016). When compared to the prototypical transporter blocker cocaine, MDPV was 50-fold more potent at DAT, 10-fold more potent at NET, and 10-fold less potent at SERT (Angoa-Pérez et al., 2017). Consistently, it was shown that MDPV increases extracellular levels of DA in the brain (Baumann et al. 2016, Schindler et al., 2016). This is likely to underlie its locomotor stimulant and addictive properties (López-Arnau et al., 2012). As an example, Huang et al. (2012) showed that repeated doses of MDPV induced the need of higher intake of MDPV, hence fueling tolerance and addiction with consequent increased likelihood of *overdosing.* (Huang et al., 2012)

Baumann et al. (2016) summarized MDPV pharmacokinetics profile: MDPV reaches peak plasma concentrations 10–20 min when injected into rats (0.5–2.0 mg/kg), and declines quickly thereafter. Furthermore, motor activation produced by the drug is positively correlated with plasma concentrations of parent drug and not its metabolites [3,4-dihydroxypyrovalerone (3,4-catechol-PV) and 4-hydroxy-3- methoxypyrovalerone (4-OH-3-MeO-PV)]. (Baumann et al., 2016)

Thus far, some of the benchmarks used to gauge the neurotoxicity induced by amphetamines include disruption of monoaminergic neurotransmitters and glial alterations. However, there is scarce information on the impact of MDPV on these parameters in animal models. Intriguingly, Anneken et al. (2015) suggested that MDPV is not neurotoxic and prevented methamphetamine-induced striatal neurotoxicity. (Anneken et al., 2015) This assumption warrants further clarification. Moreover, emotional parameters associated with MDPV consumption are far from being elucidated.

1.3. Aims and Thesis outlines

This present thesis aimed to characterize, for the first time, the impact of MDPV on frontal cortex glial cells and innate immune players including receptor for advanced glycation end-products (RAGE) and its ligand S100β, within first 24 hours following a binge MDPV regimen. In addition, emotional behavior was assessed. A binge neurotoxic regimen of METH was also employed to deepen current knowledge on METH neurotoxicity.

Chapter 2

Materials and Methods

2.1. Drugs and chemicals

The psychostimulants used herein were the following: metilenedioxipirovalerone hydrochloride (MDPV.HCl) and metanfetamine hydrochloride (METH.HCl). Our laboratory was issued permission to import Methamphetamine-HCl from Sigma–Aldrich (Sigma–Aldrich, St. Louis, USA) by INFARMED, Portugal (National Authority for approval of Medicines and Health Products). MDPV was kindly gifted by Prof. Félix Carvalho (UCIBIO, REQUIMTE - Laboratory of Toxicology, Department of Biological Sciences, Faculty of Pharmacy, University of Porto, Portugal). All other chemicals (ultrapure and pro analysis quality) were purchased from Sigma-Aldrich and Merck AG (Darmstadt, Germany) and Santa-Cruz Biotecnology.

2.2. Animals

In the present work, male C57BL/6 mice with 10 weeks old and weighing 20-30g (Charles River Laboratories, Barcelona, Spain) were housed four per cage, under controlled environmental conditions. Such conditions included a 12 hour of light/dark cycles at room temperature (RT) of 22 ±1°C, with food and water supplied *ad libitum.* All experiments were approved by the Institutional Animal Care and Use Committee from Faculty of Medicine, Coimbra University, and were conducted according to the European Community directive (2010/63/EU) as well as with ARRIVE guidelines. (Kilkenny et al, 2010). Additionally, animal procedures were performed in strict accordance with the "Guide for the Care and Use of Laboratory Animals" (Institute of Laboratory Animal Resources, National Academy Press 1996). All efforts were made to minimize animal suffering and to reduce the number of used animals.

2.3. Drug Administration

Animals were randomly divided into three different groups and injected intraperitoneally (i.p.) with four injections of 10mg/kg METH (n= 9) or MDPV (n= 8) or saline solution, 0.9% de NaCl, SAL (n=9), every two hours, in volumes of 0.1 mL/10 g (body weight), as described by Fantegrossi and colleagues (2013). The MDPV regimen used herein compared with a well characterized METH binge regimen in terms of neurotoxicity and behavioral changes (Moratalla et al. ,2017). Furthermore, behavioral tests were conducted approximately 18 hours after last injection. Also, mice were sacrificed within 24 hours after last injection for subsequent molecular assays, as seen in the experimental design bellow **(Figure 1).** This time-point (24 hours) was

chosen since we aimed to evaluate innate immune players, glial changes and behavioral alterations while neurotoxic phenomenon unravels.

Noteworthy, animals were grouped into three independent cohorts of animals. The first two sets of animals, n=18, (n =6 SAL; n = 7 METH; n =5 MDPV) were sacrificed by decapitation and the whole brains were removed from the skull with the aid of blunted curved forceps. Frontal Cortex was dissected on a cold plate and immediately frozen in liquid nitrogen and stored at -80°C (Glowinski & Iversen, 1966) The right hemispheres of frontal cortices of each experimental group were stored in RNA *later* RNA stabilization Reagent (QiaGen, GmbH Hilden) for subsequent RNA extraction followed by RT-qPCR analysis. On the other hand, the left hemispheres were processed for Western Blot (WB) analysis. Next, the third set of animals, n=8, (n=3 SAL; n=2 METH; n=3 MDPV) was deeply anesthetized with 100mg/kg pentobarbital and transcardially perfused with 0.1 M phosphate buffer saline pH 7.4 (PBS) followed by 4% paraformaldehyde (PFA) in 0.1 M PBS. Finally, brains were removed, post-fixed for 24 h in 4% paraformaldehyde and dehydrated in 30% sucrose in 0.1 M PBS for 24 h for subsequent immunohistochemistry (IHC) analysis.

It is also relevant to note that we focused our study on frontal cortex because it is a rich dopaminergic region and is associated with mood conditions such as depressive-like behavior (Krishnan and Nestler, 2010).

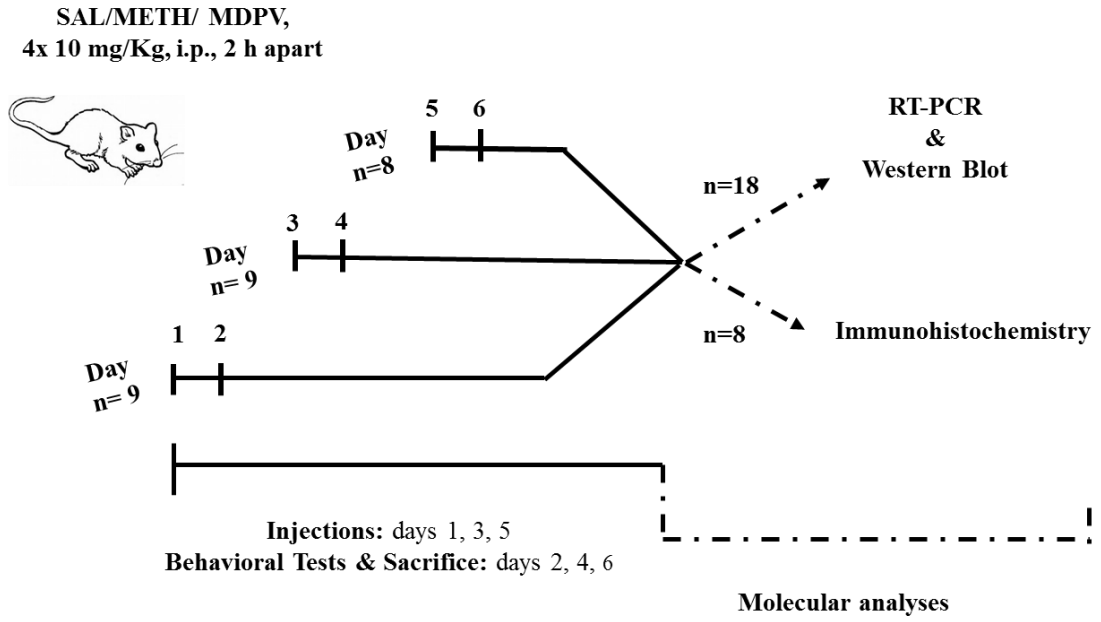

Figure 2.1 Experimental study design performed for METH and MDPV binge drug regimen.

2.4. Behavioral analysis

Within 24 hours after i.p. injection of METH or MDPV or SAL (4 x 10 mg/kg), behavioral tests were conducted in three independent cohorts of animals. All tests were carried out between 9:00 and 15:00 h in a sound-attenuated room under low-intensity light (12 lx) and they were scored by the same rater in an observation room where the mice had been habituated for at least 1 h before the beginning of the tests. Behavior was monitored by a video camera positioned above the apparatuses and the images were later analyzed with the ANY Maze video tracking (Stoelting Co., Wood Dale, IL, USA) by an experienced researcher who was unaware of the experimental group of the animals tested.

2.4.1. Elevated Plus Maze

Elevated plus maze (EPM) probed anxiety-like behavior associated with the use of MDPV and METH. A four-arm apparatus was used consisting of two open and two other closed arms (29,5 cm of length and 6 cm of width). Each animal was placed in the center of the apparatus, facing an open arm, and its exploratory behavior measured during 5 min. All four paws placed on an arm qualified as an entry. The following parameters were evaluated: time spent and the number of entries into open arms and total number of entries in the four arms. The total number of entries in the four arms was used as a measure of locomotor activity. The maze was wiped clean with 10% ethanol between trials (Fonseca et al., 2017).

2.4.2. Open-field test

Open-field (OF) test assessed locomotor and exploratory activity following MDPV and METH injection. Mice were placed in the center of an unexplored arena (45x45 cm) during 15 minutes. The following parameters were scored: total distance travelled (meters) (5 and 15 minutes), rearing number and rearing time (seconds) (5 minutes) (Coelho et al. 2014). The Open field was wiped clean with 10% ethanol between trials (Fonseca et al., 2017).

2.4.3. Splash test

The splash test evaluated grooming behavior following MDPV and METH injection, as an index of self-care and motivational behavior phenotype of experimental groups. This test was performed in each home cage (one mouse at a time) and began after vaporization of a 10% sucrose solution on the dorsal coat of mice. For 5 minutes, grooming time (seconds) was recorded. Grooming parameters scored consisted in nose/face grooming (along the snout), head washing (semicircular movements over the top of the head and behind ears) and body grooming (cleaning of the fur by licking or scratching) (Moretti et al. 2015; Fonseca et al., 2017).

2.4.4. Tail Suspension

Tail suspension test assessed despair-like behavior of mice following MDVA and METH injection. This is a widely used test for characterizing depressive-like behavior in mice (Silva et al. 2014). Briefly, mice were subjected to a short inescapable stress as follows: mice were hanged down by its tail, approximately 50 cm above the flour, using adhesive tape, placed 1 cm from tail tip. Immobile state, characterized by a motionless state, was recorded for 6 minutes (Steru et al. 1985).

2.5. Real-Time Quantitative PCR (RT-qPCR)

RNA was isolated from right frontal cortices according to protocol from Recover All™ Total Nucleic Acid isolation kit (AM1975, Alfagene), as previously performed by Viana and collegues (Viana et al. 2016). Total amounts of RNA extracted, RNA integrity (RIN, RNA Integrity Number) and purity (A260/A280) were measured by RNA Nano Chip kit in Agilent 2100 Bioanalyzer (2100 expert software, Agilent Technologies, Walbronn, Germany) and ND-1000 spectrophotometer (NanoDrop Technologies, Wilmington, DE, USA), respectively. RNA was reverse transcribed with Transcriptor Universal cDNA Master (Roche Diagnostics, Mannheim, Germany): one microgram of total RNA was mixed with a 5x Transcriptor Universal Reaction Buffer and 20x Transcriptor Universal Reverse Transcriptase (Roche Diagnostics) in a total reaction volume of 20 uL. Afterwards, reactions were carried out in a thermocycler Eppendorf vapo.protect with the following thermal profile: 5 min at 25°C, 10 min at 55°C and 5 min at 85°C. Gene expression was performed by Real Time quantitative Polymerase chain

Reaction (RT-qPCR) using LightCycler 480 II system (Roche Diagnostics). RT-qPCR amplification of S100□, RAGE and endogenous controls 18SrRNA used optimized primers from Real time ready catalog assays (Cat. No 315571, 31148 and 300236, respectively, Roche Diagnostics) and LightCycler® 480 Probes Master 2x (Roche Diagnostics), according to manufacturer's instructions. The primer mouse sequences used were as follows: RAGE, 50-GTC AGCATCAGGGTCACAGA-30 (forward) and 50-AAGGCCAGGG CTAGCGTA-30 (reverse); S100β, 50-AACAACGAGCTCTCTC ACTTCC-30 (forward) and 50-CTCCATCACTTTGTCCACCA-30 (reverse); 18SRNA, 50-GCAATTATTCCCCATGAACG-30 (forward) and 50-GGGACTTAATCAACGCAAGC-30 (reverse). Non-template control reactions were performed for each gene, in order to assure that there was no unspecific amplification. RT-qPCR results were analyzed with qbase+ software (Biogazelle, Gent, Belgium). The relative expression ratio of each of the target genes was computed based on its real-time PCR efficiencies (E) and the crossing point difference (ΔCq) for an unknown sample versus a control ($E^{\Delta Cq}$ method). Results were obtained in normalized relative quantities and then converted to percentage using control group as reference.

2.6. Western Blot analysis

Left frontal cortices were used for total protein extracts as previously described (Simões et al. 2008; Viana et al. 2016). Total tissue was homogenized in lysis buffer (50 mM TrisHCl pH 7.4, 0.5% Triton X-100) containing protease inhibitor cocktail [1 mM PMSF, 1 Mm DTT, 5 μg/mL CLAP (5 μg/mL chymostatin, 5 μg/mL leupeptin, 5 μg/mL antiparin, 25 mg/mL pepstatin, - Sigma-Aldrich]. Afterwards, total protein concentration was determined by the bicinchoninic acid (BCA) protein assay (Pierce Biotechnology, Rockford, IL, USA). Protein amounts **(Table 2.1**) were separated using 8–15% sodium dodecyl sulfate–polyacrylamide gel electrophoresis (SDS-PAGE) and electrophoretically transferred to a polyvinylidene difluoride membrane (Merck Millipore, Madrid, Spain) and blocked by 5% defatted milk for 2 hours (Silva et al. 2014). Membranes were incubated overnight at 4°C with primary antibodies **(Table 2.1)**. Membranes were then incubated with alkaline phosphatase-conjugated IgG secondary antibodies (**Table 2.1**). Finally, membranes were visualized on Typhoon FLA 9000 (GE Healthcare) and analyzed using Image Studio™ Lite Software (LI-COR Corporate Offices - US, Inc., Lincoln, Nebraska, USA).

Results were normalized against internal controls β-actin (1:1000; A5316,) and then expressed as percentage of control.

Table 2.1 List of primary and secondary antibodies used in western blot analysis.

Primary Antibody	*Dilution*	*Protein amount (µg)*	*Reference*	*Secondary Antibody*	*Dilution*	*Reference*
Rabbit anti-RAGE	1:500	40	Ab3160, Abcam	Goat anti-rabbit	1: 5000	GE Healthcare, Little Chalfont, UK
Goat anti-RAGE	1:200	40	Sc-8230, Santa-Cruz Biotecnology	Donkey anti-goat	1: 5000	Sc-2022, Santa-Cruz Biotecnology
Mouse anti-GFAP	1:2000	10	IF03L, Merck Millipore	Goat anti-mouse	1: 5000	GE Healthcare, Little Chalfont, UK
Rabbit anti-MBP	1:500	30	Ab40390, Abcam	Goat anti-rabbit	1:5000	GE Healthcare, Little Chalfont, UK
Rabbit anti-TH	1:1000	20	AB152, Merck Millipore	Goat anti-rabbit	1: 5000	GE Healthcare, Little Chalfont, UK

2.7. Immunohistochemistry

Frontal cortex anatomical limits were identified (AP, +1.32 to +0.5 mm) by the use of a mouse brain atlas (Paxinos and Frankling 2004), being the following protocol performed as previously described by Viana and colleagues (Viana et al. 2016). Cortical coronal sections of 40 µm thickness were obtained from cryostat (Leica CM3050S, Nussloch, Germany) in 0.1 M PBS and used for free-floating immunohistochemistry. Firstly, slices were washed twice with 0.1 M PBS, blocked with 0.25% Triton X-100 and 5% normal fetal bovine serum (FBS) in 0.1 M PBS for 1 h at room temperature, and secondly slices were incubated for 24 h at 4°C with the primary antibodies reported in **Table 2.2**. Afterwards, sections were rinsed with 0.1 M PBS (3 x 10 min) and incubated with 4´,6-diamidino-2-phenylindole (DAPI; 1:200; D1306, Invitrogen, Carlsbad,

CA, USA) for nuclear staining and the secondary fluorescent antibodies for 2 hours at room. In the end, sections were rinsed with 0.1 M PBS (3 x 10 min), so as to mount with glycergel (Dako mounting medium). Samples were imaged using a confocal laser scanning microscope (LSM 710 Meta, Carl Zeiss, Gottingen, Germany), in which lenses amplifying 40x and 10x were employed. Herein, we draw your attention to three particular areas within frontal cortex, namely, cingulate cortex, area 1 (Cg 1), cingulate cortex, area 2 (Cg 2), and secondary motor cortex (M2) (**Figure 2.2**). Moreover, for presentation purposes, we will show areas in which immunofluorescence is representative for each group.

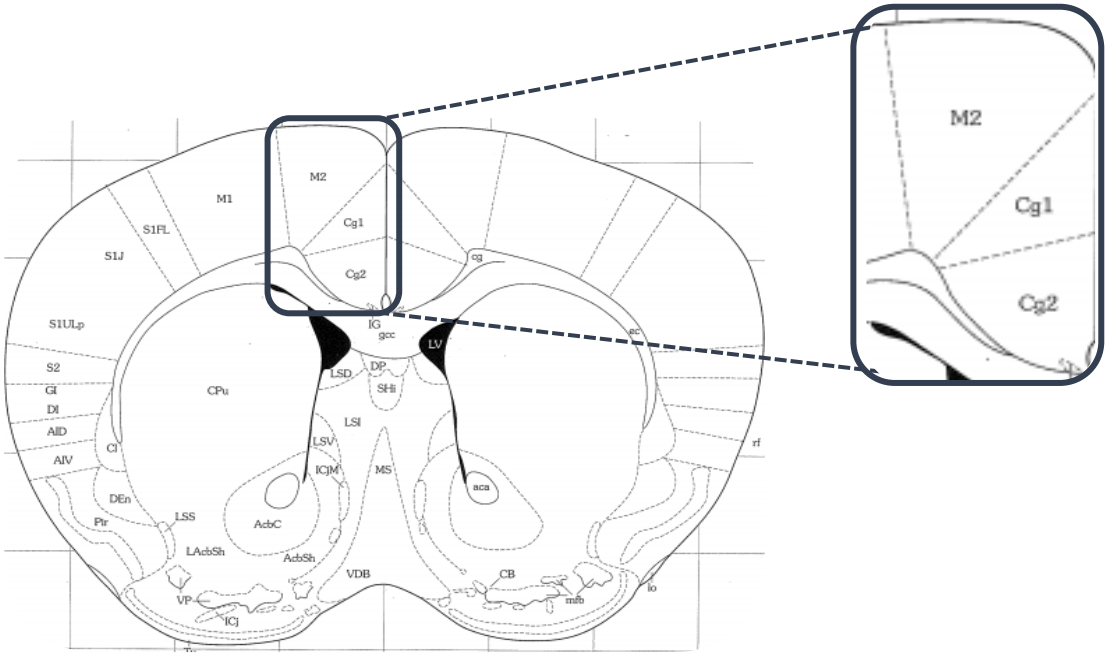

Figure 2.2 Drawing of a coronal section at +0.98 mm anterior from Bregma depicting the diverse areas in mice brain, with particular focus on cingulate cortex, area 2 (Cg 2), cingulate cortex, area 1 (Cg 1), and secondary motor cortex (M2), which are highlighted at the inset at the right-hand side (Paxinos and Frankling 2004).

Table 2.2 List of primary and secondary antibodies used in Immunohistochemistry analysis.

Primary Antibody	*Dilution*	*Reference*	*Secondary Antibody*	*Dilution*	*Reference*
Rabbit anti-RAGE	1:500	Ab3160, Abcam	donkey anti-rabbit Alexa Fluor 594	1: 1000	Invitrogen, Carlsbad, CA, USA
Goat anti-RAGE	1:100	Sc-8230, Santa-Cruz Biotecnology	donkey anti-goat Alexa Fluor 488	1: 1000	Invitrogen, Carlsbad, CA, USA
Rabbit anti-s100β	1:500	ABN59, Merck Millipore	donkey anti-rabbit Alexa Fluor 594	1:1000	Invitrogen, Carlsbad, CA, USA
Mouse anti-GFAP	1:100	IF03L, Calbiochem	donkey anti-mouse Alexa Fluor 488	1: 1000	Invitrogen, Carlsbad, CA, USA
Rabbit anti-iba-1	1:250	019-19741, Wako	donkey anti-rabbit Alexa Fluor 594	1: 1000	Invitrogen, Carlsbad, CA, USA
Rabbit anti-MBP	1:1000	Ab40390, Abcam	goat anti-rabbit Alexa Fluor 488	1:1000	Invitrogen, Carlsbad, CA, USA
Rabbit anti-TH	1:250	AB152, Merck Millipore	goat anti-rabbit Alexa Fluor 488	1: 1000	Invitrogen, Carlsbad, CA, USA

2.8. Statistical analysis

Results are presented as mean values ± standard error of mean (S.E.M.). Data concerning to molecular and behaviour tests were analysed by a one-way ANOVA followed by Tukey´s *post hoc* multiple comparison test, or by Kruskal-Wallis followed by Dunn's *post hoc* test. All tests were considered significant at $P < 0.05$ (*/$^{\#}$), $P < 0.01$ (**/$^{\#\#}$) and $P < 0.001$ (***/$^{\#\#\#}$). The symbol * refers to a comparison between each drug and SAL and # refers to a comparison between MDPV and METH. Analyses were performed using GraphPad Prism 6.01 software for Windows (GraphPad Software, San Diego, CA, USA, www.graphpad.com).

Chapter 3

Results

3.1. Behavioral consequences of METH and MDPV administration to mice

Considerable body of evidence has described locomotor and emotional alterations underpinning METH ab(use). However, the impact of the psychostimulant MDPV on emotional behavior has yet to be characterized. In this context, behavioral tests were conducted to assess the influence of a binge dosage of MDPV, in comparison with a binge dosage of METH, in emotion and locomotor parameters in 10-weeks-old male adult C57BL/6J mice.

First, anxiety-like mood was addressed by the use of Elevated Plus Maze. Both METH and MDPV did not significantly change time spent in open arms (**Figure 3.1b**; $P > 0.05$ vs SAL). However, there was a significant increment in the number of METH-mice entries into open arms (**Figure 3.1a**; $^{**}P < 0{,}01$ vs SAL). In addition, METH-mice but not MDPV-mice, showed a statistically significant reduction in the total number of arm entries (**Figure 3.1c**; $^{**}P < 0{,}01$ vs SAL; $^{\#}P < 0{,}05$ vs MDPV). Together, these observations suggest that METH and MDPV exerted no anxiogenic-like behavior in mice. Additionally, these data led us to speculate whether METH, but not MDPV, elicited locomotor deficits.

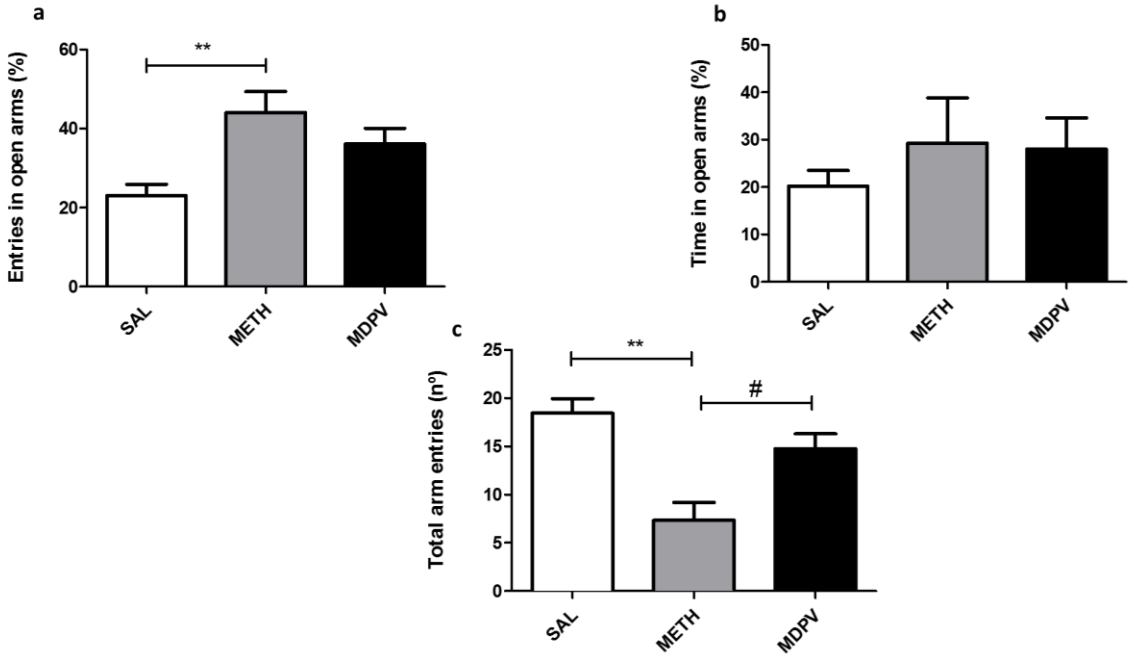

Figure 3.1 Impact of METH and MDPV on anxiety-like behavior in mice (Elevated Plus Maze test). Effects of METH and MDPV (4 x 10 mg/kg, i.p., 2-hours apart) in mice on (**a)** the entries in open arms (%), on (**b**) the time spent in open arms (%), and on **(c)** total arm entries (nº), within 24 hours post-injection. Data are presented as mean % of control ± S.E.M (n=8-9) and was considered significant at ***P* <0.01; vs SAL; #*P* <0.05; vs METH. Statistical analysis was performed Kruskal-Wallis followed by Dunn's *post hoc* test (**a, b**), or by one-way ANOVA followed by Tukey´s *post hoc* multiple comparison test (**c).**

Locomotor profile of mice was further elucidated by using Open Field test. Our findings indicated a statistically significant decrease in total distance traveled (meters) in the METH group, but not in the MDPV group, further confirming locomotor deficits in METH-mice (**Figures 3.2a, b).** Figure 2c illustrates a representative track plot for each experimental group during the first 5 minutes.

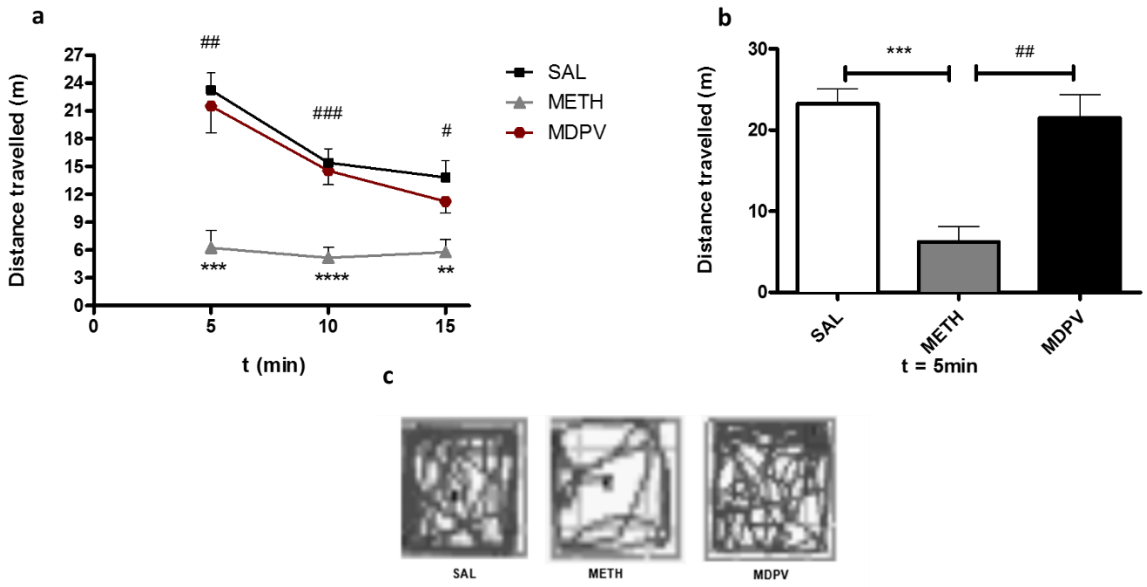

Figure 3.2 Impact of METH and MDPV on locomotor behavior in mice (Open Field test). Effects of METH and MDPV (4 x 10 mg/kg, i.p., 2-hours apart) in mice on distance travelled during 15 minutes (m) and during first 5 minutes (**a, b**), within 24 hours post-injection. **c** represents a schematic track plot of the path made by the three groups of mice in a 5 minute-test. Data are presented as mean % of control ± S.E.M (n=8-9) and was considered significant at ***P* <0.01; ****P* <0.001; *****P* <0.0001 vs SAL; #*P* <0.05; ##*P* <0.01; ###*P* <0.001 vs METH. Statistical analysis was performed by Kruskal-Wallis followed by Dunn's *post hoc* test in 5 minute-test in (**b)** as well as in **(a)**, and, by One-way ANOVA followed by Tukey´s *post hoc* test in 10 and 15 minute-test, (**a)**.

Furthermore, mice exploratory behavior was also addressed with Open Field. METH and MDPV displayed opposite effects on rearing behavior: while METH decreased number of rearings and rearing time, MDPV showed increased rearing behavior (**Figure 3.3a, b**). These data suggest that MDPV increases exploratory behavior. The decrease in rearing behavior in METH-mice might be shadowed by a decrease in general locomotor behavior in these mice.

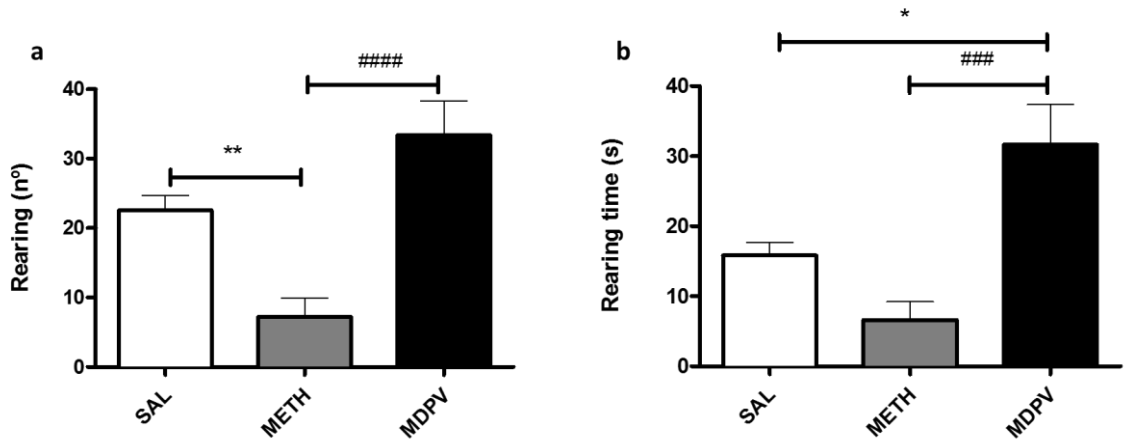

Figure 3.3 Impact of METH and MDPV on exploratory activity in mice (Open Field test (5 minutes)). Effects of METH and MDPV (4 x 10 mg/kg, i.p., 2-hours apart) in mice on **(a)** number of rearings, and on (**b)** rearing time (s), within 24 hours post-injection. Data are presented as mean % of control ± S.E.M (n=8-9) and was considered significant at **P* <0.05; ** *P* <0.01 vs SAL; $^{\#\#\#}P$ <0.001; $^{\#\#\#\#}P$ <0.0001vs METH. Statistical analysis was performed by One-way ANOVA followed by Tukey´s *post hoc* test (**a**), and by Kruskal-Wallis followed by Dunn's *post hoc* test (**b).**

We consolidated emotional characterization by evaluating depressive-like alterations in mice using both tail suspension test and splash test. METH, but not MDPV, significantly increased immobility time in tail suspension test **(Figure 3.4a;** ***P* <0,01 vs SAL; $^{\#\#\#}P$ <0,001 vs MDPV). Again, the general locomotor impairment triggered by METH might contribute to this effect. Additionally, no significant changes were observed in mice grooming in both METH and MDPV groups (**Figure 3.4b***; P* >0,05). This is suggestive that there are no self-care and motivational behavior alterations in place.

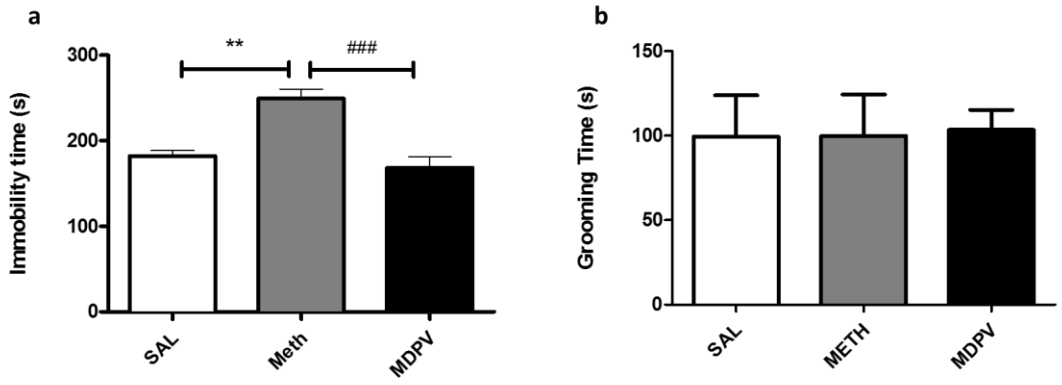

Figure 3.4 Impact of METH and MDPV on depressive-like behavior in mice, with Tail Suspension test (a) and Splash test (b). Effects of METH and MDPV (4 x 10 mg/kg, i.p., 2-hours apart) in mice on **(a)** immobility time (s), and on **(b)** grooming time (s) Data are presented as mean % of control ± S.E.M (n=7-9) and was considered significant at $^{**}P$ <0.01 vs SAL; $^{\#\#\#}P$ <0.001 vs METH. Statistical analysis was performed by Kruskal-Wallis followed by Dunn's post hoc test **(a)** and by a one-way ANOVA followed by Tukey´s *post hoc* multiple comparison test **(b).**

3.2. Molecular and glial changes in frontal cortex induced by METH and MDPV administration to mice

3.2.1. Impact of METH and MDPV on dopaminergic terminals

TH levels were not changed in frontal cortices of both METH-and MDPV-mice compared to saline as gauged by immunoblotting (**Figure 3.5a**; P >0,05) and immunofluorescence labeling (**Figure 3.5b**).

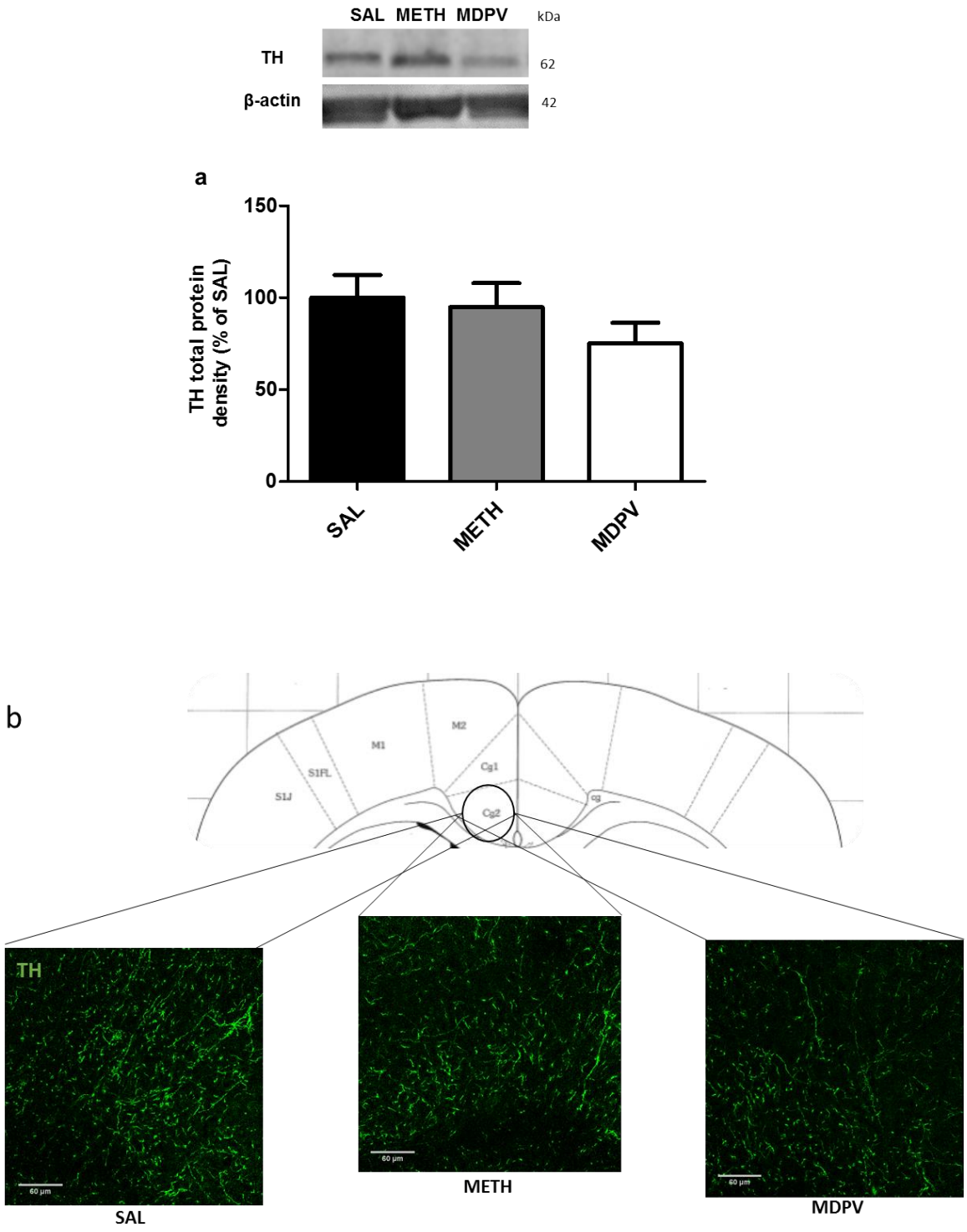

Figure 3.5 Impact of an acute binge dose of METH and MDPV on TH density in mice frontal cortices. TH density was evaluated by western blot, expressed as mean % of control ± S.E.M (n=5-7) **(a),** and by immunofluorescence (n=2-3) **(b),** 24 h post-injection of METH and MDPV (4 x 10 mg/kg, i.p. 2-hours apart). Statistical analysis was performed by Kruskal-Wallis followed by Dunn's post hoc test (**a**). In

(**b**) illustrative imagens of immunofluorescence of dopaminergic fibers through TH staining (green), particularly in cingulate cortex, area 2 (Cg 2), are shown. *Scale bars* = 60 µm.

3.2.2. Impact of METH and MDPV on innate immune players in frontal cortex

3.2.2.1. Impact of METH and MDPV in RAGE and S100β density

Firstly, RAGE biology was characterized. This is a pattern-recognition receptor which is operative in the innate immune system. RAGE gene expression was analyzed by RT-qPCR. RAGE mRNA levels were not significantly changed by both drugs when compared to saline (**Figure 3.6a**; P >0,05). Then RAGE protein levels were assessed. To this end, total C-terminal and N-terminal RAGE terminally truncated isoforms density were analysed to dissect the complex proteomic of RAGE variants. We used an antibody raised against C-terminal, intracellular domain of RAGE (anti-C-terminal RAGE Ab) that revealed immunoreactivity at 50, 45 and 37 kDa, which probably reflect monomeric flRAGE, pre-glycosylated flRAGE/N-truncated isoforms and a proteolytic product of RAGE, respectively. Neither METH nor MDPV changed RAGE density, when quantifying all obtained bands (**Figure 3.6b, c**; P >0,05). Also, the absence of alterations was verified when quantifying each band individually (data not shown). RAGE proteomic analysis was further performed by immunohistochemistry.

In saline mice, RAGE was predominantly found in cytosol, when labeling was performed with anti-N-terminal RAGE Ab (**Figure 3.6d**). In, contrast, cells displayed RAGE immunoreactivity in the nucleus and practically no cytoplasmic immunoreactivity when anti-C terminal RAGE Ab was used (**Figure 3.6d**). These distinct immunolabeling patterns were confirmed by the absence of co-localization profile obtained when both anti-RAGE antibodies were used (**Figure 3.6d**). Importantly, again, neither MDPV nor METH changed RAGE immunolabeling pattern as gauged by both RAGE antibodies (**Figure 3.6d**). These observations indicate that neither MDPV nor METH changed RAGE proteomic at this time point at frontal cortex.

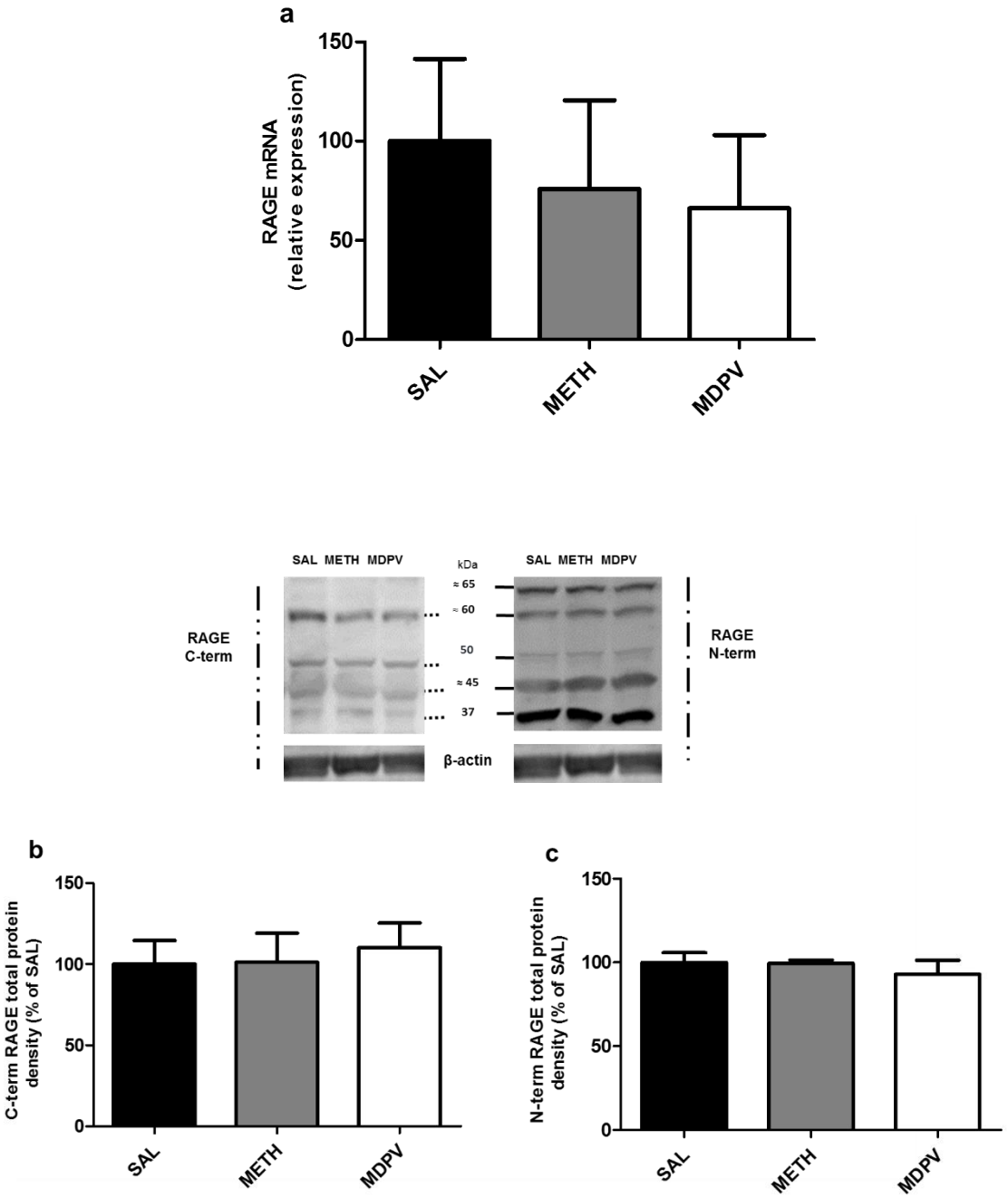
a
RAGE mRNA (relative expression)
150
100
50
0
SAL
METH
MDPV
SAL METH MDPV
kDa
≈ 65
≈ 60
50
≈ 45
37
β-actin
SAL METH MDPV
RAGE C-term
RAGE N-term
b
C-term RAGE total protein density (% of SAL)
150
100
50
0
SAL
METH
MDPV
c
N-term RAGE total protein density (% of SAL)
150
100
50
0
SAL
METH
MDPV

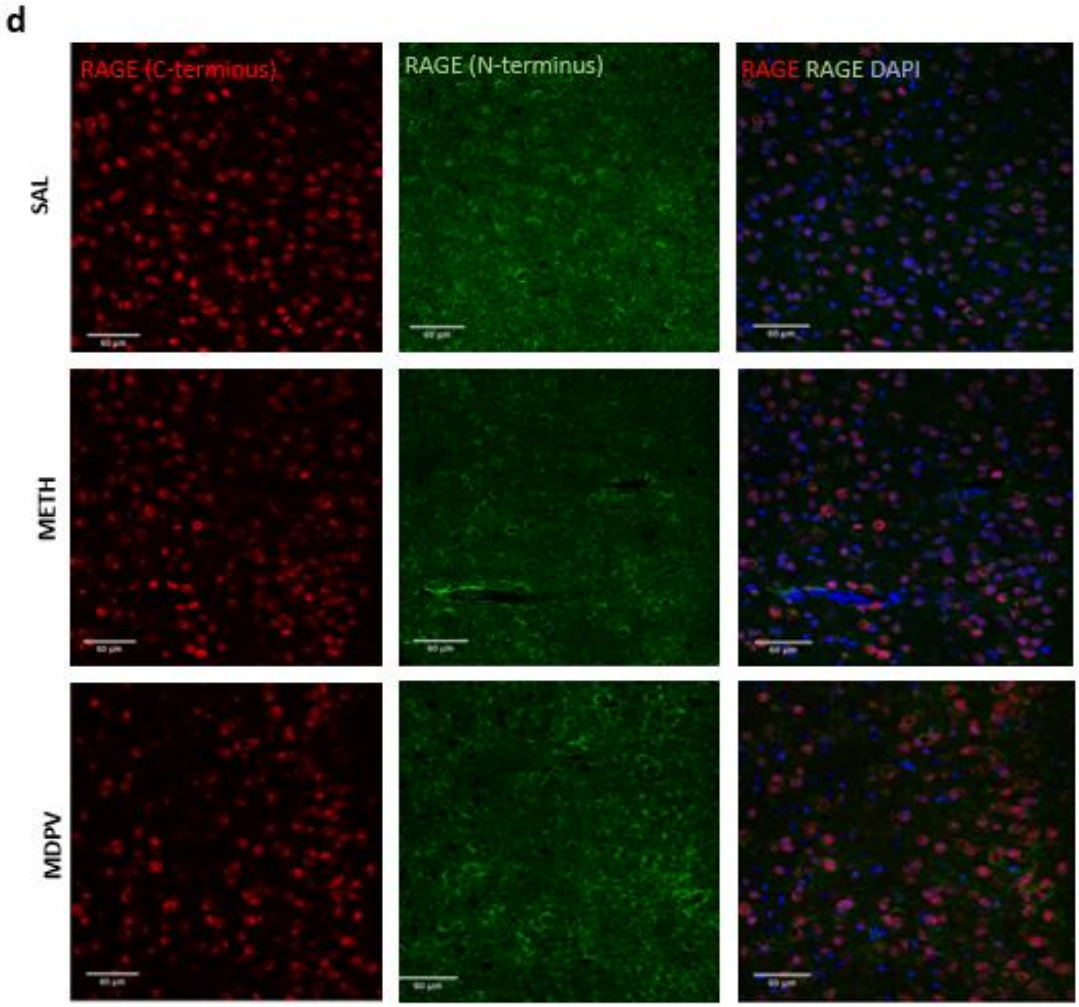

Figure 3.6 Influence of an acute binge dose of METH and MDPV on receptor RAGE gene expression and protein density in frontal cortex. RAGE mRNA quantification (**a),** RAGE protein levels (**b, c**), and its cellular distribution (**d, e**) were assessed 24 h post-injection of METH and MDPV (4 x 10 mg/kg, i.p. 2-hours apart). Above, RAGE mRNA quantification by RT-PCR**,** expressed as mean % of control ± S.E.M (n=4-5) (**a**). Representative quantification by western blot of RAGE protein with polyclonal rabbit anti-RAGE C-terminal antibody**,** expressed as mean % of control ± S.E.M (n=5-7) (**b**), and polyclonal anti-RAGE N-terminal antibody**,** expressed as mean % of control ± S.E.M (n=2-4) (**c**) are shown. In (**d)**, illustrative imagens of immunofluorescence (n=2-3), particularly in cingulate cortex, area 2 (Cg 2), are shown (RAGE C-terminus (red), RAGE N-terminus (green) and nuclei stained with DAPI (blue)). *Scale bars* = 60 µm. Statistical analysis was performed by Kruskal-Wallis followed by Dunn's post hoc test (**a, b, c**).

Secondly, we aimed to characterize the impact of both MDPV and METH in s100β, which acts as a DAMP (dangerous-associated molecular pattern) and is a well-known RAGE ligand. S100β gene expression was not significantly changed by any of the tested drugs (**Figure**

3.7a; *P* >0,05). S100β protein levels were assessed by immunofluorescence and no statistically significant alterations in S100β immunolabeling were detected between groups (**Figure 3.7b, c**; *P* >0,05).

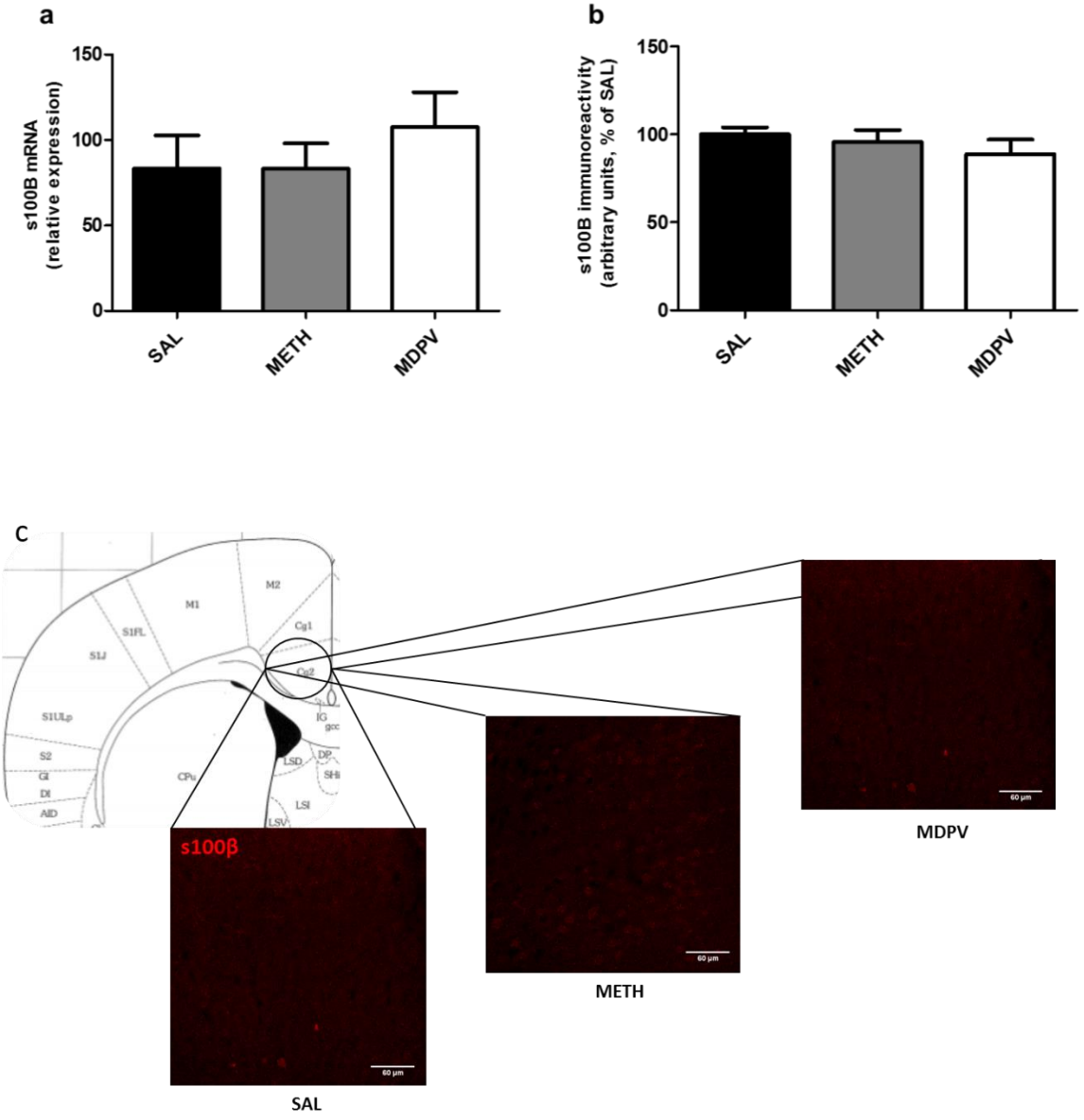

Figure 3.7 Influence of an acute binge dose of METH and MDPV on s100β gene expression and protein levels in frontal cortex. S100β mRNA quantification was assessed by RT-PCR, expressed as mean % of control ± S.E.M (n=5-7) (**a),** S100β density by immunofluorescence, expressed as mean % of control ± S.E.M (n=2-3) (**b**), 24 h post-injection of METH and MDPV (4 x 10 mg/kg, i.p. 2-hours apart). In (**c**) illustrative imagens of S100β immunostaining (red), particularly in cingulate cortex, area 2 (Cg 2),

are shown. *Scale bars* =60 µm. Statistical analysis was performed by Kruskal-Wallis followed by Dunn's post hoc test (**a),** or by One-way ANOVA followed by Tukey´s *post hoc* test, **b**).

3.2.3. Impact of METH and MDPV in glial cells

Several lines of evidence have demonstrated that METH consumption has implications on microglia and astrocytes that belong to brain innate immune system. However, the effects of MDPV in glial cells was never studied. The influence of MDPV and METH in microglia, astrocytes from frontal cortices in mice was also assessed. Both MDPV and METH did not significantly change Iba-1, GFAP density, as seen by western blot analysis and confirmed by immunofluorescence (**Figures 3.8, 3.9;** *P* >0,05). Additionally, the impact of MDPV and METH in cortical myelin fibers was evaluated. Again, both MDPV and METH did not significantly change MBP density, as seen by western blot analysis, in which, all obtained bands were quantified (**Figures 3.10a;** *P* >0,05) and each band was individually quantifying (data not shown), as well. Such assumption was thereafter confirmed by immunofluorescence.

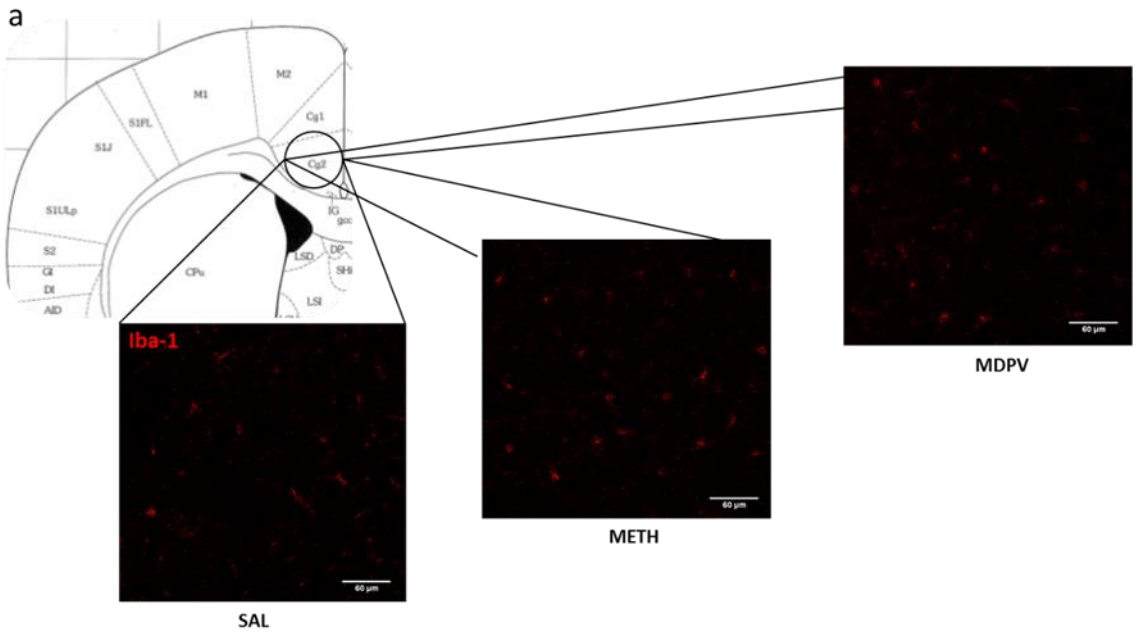

Figure 3.8 Influence of an acute binge dose of METH on Iba-1 immunolabeling in frontal cortex. Iba-1 density was evaluated by immunofluorescence (red), particularly in cingulate cortex, area 2

(Cg 2), (n=2-3) (**a**), 24 h post-injection of METH and MDPV (4 x 10 mg/kg, i.p. 2-hours apart). *Scale bars* = 60 µm.

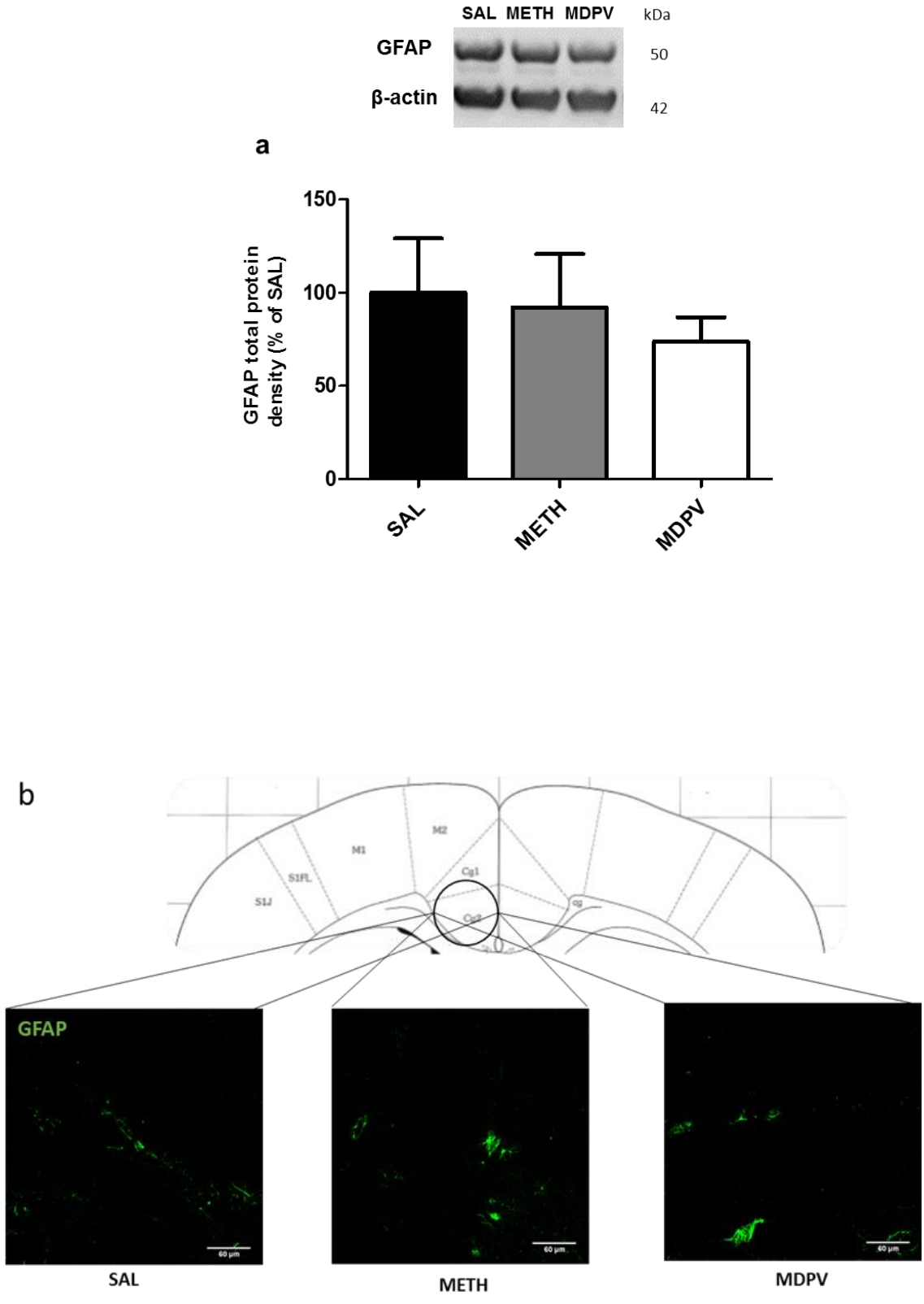

Figure 3.9 Influence of an acute binge dose of METH on GFAP levels in frontal cortex. GFAP density was evaluated by western blot, expressed as mean % of control ± S.E.M (n=5-7) **(a),** and by immunofluorescence (n=2-3) **(b),** 24 h post-injection of METH and MDPV (4 x 10 mg/kg, i.p. 2-hours apart). Statistical analysis was performed by Kruskal-Wallis followed by Dunn's post hoc test (**a**) In (**b**), illustrative imagens of GFAP immunostaining (green), particularly in cingulate cortex, area 2 (Cg 2), are shown *Scale bars* = 60 μm.

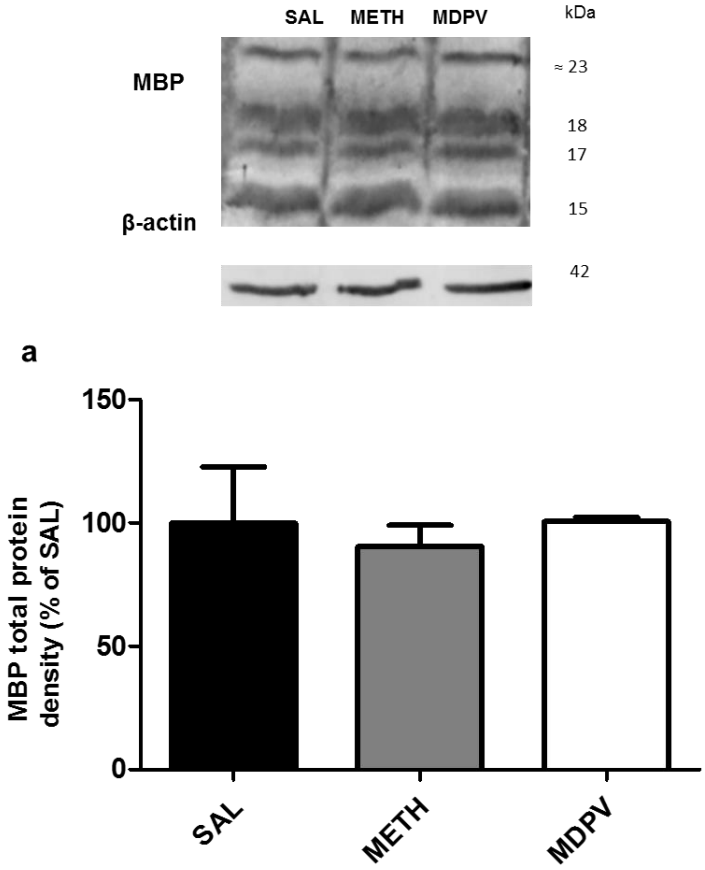

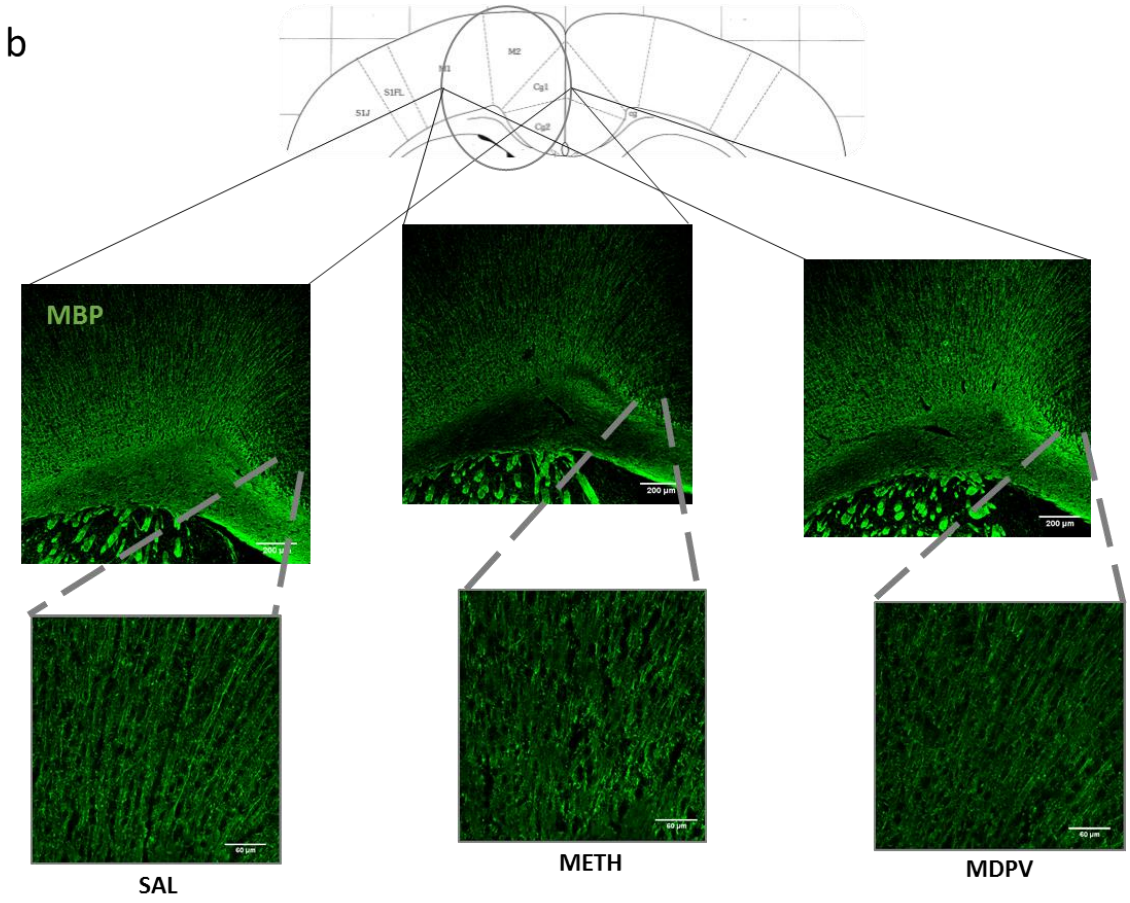

Figure 3.10 Influence of an acute binge dose of METH on MBP levels in frontal cortex. MBP density was evaluated by western blot, expressed as mean % of control ± S.E.M (n=4-6) **(a),** and by immunofluorescence (n=2-3) **(b),** 24 h post-injection of METH and MDPV (4 x 10 mg/kg, i.p. 2-hours apart). Statistical analysis was performed by Kruskal-Wallis followed by Dunn's post hoc test (**a**) In (**b**), illustrative imagens of MBP immunostaining (green), particularly in cingulate cortex, area 2 (Cg 2), are shown. *Scale bars* = 200 µm (pictures at the top); 60 µm (pictures at the bottom).

Chapter 4

Main findings and discussion

4.1. Main findings and discussion

Nowadays, drug misuse and addiction, including METH addition, is a major worldwide issue with an undeniable impact on public health, human rights and security (UNODOC, 2017). In parallel, the rapid emergence and abuse of new psychoactive substances (NPS) regarding the synthetic cathinone, Methylenedioxypyrovalerone (MDPV), known as "bath salt", clearly seems to worsen this scenario (Baumann et al. 2016). Nevertheless, there is currently sparse information regarding MDPV neurotoxicity, including in frontal cortex. Therefore, herein we aimed to characterize, for the first time, the impact of MDPV on frontal cortex glial cells and innate immune players including receptor for advanced glycation end-products (RAGE) and its ligand S100β, within first 24 hours following a binge MDPV regimen. In addition, emotional behavior was assessed. A binge neurotoxic regimen of METH was also employed to deepen current knowledge on METH neurotoxicity.

METH is implicated in dopaminergic system alterations and in emotional impairment including depressive-like behavior (Krishnan and Nestler, 2010; Silva et al., 2013; Fonseca et al., 2016). Herein, METH animals showed undoubtedly impaired locomotor function, as seen by a robust decrease in the distance travelled in the open field arena. This is consistent with previous findings within 24 hours following a similar METH binge protocol (Boger et al., 2007; Grace et al., 2010; Leitão et al., 2017). This further consolidates our previous findings following 24 and 48 hours post-an acute single dose of 30 mg/kg of METH (Pereira et al., 2012). This locomotor impairment might have shadowed emotional characterization due to a putative carry over effect to other behavioral tests. In fact, one cannot exclude the hypothesis whereby locomotor impairment might have contributed to the increasing immobility time seen in METH animals, in the Tail Suspension test. Although both Leitão et al., (2017) and Fonseca et al., (2016) reported a decrease in grooming time in METH-mice, herein we failed to see alterations in this test in the METH group. Again, locomotor impairment together with low basal grooming activity seen in control animals might contribute to our apparently contradictory result with METH. This locomotor impairment is seemingly transient since we previously showed that at 3 days post-single high METH there were no longer statistical significant differences in distance travelled compared to saline (Fonseca et al., 2016). In spite of locomotor confounds, elevated plus maze test suggested that METH did not apparently induce an anxiogenic-like effect. This is consistent with our previous data (Fonseca et al., 2016).

Surprisingly, the behavioral profile of rodents after a single binge episode of MDPV has not yet been documented so far. Regarding MDPV binging, there is only one work recently published by Philogene and colleagues (2017). These authors verified that rats displayed anxiety-

and depressive-like behavior 48 hours after a chronic MDPV binging paradigm (1 mg/kg MDPV 3 x/day for 10 days) (Philogene-Khalid et al., 2017). We newly show that a single binge MDPV paradigm did not change emotional and locomotor behavior in mice. Although, and interestingly, high MDPV doses (1–20 mg/kg) facilitated the spontaneous locomotor activity in mice within 2 hours after drug administration. In fact, psychomotor stimulants are known to increase locomotor motion in rodents, which is strongly associated with their high addiction potential (Wise and Bozarth, 1987; Calabrese et al., 2008). Moreover, it is plausible that more than 12 hours following the last MDPV administration, locomotor activity returned to basal values. Consistently with our observations, MDPV is reported as a with rapid initial rises in locomotor activity which deteriorated throughout time. (Calabrese et al.,2008; Fischman et al., 1989)

Nonetheless, and interestingly, MDPV enhanced exploratory activity in mice as gauged by an increase in rearing numbers and duration in the Open Field test. In agreement with our results but in a different behavioral assessment, Marusich and colleagues, also verified an increase in exploratory activity, after administration doses ranging from 1 to 30mg/kg, Functional Observational Battery (FOB**)** (Marusich et al., 2012). This increased spontaneous exploratory behavior seemingly outlasts the well-known increase in locomotor activity, which is no longer apparent. In this study, operative neuronal mehanisms underlying this behavioral phenomenon were not evaluated, reinforcing the need to dissected such occurence.

This increase in exploratory behavior is consistent with MDPV-mice portraying normal emotional behavior, for example, mice showing depressive-like behavior tended to exhibit a lower level of exploratory activity (Kalueff et al. 2004). Conversely, METH mice showed a decrease in number and duration of rearings as previously shown by Leitão et al. (2017). This exploratory behavior impairment is aligned with METH-mice also showing a decrease in spontaneous locomotor in the open field arena.

Disruption in dopaminergic structures structures are a well-known hallmark of METH neurotoxicity **(**Krasnova and Cadet 2009; Silva et al., 2013). Also, mesocorticolimbic dopaminergic system, involving dopaminergic projections from ventral tegmental area onto frontal cortex plays a major role in motivation and reward (Phillips et al. 2008; Yim et al. 1980; D´Ardenne et al. 2008). Therefore, frontal cortex is thought to be affected by drugs of abuse (Goldstein & Volkow, 2011). In fact, METH users were reported to display anomalies in the frontal cortical structure and function (for review see Goldstein & Volkow, 2011). Also, MDPV is documented to have a greater potency as a reinforcer compared to cocaine or methamphetamine (Aarde et al., 2013; Watterson et al., 2014) and also, the psychostimulant effects of synthetic cathinones are sugested to be underlined by dopaminergic mechanisms (Simmler et al. 2012). Herein, neither METH nor MDPV significantly changed TH density in mice frontal cortices. Our

group previously showed that a single-high dose of METH (30 mg/kg) evoked DA and TH depletion 3 days following METH-dosing (Silva et al. 2013). This is suggestive that dopaminergic derangements are not yet in place as early as 24 hours post-METH. Importantly, this is the first report showing the impact of MDPV in frontal cortex. It is not surprising that MDPV is not inducing dopaminergic toxicity, considering that MDPV is a non-substrate blocker of the DA transporter and also inhibits reuptake of norepinephrine (Meltzer et al., 2006; Psychonaut et al., 2009), effects that are similar to those produced by cocaine (Rothman et al., 2001). This is in contrast with METH which is a substrate for DAT-mediated uptake. Moreover, MDPV failed to affect striatal dopaminergic markers of neurotoxicity, (DA, DAT or TH expression) in mice 2–3 days following drug administration (Lopez-Arnau et al., 2014; Anneken et al., 2015). However, *in vivo* dopaminergic toxicity data regarding MDPV seems parsimonious and warrants further investigation.

Considering that microglial activation represents an early step in methamphetamine-induced neurotoxicity (Thomas et al., 2004a), we aimed to characterize for the first time the cellular and molecular elements of the innate immune players residing in frontal cortex following MDPV administration. METH effect in the same parameters was also evaluated.

In the first place, we aimed to quantify RAGE expression and levels following MDPV and METH dosing. We measured RAGE mRNA levels by RT-PCR and RAGE protein levels by western blot and immunohistochemistry. Gene expression data revealed that neither MDPV nor METH changed RAGE gene transcription. In order to explore the influence of MDPV and METH on cortical RAGE variants, two different anti-RAGE antibodies raised against extracellular as well as intracellular epitopes were employed. We observed RAGE immunoreactivity in a broad spectrum of molecular weight patterns likely reflecting diverse RAGE isoforms, as previously shown (Viana et al., 2016). Again, neither drug changed RAGE levels. This is highly suggestive that RAGE inhibitory isoforms as well as full-length RAGE were not affected by any tested drug at this time-point. These data were confirmed by immunohistochemistry analysis. We found RAGE immunoreactivity homogeneously distributed in cellular cytoplasm when an antibody raised against the extracellular portion of receptor was utilized. This is consistent with our previous observations in striatum using the same antibody (Viana et al., 2016). On the other hand, a very dense nuclear staining was observed when an antibody raised against RAGE cytosolic tail was employed, in agreement with other reports focused on RAGE expression in rat cortical neurons using an anti-C-terminal RAGE antibody (Greco et al., 2012; Li et al., 2014). Importantly, this RAGE immunolabeling pattern was not altered by both drugs. These data may suggest that there is no RAGE-dependent *immune response deregulation* occurring within 24 hours post-drug administration.

Brain deleterious events have been linked to RAGE ligands, including S100β. This protein plays a crucial role in astrocytes, including cytoskeleton organization and dynamics, astrocytic cell shape as well as migration (Donato et al., 2009). Regarding extracellular functions, S100β can either act as a neurotrophic or neurotoxic molecule, depending on the concentration reached. Herein, S100β mRNA as well S100β levels were not altered by any of the tested drugs. This is, definitely, the first report combining psychostimulants and S100β targeting. This data is suggestive that S100β remains within physiological levels, thus maintaining its neurotrophic properties.

Microglia are a widely described resident macrophages within the CNS, comprising the first line of defense in response to diverse injurious stimuli, including viral infection, neuron injury or exposure to drug abuse. In the absence of a stimuli, they are characterized by a quiescent state, or resting state, but upon certain stimuli, microglia undergo morphological changes resulting in the production and secretion of a plethora of cytokines, chemokines, and neurotoxic factors (Streit et al. 1999; Streit et al. 2002). Moreover, microglial activation is known to be the hallmark as a cellular response related with neuroinflammation (Kreutzberg 1996; Graeber and Streit 2010; Streit 2010; Prinz et al. 2011). Importantly, it was demonstrated that microglial activation represents an early step in methamphetamine-induced striatal neurotoxicity (Thomas et al. 2004b). Furthermore, it was demonstrated that a single high dose of METH (30 mg/kg, i.p.) triggered the activation of microglia in mice hippocampi (Gonçalves et al. 2010). However, neither METH nor MDPV changed Iba-1 immunolabeling, thus suggesting that there were no morphological alterations, and so microgliosis is not in place in frontal cortex at 24 hours post-injection. This is aligned with 20 mg/kg METH (i.p.) having not caused cause a change in proinflammatory cytokine or chemokine expression in the frontal cortex at 12 hours post-dosing (Kelly et al., 2012). Furthermore, these authors argued that only subtle neurotoxic effects of METH have been seen in frontal cortex. As for MDPV, this is the first report looking at microglia. However, further studies are warranted to finely dissect the time-course of putative microglia morphology alterations, if any, following MDPV injection.

It is now accepted that astrocytes, the most abundant glial cell population of the CNS, participate in the local innate immune response triggered by a variety of insults, including neurotoxicity triggerd by methanphetamine (Farina et al. 2007; Zhang et al., 2015). Additionally, these cells express RAGE receptors, similarly to microglia (Viana et al., 2016). Glial fibrillary acidic protein (GFAP) is the hallmark intermediate filament protein in astrocytes (Hol and Pekny, 2015). Astrocytes assume a reactive phenotype following administration of neurotoxins, including drugs of abuse (Hol and Pekny, 2015; Loftis and Janowsky, 2015). This coincides with an upregulation of GFAP.

Increase in GFAP expression occurs following to a decrease in striatal dopaminergic markers following METH (O'Callaghan and Miller, 1994; O'Callaghan et al., 2014). On the other hand, MDPV failed to alter striatal TH and GFAP levels (Anneken et al., 2015). Herein we characterize the impact of MDPV and METH on astrocytes in frontal cortex. Our data showed that both drugs failed to change GFAP levels as evidenced by western-blot and as gauged by the unaltered astrocytic morphology, in immunohistochemistry. GFAP data regarding METH is not surprising considering that TH levels were not altered at this time-point. Moreover, we also showed that frontal cortical GFAP levels were still unchanged in mice, 3 days post-METH injection (30 mg/kg of METH) (Silva et al., 2013). Consistently, Kelly and colleagues (2012) demonstrated that GFAP levels, in frontal cortex, were normal 12 and 72 hours, following a METH single dose of 20 mg/kg (s.c.) (Kelly et al., 2012). As for MDPV, again, this is the first report looking at astrocytes in frontal cortex. GFAP data further suggests that MDPV is not inducing an overt neurotoxic effect at this time-point. Further studies are warranted to fully characterize MDPV impact on astrocytic function. Overall. GFAP data is consistent with S100β results. Together it suggests that both drugs are not inducing astrocytic reactivity in frontal cortex.

Myelin is a cholesterol and glycolipidic rich plasma membrane structure, known as an extension of oligodendrocytes (myelin forming cells) in the central nervous system (CNS) that comprises an insulation sheath for axons. (Baumann et al., 2001; Miron and Franklin, 2014). Myelin is expressed in oligodendrocytes in the CNS and is localized in the cytoplasmic surface of the plasma membrane and myelin membrane produced by these cells (Barbarese et al., 1988). As an essential component for axons structure, function and sustainment (Nave and Trapp, 2008), myelin disruption, characterized by demyelination, caused by an insult, leads to major CNS pathologies from congenital and autoimmune disorders to metabolic disturbances (Love, 2006). Importantly, myelin, is drawing investigators attention due to its apparent involvement not only in various psychiatric disorders (such as schizophrenia, bipolar disorder and depression) but also in drug addiction, and in particular, recently myelin was identified as a potential target of many psychotropic drugs. (Bora et al., 2012; Eschenroeder et al., 2012) Nevertheless, only a few scientists have explored the impact of METH in myelin. Bowyer and colleagues, are the mentioned authors, who provided the first insights of CPu myelin damage, 4 hours post-METH administration (40 mg/kg, s.c.) to mice (Bowyer et al. 2008). Myelin basic protein (MBP) is a structural protein that plays a vital role in myelin compaction and thickening in the CNS (Condorelli et al., 2003; Eftekharpour et al., 2007). Herein we characterized MBP levels, as an evaluation of myelinization, in frontal cortex following MDPV and METH. MBP levels were not altered by any drug as assessed by western-blot and displayed by inaltered morphologic profile, in immunohistochemistry. This is suggestive that fibers demyelinization in frontal cortex were

not grossly perturbed by both drugs at this time-point. Again, one should stress that, to our knowledge, this is the first report on the impact of a binge episode of MDPV in myelinated structures.

4.2. Concluding remarks

Overall, our study characterizes for the first-time behavioral profile as well as cortical innate immune parameter, 24 hours following a binge MDPV paradigm. Therefore, we offer a first evidence that a single binge MDPV regimen did not come with any changes in both emotional and locomotor parameters, but curiously enhanced exploratory activity in mice. Moreover, MDPV did not impose any changes in innate immunity as well as in neurotoxicity parameters including RAGE, microglial, astrocytic, myelin and dopaminergic markers. Finally, METH is not seemingly imposing any innate immune deregulation at this time-point. One cannot exclude the hypothesis whereby this is a premature time-window to observe significative molecular changes in frontal cortices following both stimulants. In this context, future studies are required to further characterize neuronal and glial effects of MDPV by using other time-points, dosing regimens and brain regions. Moreover, despite pharmacological effects of synthetic cathinones is described to have similar effects to known stimulants of abuse, further studies will be required with a larger spectrum of substances, reported in available illegal products.

Chapter 5

References

Aarde, S.M. et al. (2013) The novel recreational drug 3,4-methylenedioxypyrovalerone (MDPV) is a potent psychomotor stimulant: self-administration and locomotor activity in rats. *Neuropharmacol.* **71**,130-40.

Abbott, N.J. *et al.* (2006) Astrocyte–endothelial interactions at the blood–brain barrier. *Nat Rev Neurosci*. **7**, 41-53.

Aghajanian, G. *et al.* (1999) Serotonin and hallucinogens. *Neuropsychopharmacol*. **21,** 168-238.

Ajami, B, *et al.* (2007) Local self-renewal can sustain CNS microglia maintenance and function throughout adult life. *Nat Neurosci*. **10**, 1538–1543.

Ajami, B. *et al.* (2007) Local self-renewal can sustain CNS microglia maintenance and function throughout adult life. *Nat Neurosci*. **10**, 1538–1543.

Akirav, E. M. *et al.* (2012) RAGE expression in human T cells: a link between environmental factors and adaptive immune responses. *PLoS One* **7**, e34698.
Chen, Y. *et al.* (2008) RAGE ligation affects T cell activation and controls T cell differentiation. *J Immunol.* **181,** 4272–4278.

Alizadeh, A. *et al.* (2015) Myelin damage and repair in pathologic CNS: challenges and prospects. *Front Mol Neurosci.* **8**, 35.

Allaman, I. *et al.* (2011) Astrocyte-neuron metabolic relationships: for better and for worse. Trends Neurosci. **34**, 76-87.

Angoa-Pérez, M. & Kuhn, D.M. (2017) Neurotoxicology of Synthetic Cathinone Analogs. *Curr Top Behav*

Neurosci. **32**, 209-230.
Anneken, J.H. *et al.* (2015) 3,4-Methylenedioxypyrovalerone prevents while methylone enhances methamphetamine-induced damage to dopamine nerve endings: β-ketoamphetamine modulation of neurotoxicity by the dopamine transporter. J Neurochem.**133**, 211-22.

Ares-Santos, S. et al. (2014) Methamphetamine Causes Degeneration of Dopamine Cell Bodies and Terminals of the Nigrostriatal Pathway Evidenced by Silver Staining *Neuropsychopharmacol.* **39**, 1066–1080.

Barbarese, E. *et al.* (1988) Expression of myelin basic protein mRNA and polypeptides in mouse oligodendrocytes in culture: differential regulation by genetic and epigenetic factors. *Brain Res.* **467**, 183-91.

Barbeau, A. (1974) High-level levodopa therapy in Parkinson's disease: five years later. *Trans Am Neurol Assoc* **99**, 160–163.

Basta, G. *et al.* (2002) Advanced glycation end products activate endo-thelium through signal-transduction receptor RAGE: a mechanism for amplification of inflammatory responses. *Circ.* **105**, 816–822.

Baumann, M. H. *et al.* (2016) Neuropharmacology of 3,4-Methylenedioxypyrovalerone (MDPV), Its Metabolites, and

Baumann, M.H. *et al.* (2012) The Designer Methcathinone Analogs, Mephedrone and Methylone, are Substrates for Monoamine Transporters in Brain Tissue. *Neuropsychopharmacol.* **37**, 1192–1203.

Baumann, N. *et al.* (2001) Biology of oligodendrocyte and myelin in the mammalian central nervous system. *Physiol Rev.***81**, 871–927.

Beaulieu, J. & Gainetdinov, R.R. (2011) The physiology, signaling, and pharmacology of dopamine receptors. *Pharmacol Rev.* **63**, 182–217.

Bierhaus A. & Nawroth P. P. (2009) Multiple levels of regulation determine the role of the receptor for AGE (RAGE) as common

soil in inflammation, immune responses and diabetes mellitus and its complications. *Diabetol.* **52**, 2251–2263.

Boger, H.A. et al. (2007) Long-term consequences of methamphetamine exposure in young adults are exacerbated in glial cell line-derived neurotrophic factor heterozygous mice. *J Neurosci.* **27**, 8816-25.

Bora, E. *et al.* (2012) White matter microstructure in opiate addiction. *Addict Biol.***17,** 141–148.

Bowyer, J. F. et al. (2008) Neurotoxic-related changes in tyrosine hydroxylase, microglia, myelin, and the blood-brain barrier in the caudate-putamen from acute methamphetamine exposure. *Synapse.* **62**, 93-204.

Boyle *et al.* (2010) Methylenedioxymethamphetamine ('Ecstasy')-induced immunosuppression: a cause for concern*? Br J Pharmacol*. **161,** 17–32.

Braley, A. *et al.* (2016) Regulation of Receptor for Advanced Glycation End Products (RAGE) Ectodomain Shedding and Its Role in Cell Function. *J Biol Chem*. **291**, 12057-73.

Brett, J. (1993) Survey of the distribution of a newly characterized receptor for advanced glycation end products in tissues. *Am J Pathol.* **143**, 1699-712.

Brown, J.M. *et al.* (2002) A single methamphetamine administration rapidly decreases vesicular dopamine uptake. *J of Pharmacol and Exp Therap* **302**, 497–501.

Bucciarelli, L.G. *et al.* (2002) RAGE blockade stabilizes established atherosclerosis in diabetic apolipoprotein E-null mice, *Circ.* **106**, 2827–2835.

Calabrese, E.J. *et al.* (2008) Addiction and dose response: the psychomotor stimulant theory of addiction reveals that hormetic dose responses are dominant. *Crit Rev Toxicol.* **387**, 599–617.

Calabresi, P. *et al*. (2007) Neuronal networks and synaptic plasticity in Parkinson's disease: beyond motor deficits. *Parkinsonism Relat Disord.* **3**, 259-262.

Callaghan, R.C. *et al.* (2010) Incidence of Parkinson's disease among hospital patients with methamphetamine-use disorders. *Mov Disord.* **25**, 2333-2339.

Callaghan, R.C. *et al.* (2012) Increased risk of Parkinson's disease in individuals hospitalized with conditions related to the use of methamphetamine or other amphetamine-type drugs. *Drug Alcohol Depend*. **120**, 35-40.

cCoy, M. *et al.* (2011) Chronic methamphetamine exposure suppresses the striatal expression of members of multiple families of immediate early genes (IEGs) in the rat: normalization by an acute methamphetamine injection. *Psychopharmacol.* **215**, 353–365

Chang, L. *et al.* (2007) Structural and metabolic brain changes in the striatum associated with methamphetamine abuse. *Addict* **102**, 16–3.

Chuah, Y.K. *et al.* (2013) Receptor for advanced glycation end products and its involvement in inflammatory diseases. *Int J Inflam.* **2013**, 403-460.

Cipollone, F. *et al.* (2003) The receptor RAGE as a progression factor amplifying arachidonate-dependent inflammatory and proteolytic response in human atherosclerotic plaques: role of glycemic control. *Circ.***108**, 1070–1077.

Collins, K. C. *et al*. (2014). Lipid tucaresol as an adjuvant for methamphetamine vaccine development. *Chem. Commun. (Camb.)* **50,** 4079–4081.

Condorelli, D. F. *et al.* (2003). Cellular expression of connexins in the rat brain: neuronal localization, effects of kainate-induced seizures and expression in apoptotic neuronal cells. *Eur. J. Neurosci.* **18**, 1807–1827.

Courtney, K.E. *et al.* (2014) Methamphetamine: an update on epidemiology, pharmacology, clinical phenomenology, and treatment literature. *Drug Alcohol Depend* **143**, 11–21.

Cunningham, J.K. & Thielemeir, M.A. (1996) Amphetamine-Related Emergency Admissions: Trends and Regional Variations in California (1985-1994). *Public Statis Instit.*

D'Ardenne, K. *et al.* (2008) BOLD responses reflecting dopaminergic signals in the human ventral tegmental area. *Science* **319,** 1264–1267.

Dalfó, E. et al. (2005) Evidence of oxidative stress in the neocortex in incidental Lewy body disease. *J Neuropathol Exp Neurol.* **64**, 816-30.

Dattilo, B. M. *et al.* (2007) The extracellular region of the receptor for advanced glycation end products is composed of two independent structural units. *Biochem.* **46**, 6957–6970.

DEA (Drug Enforcement Agency) Synthetic Cathinones - DEA Request for Information. 2011.

del Rio-Hortega, P. &Penfield, W. (1892) Cerebral cicatrix: The reaction of neuroglia and microglia to brain wounds. *Bull Johns Hopkins Hospital*. **41**, 278–303.

Donato, R. & Heizmann, C. W. (2010) S100B Protein in the Nervous System and Cardiovascular Apparatus in Normal and Pathological Conditions. *Cardiovasc Psychiatry Neurol.* 2010, 929-712.

Donato, R. *et al.* (2009) S100B's double life: intracellular regulator and extracellular signal. *Biochim Biophys Acta***. 1793,** 1008–1022.

Donato, R. *et al.* (2009) S100B's double life: intracellular regulator and extracellular signal. *Biochim Biophys Acta.* **1793,** 1008-1022

Dopaminergic Receptors. *Front Cell Neurosci*. **11**, 27.

Downes, M. A., and Whyte, I. M. (2005). Amphetamine-induced movement disorder. *Emerg. Med. Australas.* **17,** 277–280.

Drug Enforcement Administration (2013) Establishment of drug codes for 26 substances. Final rule. *Fed Regist.* **78**, 664–666.

Dumitriu, I. E. *et al.* (2007) The secretion of HMGB1 is required for the migration of maturing dendritic cells. *J Leukoc Biol.* **81**, 84–91.

Eftekharpour, E. *et al.* (2007). Myelination of congenitally dysmyelinated spinal cord axons by adult neural precursor cells results in formation of nodes of Ranvier and improved axonal conduction. *J. Neurosci.* **27**, 3416–3428.

Ellis, R. J. *et al.* (2003). Increased human immunodeficiency virus loads in active methamphetamine users are explained by reduced effectiveness of antiretroviral therapy. *J. Infect. Dis*. **188**, 1820–1826.

EMCDDA (European Monitoring Centre for Drugs and Drug Addiction) EMCDDA and Europol step up information collection on mephedrone. 2013.

Ernst, T. *et al.* (2000) Evidence for longterm neurotoxicity associated with methamphetamine abuse: a 1HMRS study. Neurology **54**, 1344–1349.

Eschenroeder, A.C. *et al.* (2012) Oligodendrocyte responses to buprenorphine uncover novel and opposing roles of mu-opioid- and nociceptin/orphanin FQ receptors in cell development: implications for drug addiction treatment during pregnancy. *Glia.* **60,** 125–136.

European Monitoring Centre for Drugs and Drug Addiction (2012) Annual report 2012: the state of the drugs problem in Europe. Publications Office of the European Union, Luxembourg.

European Observatory on Drugs and Toxic dependence (2017), *European Report on Drugs 2017: Trends and evolutions*, Union European Publisher Department, Luxemburg.

Everitt, B.J.& Robbins, T.W. (2013) From the ventral to the dorsal striatum: devolving views of their roles in drug addiction. *Neurosci Biobehav Rev* **37**, 1946-1954.

Fang, F. *et al.* (2010) RAGE-dependent signaling in microglia contributes to neuroinflammation, Abeta accumulation, and impaired learning/memory in a mouse model of Alzheimer's disease. *FASEB J*. **24**, 1043–1055.

Farina, C. (2007) Astrocytes are active players in cerebral innate immunity. *Trends Immunol.* **28,** 138-45.

Fischman, M.W. *et al.* (1989) Relationship between self-reported drug effects and their reinforcing effects: Studies with stimulant drugs. *NIDA Res Monogr.* **92**, 211–230.

Fleckenstein, A. E. *et al.* (2007) New insights into the mechanism of action of amphetamines *Annu Rev Pharmacol Toxicol.* **47**,681-98.

Fonseca, R. et al. (2016) Methamphetamine induces anhedonic-like behavior and impairs frontal cortical energetics in mice. *CNS Neurosci & Ther*. 1-8.

Frank, M.G. *et al.* (2016) The danger-associated molecular pattern HMGB1 mediates the neuroinflammatory effects of methamphetamine. *Brain Behav Immun*.**51**, 99-108.

Fry, J.L. & Toker, A. (2010) Secreted and membrane-bound isoforms of protease ADAM9 have opposing effects on breast cancer cell migration. Cancer Res. **70,** 8187-98.

Galichet, A. et al. (2008) Calcium-regulated intramembrane proteolysis of the RAGE receptor. *Biochem Biophys Res Commun.* **370**, 1-5.

Gangarossa, G. *et al.* (2012) Characterization of dopamine D1 and D2 receptor-expressing neurons in the mouse hippocampus. *Hippocamp.* **22**, 2199-2207.

Geissmann, F. (2010) Unravelling mononuclear phagocyte heterogeneity. *Nat Rev Immunol*. **10**, 453–460.

Geissmann, F. *et al.* (2010) Unravelling mononuclear phagocyte heterogeneity. *Nat Rev Immunol*. **10**, 453–460.

Ginhoux, F. et al. (2010) Fate mapping analysis reveals that adult microglia derive from primitive macrophages. *Sci.* **330**, 841–845.

Ginhoux, F. *et al.* (2010) Fate mapping analysis reveals that adult microglia derive from primitive macrophages. *Science*. **330,** 841–845.

Global Drug Survey 2017 (*Report released by the GDS Core Research Team,* Dr Adam Winstock, Dr Monica Barratt, Dr Jason Ferris & Dr Larissa Maier).

Goldstein, R. Z. & Volkow, N. D. (2011) Dysfunction of the prefrontal cortex in addiction: neuroimaging findings and clinical implications *Nat Rev Neurosci.* **12**, 652–669.

Gonçalves, J. *et al.* (2010) Methamphetamine-induced neuroinflammation and neuronal dysfunction in the mice hippocampus: preventive effect of indomethacin. *Eur J Neurosci.* **31**, 315-26.

Grace, C.E. *et al.* (2010) Effect of a neurotoxic dose regimen of methamphetamine on behavior, plasma corticosterone, and brain monoamines in adult C57BL/6 mice. *Neurotoxicol Teratol.* **32**, 346–355.

Graeber, M.B. & Streit, W.J. (2010) Microglia: biology and pathology. *Acta Neuropathol*. **119,** 89–105.

Granado, N. *et al.* (2008a) D1 but not D5 dopamine receptors are critical for LTP, spatial learning, and LTP-Induced arc and zif268 expression in the hippocampus. *Cereb. Cortex* **18**, 1 -12.

Granado, N. *et al*. (2008b) Persistent MDMAinduced dopaminergic neurotoxicity in the striatum and substantia nigra of mice. *J Neurochem.***107**, 1102-1112.

Greco, R. et al. (2012) Modulation of RAGE isoforms expression in the brain and plasma of rats exposed to transient focal cerebral ischemia. *Neurochem. Res.* **37,** 1508–1516.

Greyer, M. *et al*. (2009) Serotonin-related psychadelic drugs. *Encyclopedia of Neuroscience*. *Oxford: Academic Press,* 741-748.

Hans, S. *et al.* (2011) RAGE: The Beneficial and Deleterious Effects by Diverse Mechanisms of Actions. *Mol Cells*. **31**, 91–97.

Hayley, S. et al. (2005) The pathogenesis of clinical depression: stressor- and cytokine-induced alterations of neuroplasticity. *Neurosci.* **135**, 659-78.

Hofmann M.A. et al. (1999) RAGE mediates a novel proinflammatory axis: a central cell surface receptor for S100/calgranulin polypeptides. *Cell.* **97**, 889–901.

Hofmann, M.A. *et al.* (1999) RAGE mediates a novel proinflammatory axis: a central cell surface receptor for S100/calgranulin polypeptides. *Cell.* **97**, 889–901.

Hol, E.M. & Pekny, M. (2015) Glial fibrillary acidic protein (GFAP) and the astrocyte intermediate filament system in diseases of the central nervous system. *Curr Opin Cell Biol*. **32**, 121-30.

Hori, O. *et al.* (1995) The Receptor for Advanced Glycation End Products (RAGE)Is a Cellular Binding Site for Amphoterin. *J Biol Chem*. **270**, 25752–25761.

Huang, P. *et al.* (2012) Contrasting effects of d-methamphetamine 3.-methylenedioxymethamphetamine 3.4-methylenedioxypyrovalerone and 4-methylmethcathinone on wheel activity in rats. *Drug Alcohol Depend*. **126,** 168–175.

Hudson, B. I. *et al.* (2008) Interaction of the RAGE cytoplasmic domain with diaphanous-1 is required for ligand-stimulated cellular migration through activation of Rac1 and Cdc42. *J Biol Chem*. **283**, 34457–34468.

Ishihara, K. *et al.* (2003) The receptor for advanced glycation end-products (RAGE) directly binds to ERK by a D-domain-like docking site. *FEBS Lett.* **550**, 107–113.

Janeway, C.A., Jr. (1989). Approaching the asymptote? Evolution and revolution in immunology. *Cold Spring Harb. Symp. Quant. Biol*. **54**, 1–13.

Kagan, J.C. (2012) Signaling organelles of the innate immune system. *Cell.* **151**, 1168–1178.

Kalea, A.Z. *et al.* (2011) Alternative splicing of RAGE: roles in biology and disease. *Front Biosci*. **16**, 2756-70.

Kalivas, P.W. & Stewart, J. (1991). Dopamine transmission in the initiation and expression of drug- and stress-induced sensitization of motor activity. *Brain Research Rev* **16**, 223–244.

Kalueff, A.V. & Tuohimaa, P. (2004) Experimental modeling of anxiety and depression. *Acta Neurobiol Exp (Wars).* **64**, 439-48.

Karila, L. *et al*. (2015) Synthetic Cathinones: A New Public Health Problem. *Cur Neuropharmacol.* **13**, 12–20.

Kaushal, N. & Matsumoto, R. R. (2011) Role of sigma receptors in methamphetamineinduced neurotoxicity. *Curr Neuropharmacol.* **9**, 54–7.

Kawasaki, T. & Kawai, T. (2014) Toll-like receptor signaling pathways. *Front Immunol*. **5**, 461.

Lester, S. N & Li, K. (2014) Toll-like receptors in antiviral innate immunity. *J Mol Biol.* **426**, 1246–1264.

Kelly, K. A. et al. (2012) Chronic exposure to corticosterone enchances the neuroinflammatory and neurotoxic responses to methamphetamine. *J Neurochem.* **122**, 995–1009.

Kesha, K. *et al.* (2013) Methylenedioxypyrovalerone ("bath salts"), related death: case report and review of the literature. *J Forensic Sci.* **58,**1654–1659.

Kettenmann, H. *et al.* (2011) Physiology of microglia. *Physiol. Rev.* **91**, 461–553.

Kierdorf, K. & Fritz, G. (2013) RAGE regulation and signaling in inflammation and beyond. *J Leukoc Biol.* **94**, 55-68.

Kilkenny, C. et al. (2010) Animal research: Reporting in vivo experiments: The ARRIVE guidelines. *Br J Pharmacol*, **160,** 1577–1579

Kim, J.H. *et al.* (2006) Blood-neural Barrier: Intercellular Communication at Glio-Vascular Interface. *J Biochem Mol Biol*. **39,** 339-345.

Kita, T. *et al.* (2003) Current research on methamphetamine-induced neurotoxicity: animal models of monoamine disruption. *J Pharmacol Sci* **92**, 178–195.

Koch, M. *et al.* (2010) Structural Basis for Ligand Recognition and Activation of RAGE. *Struct.* **18,** 1342–1352.

Kogan, F.J. *et al.* (1976) Influence of methamphetamine on nigral and striatal tyrosine hydroxylase activity and on striatal dopamine levels. *Eur J Pharmacol.* **36**, 363–371.

Koob, G.F. (1992) Drugs of abuse: anatomy, pharmacology and function of reward pathways. *Trends Pharmacol Sci* **13**, 177–184.

Kovach, M. A. & Standiford T.J. (2011) Toll like receptors in diseases of the lung. *Int Immunopharmacol.* **11,**1399–1406.

Krasnova, I.N. & Cadet, J.L. (2009) Methamphetamine toxicity and messengers of death. *Brain Res Rev.* **60**, 379–407.

Krasnova, I.N. *et al.* (2009) Methamphetamine toxicity and messengers of death. *Brain Res Rev* **60**, 379–407.

Krasnova, I.N. *et al.* (2011) Chronic methamphetamine administration causes differential regulation of transcription factors in the rat midbrain. *PLoS ONE* **6**, e19179.

Kreutzberg, G.W. (1996) Microglia: a sensor for pathological events in the CNS. *Trends Neurosci*. **19**, 312–318.

Krishnan, V. & Nestler, E.J. (2010) Linking molecules to mood: new insight into the biology of depression. *Am J Psychiatry* **167**, 1305–1320.

Leclerc, E. *et al.* (2008) Binding of S100 proteins to RAGE: an update. *Biochim Biophys Acta*. **1793**, 993-1007.

Leclerc, E. *et al.* (2010) The S100B/RAGE Axis in Alzheimer's Disease. *Cardiovasc Psychiatry Neurol.* **2010**, 1–11.

Ledonne, A. & Mercuri, N.B. (2017) Current Concepts on the Physiopathological Relevance of

Leitão, R. et al. (2017) Aquapurin-4 as a New Target against Methamohetamine-induced brain alterations: focus on the neurogliovascular unit and motivational behavior. *Mol Neurobiol.*

Leonard, B. E. (2007) Inflammation, depression and dementia: are they connected? *Neurochem Res.* **32,** 1749-56.

Lester, S.N. & Li, K. **(2014)** Toll-like receptors in antiviral innate immunity. *J Mol Biol.* **426,** 1246-64.

Li, H. *et al.* (2014) Expression and cell distribution of receptor for advanced glycation end-products in the rat cortex following experimental subarachnoid hemorrhage. *Brain Res.* **1543,** 315–323.

Lim, S.A. *et al.* (2014) Striatal cholinergic interneuron regulation and circuit effects.*Front Synaptic Neurosci.***6,** 22**.**

Lister R. (1990) Ethologically-based animal models of anxietydisorders. *Pharmacol Ther*. **46**, 321–340.

Loftis, J.M. & Janowsky, A. (2015) Neuroimmune Basis of Methamphetamine Toxicity *Int Rev Neurobiol.* **118**, 165–197.

Loi, B. *et al.* (2015) Deaths of individuals aged 16-24 years in the UK after using mephedrone. *Hum Psychopharmacol.* **30,** 225-32.

López-Arnau, R. *et al.* (2012) Comparative neuropharmacology of three psychostimulant cathinone derivatives: butylone, mephedrone and methylone. *Br. J. Pharmacol.* **126**, 168–175.

López-Arnau, R. *et al.* (2014) Repeated doses of methylone, a new drug of abuse, induce changes in serotonin and dopamine systems in the mouse. *Psychopharmacol. (Berl).* **231**, 3119-29.

López-Díez, R. *et al.* (2013) Complex tissue-specific patterns and distribution of multiple RAGE splice variants in different mammals.*Genome Biol Evol.* **5**, 2420-35.

Lotze, M.T & Tracey, K.J. (2005) High-mobility group box 1 protein (HMGB1): nuclear weapon in the immune arsenal. *Nat Rev Immunol*. **5,** 331–342.

Love, S. (2006) Demyelinating diseases. *J Cli. Pathol.* **59-**1151–1159.

Manfredi, A. A. *et al*. (2008) Maturing dendritic cells depend on RAGE for in vivo homing to lymph nodes. *J Immunol.* **180**, 2270–2275.

Mansergh, G. *et al.* (2006). CDC consultation on methamphetamine use and sexual risk behavior for HIV/STD infection: summary and suggestions. *Public Health Rep*. **121**, 127–132.

Martinez-Clemente, J. et al. (2012)Interaction of mephedrone with dopamine and serotonin targets in rats. *Eur Neuropsychopharmacol.***22**, 231–236.

Martins, T. *et al.* (2011) Methamphetamine transiently increases the blood-brain barrier permeability in the hippocampus: role of tight junction proteins and matrix metalloproteinase-9. *Brain Res.* **1411**, 28–40.

Marusich, J. A. *et al.* (2012) Effects of Synthetic Cathinones Contained in "Bath Salts" on Motor Behavior and a Functional Observational Battery in Mice. *Neurotoxicol.* **33**, 1305–1313.

McCann, U.D. *et al.* (2008) Persistent cognitive and dopamine transporter deficits in abstinent methamphetamine users. *Synapse.* **62**, 91–100.

McGuinness, T. (2006) Methamphetamine abuse. *Am J Nurs.* 106**, 54-59.**

McKimmie, C.S. & Graham, G.J. (2010) Astrocytes modulate the chemokine network in a pathogen-specific manner. *Biochem Biophys Res Commun*. **394,** 1006–1011.

Meiser, J. *et al.* (2013) Complexity of dopamine metabolism. *Cell communication and signaling: CCS*, **11**, 34.

Meltzer. P.C. *et al.* (2006) 1-(4-Methylphenyl)-2-pyrrolidin-1-yl-pentan-1-one (Pyrovalerone) analogues: a promising class of monoamine uptake inhibitors. *J Med Chem*. **49**, 1420–1432.

Meredith, C.W. *et al.* (2005) Implications of Chronic Methamphetamine Use: A Literature Review. *Harv Rev Psychiatry* 13**, 141 -154.**

Metz, V.V. *et al*. (2012) Induction of **RAGE** shedding by activation of G protein-coupled receptors. *PLoS One.* **7**, e41823.

Miller, D.B. & O'Callaghan, J.P. Environment-, drug- and stress-induced alterations in body temperature affect the neurotoxicity of substituted amphetamines in the C57BL/6J mouse. *J Pharmacol Exp Ther*. **270**, 752-60.

Miron, V. E. & Franklin, R. J. (2014). Macrophages and CNS remyelination. *J. Neurochem.* **130**, 165–171.

Miyazaki, M. *et al.* (2013) Role of convergent activation of glutamatergic and dopaminergic systems in the nucleus accumbens in the development of methamphetamine psychosis and dependence. *Int J Neuropsychopharmacol.* **16,** 1341-50.

Mizoguchi, H. & Yamada, K. (2011) Pharmacologic Treatment with GABA(B) Receptor Agonist of Methamphetamine-Induced Cognitive Impairment in Mice. *Curr Neuropharmacol.* **9,** 109-112.

Monk, P.N. & Shaw, P.J. (2006) ALS: life and death in a bad neighborhood. *Nat Med*. **12**, 885-7.

Moratalla, R. *et al.* (1996) Cellular responses to psychomotor stimulant and neuroleptic drugs are abnormal in mice lacking the D1 dopamine receptor. Proc Natl Acad Sci U S A. 93, 14928-33.

Moretti, M. *et al.* (2015) Effects of agmatine on depressive-like behavior induced by intracerebroventricular administration of 1-methyl-4-phenylpyridinium (MPP(+)). *Neurotox Res.* 2015; **28**, 222–231.

Muda, M. *et al.* (2005) Splice variants of the relaxin and INSL3 receptors reveal unanticipated molecular complexity. *Mol Hum Reprod.* **11**, 591-600.

Nagai, F. *et al.* (2007) "The effects of non-medically used psychoactive drugs on monoamine neurotransmission in rat brain". *Eur J Pharmacol.* **559**, 132–137.

Nagai, T. & Kamiyama, S. (1988) Forensic toxicologic analysis of methamphetamine and amphetamine optical isomers by high performance liquid chromatography. *Int J Legal Med.***101**, 151 -159.

Nakamura, N. *et al.* (2011). HIV risk profiles among HIV-positive, methamphetamine-using men who have sex with both men and women. *Arch. Sex. Behav*. **40**, 793–801.

Nash, B. *et al.* (2011) Functional duality of astrocytes in myelination. *J Neurosci*. **31**, 13028–13038.

Nash, B. *et al.* (2011) Functional duality of astrocytes in myelination. *J Neurosci*. **31**, 13028-38.

Nave, K. A. &Trapp, B. D. (2008). Axon-glial signaling and the glial support of axon function. *Annu. Rev. Neurosci.* **31**, 535–561.

Neeper, M. et al. (1992) Cloning and expression of a cell surface receptor for advanced glycosylation end products of proteins. *J Biol Chem*. **267**, 14998-5004.

Newton, K. &Dixit, V.M. (2012) Signaling in innate immunity and inflammation. *Cold Spring Harb. Perspect. Biol*. **4**, a006049

O'Callaghan, J.P. *et al.,* (2014) Early activation of STAT3 regulates reactive astrogliosis induced by diverse forms of neurotoxicity. *PLoS One*. **9,** e102003.

Parkinsonian brains. *Mov Disord* **23,** 534–547.

Paxinos, G. & Franklin, K. B. J. (2004) *The mouse brain in stereotaxic coordinates*. Elsevier Academic Press, Amsterdam; Boston.

Penders, T.M. *et al.* (2012) Intoxication delirium following use of synthetic cathinone derivatives. *Am J Drug Alcohol Abuse* **38**, 616–617.

Pereira, F. C. *et al.* (2004) Lack of hydroxyl radical generation upon central administration of methamphetamine in rat caudate nucleus: a microdialysis study. *Neurotox Res.* **6,** 149-52**.**

Pereira, F. C. *et al.* (2011) Buprenorphine modulates methamphetamine-induced dopamine dynamics in the rat caudate nucleus. *Neurotox Res.* **19,** 94-101.

Pereira, F.C. *et al.* (2002) Acute changes in dopamine release and turnover in rat caudate nucleus following a single dose of methamphetamine. *J Neural Transm (Vienna).* **109**, 1151-1158.

Pereira, F.C. et al. (2012) Disruption of striatal glutamatergic/GABAergic homeostasis following acute methamphetamine in mice. *Neurotoxicol Teratol.* **34,** 522–529.

Pereira, F.C. *et al.* (2012)Disruption of striatal glutamatergic/GABAergic homeostasis following acute methamphetamine in mice. *Neurotoxicol Teratol.* **34**, 522-9.

Phillips, A.G. *et al.* (2008) A top-down perspective on dopamine, motivation and memory. *Pharmacol Biochem Behav.* **90,** 236–249.

Philogene-Khalid, H. L. et al. (2017) Synthetic cathinones and stereochemistry: S enantiomer of mephedrone reduces anxiety- and depressant-like effects in cocaine- or MDPV-abstinent rats. *Drug Alcohol Depend.* **178**, 119–125.

Prinz, M. et al. (2011) Heterogeneity of CNS myeloid cells and their roles in neurodegeneration. *Nat Neurosci.* **14**, 1227–12235.

Prosser, J.M. *et al.* (2012) The toxicology of bath salts: a review of synthetic cathinones. *J Med Toxicol* **8**, 33–34.

Psychonaut Research Web Mapping Project. (2009) MDPV report. Institute of Psychiatry, King's College London; London, UK.

Ramasamy, R. *et al.* (2005) The RAGE axis and endothelial dysfunction: maladaptive roles in the diabetic vasculature and beyond.*Trends Cardiovasc Med.* **15**, 237-43.

Ransohoff, R. M. *et al.* (2012) Innate immunity in the central nervous system. *J Clin Invest.* **122,** 1164–1171.

Ransohoff, R.M. *et al.* (1993) Astrocyte expression of mRNA encoding cytokines IP-10 and JE/MCP-1 in experimental autoimmune encephalomyelitis. *FASEB J.* **7**, 592–600.

Regulation n. º 7/2017, 2nd March concerning *Decreto-Lei* n.º 15/93, 22th January, *in Diário da República.*

Related Analogs. *Curr Top Behav Neurosci.* **32**, 93-117.

Ricaurte, G.A. *et al.* (1980) Long-term effects of repeated methamphetamine administration on dopamine and serotonin neurons in the rat brain: a regional study. *Brain Res.* **193**, 153–163.

Rojas A. *et al.* (2010) Fueling inflammation at tumor microenvironment: the role of multiligand/RAGE axis. *Carcinogen.* **31**, 334–341

Roll, J.M. *et al.* (2006) Contingency management for the treatment of methamphetamine use disorders. *Am J Psychiatry. **163***, 1993-1999.

Rose, M.E. & Grant, J.E. (2008) Pharmacotherapy for methamphetamine dependence: a review of the pathophysiology of methamphetamine addiction and the theoretical basis and efficacy of pharmacotherapeutic inter ventions. *Ann Clin Psychiatry* **20,** 145–155.

Ross, E.A. *et al.* (2012) Psychoactive "bath salts" intoxication with methylenedioxypyrovalerone. *Am J Med.* **125**, 854–858.

Rothman, R.B. *et al.* (2001) Amphetamine-type central nervous system stimulants release norepinephrine more potently than they release dopamine and serotonin. *Synapse.* **39,** 32–41.

Rothman, R.B. *et al.* (2001) Amphetamine-type central nervous system stimulants release norepinephrine more potently than they release dopamine and serotonin. *Synapse.* **39**, 32–41.

Rowitch, D.H. & Kriegstein, A. R. (2010) Developmental genetics of vertebrate glial-cell specification. *Nat.* **468**, 214-222.

Saleh, A. *et al.* (2013) Receptor for advanced end-products (RAGE) activates diverse signaling pathways to augment neurite outgrowth of adult sensory neurons. *Exp Neurol*. **249**, 149-159.

Schifano, F. *et al.* (2012)Suspected and confirmed fatalities associated with mephedrone (4-methylmethcathinone, "meow meow") in the United Kingdom. *J Clin Psychopharmacol*. **32**, 710-4.

Schifano, F. *et al.* (2016) NPS: Medical Consequences Associated with Their Intake. *Curr Topics Behav Neurosci.*

Schindler, C. W. (2016) Reinforcing and neurochemical effects of the "bath salts" constituents 3,4 methylenedioxypyrovalerone (MDPV) and 3,4-methylenedioxy-N-methylcathinone (methylone) in male rats. *Psychopharmacol (Berl).* **233**, 1981-90.

Schmidt, A. M. *et al.* (1999) Activation of Receptor for Advanced Glycation End Products/A Mechanism for Chronic

Schmidt, A. M. et al. (2001) The multiligand receptor RAGE as a progression factor amplifying immune and inflammatory responses. *J Clin. Invest.* **108**, 949–955.

Schmidt, A.M. *et al.* (1992) Isolation and characterization of two binding proteins for advanced glycosylation end products from bovine lung which are present on the endothelial cell surface. *J Biol Chem*. **267**, 14987–14997.

Scott, J.C. *et al.* (2007) Neurocognitive effects of methamphetamine: a critical review and meta-analysis. Neuropsychol Rev **17**, 275–297.

Seiden, L.S. & Sabol, K.E. (1996) Methamphetamine and methylenedioxymethamphetamine neurotoxicity: possible mechanisms of cell destruction. *NIDA Res Monogr.* **163**, 251 -76.

Shanks, K.G. *et al.* (2012) Analysis of first and second generation legal highs for synthetic cannabinoids and synthetic stimulants by ultra-performance liquid chromatography and time of flight mass spectrometry. *J Anal Toxicol.* **36**,360–371.

Shen, H. *et al.* (2013) A stress steroid triggers anxiety via increased expression of α4βδ GABAA receptors in methamphetamine dependence. *Neurosci.* **254**, 452-475.

Shoptaw, S.J. *et al.* (2009) Treatment for amphetamine withdrawal. *Cochrane Database Syst Rev* 15, CD003021.

Silva, C. D. *et al.* (2013) A Single Neurotoxic Dose of Methamphetamine Inducesa Long-Lasting Depressive-Like Behaviour in Mice. *Neurotox Res.* **25**, 295-304.

Simmler, L.D, *et al.* (2012) Pharmacological characterization of designer cathinones in vitro. *Br J Pharmacol.* **168**, 458–70.

Simões, P.F. *et al.* (2007) Methamphetamine induces alterations on hippocampal NMDA and AMPA receptor subunit levels and impairs spatial working memory. *Neurosci.* 150, 433-41.

Sofroniew, M.V. & Vinters, H.V. (2010) Astrocytes: biology and pathology. *Acta Neuropathol.* **119**, 7-35.

Spiller, H.A. *et al.* (2011) Clinical experience with and analytical confirmation of "bath salts" and "legal highs" (synthetic cathinones) in United States. *Clin Toxicol (Phila).* **49**,499–505.

Srisurapanont, M. et al. (2011) Comparisons of methamphetamine psychotic and schizophrenic symptoms: a differential item functioning analysis. *Prog. Neuropsychopharmacol. Biol. Psychiatry* **35**, 959–964

Steru, L. et al. (1985) A new method for screening antidepressants in mice. *Psychopharmacol.* **85**, 367–370.

Stoll, G. *et al.* (1998) Inflammation and glial responses in ischemic brain lesions. *Prog Neurobiol*. **56,** 149–171

Streit, W.J. (2010) Microglia activation and neuroinflammation in Alzheimer's disease: a critical examination of recent history. *Front Aging Neurosci.* **2**, 1–5.

Streit, W.J. *et al.* (1999) Reactive microgliosis. *Prog Neurobiol.* **57**, 563-81

Streit, W.J. *et al.* (2002) Microglia and the response to brain injury. *Ernst Schering Res Found Workshop.* **39**,11-24

Sugaya, K. *et al.* (1994) Three genes in the human MHC class III region near the junction with the class II: gene for receptor of advanced glycosylation end products, PBX2 homeobox gene and a notch homolog, human counterpart of mouse mammary tumor gene int-3. *Genomics.* **23,** 408-419.

Szabo, A. *et al.* (2015) Psichostimulants and immunomodulation: novel approaches and therapeutic opportunities. *Front in Immunol*. **6**, 358.

Takeuchi, O. & Akira, S. (2010) Pattern recognition receptors and inflammation. *Cell*. **140**, 805–20.

Thomas, D.M. *et al.* (2004) Microglial activation is a pharmacologically specific marker for the neurotoxic amphetamines.*Neurosci Lett.* **367**,349-54.

Thomas, D.M. et al. (2004a) Microglial activation is a pharmacologically specific marker for the neurotoxic amphetamines. *Neurosci Lett*. **367**, 349–354.

Thomas, D.M. *et al.* (2004b) Methamphetamine neurotoxicity in dopamine nerve endings of the striatum is associated with microglial activation. *J Pharmacol Exp Ther*. **311**, 1–7.

Tian, J. *et al.* (2007) Toll-like receptor 9-dependent activation by DNA-containing immune complexes is mediated by HMGB1 and RAGE. *Nat. Immunol.* **8**, 487–496.

Traherne, J. A. (2008) Human MHC architecture and evolution: implications for disease association studies. *Int J Immunogenet.* **35,** 179-192.

United Nations Office on Drugs and Crime (UNODC) (2014) World Drug Report. United Nations Publication.

United Nations Office on Drugs and Crime (UNODOC), "Amphetamines and Ecstasy." 2011 Global ATS Assessment.

United Nations Office on Drugs and Crime, World Drug Report, 2015 (United Nations publication).

United Nations Office on Drugs and Crime, World Drug Report, 2017 (United Nations publication).

Unterholzner, L. *et al.* (2010) IFI16 is an innate immune sensor for intracellular DNA. *Nat Immunol.* **11**, 997–1004.

Urbina, J. A. *et al.* (2004). In vitro and in vivo activities of E5700 and ER-119884, two novel orally active squalene synthase inhibitors, against Trypanosoma cruzi. Antimicrob. *Agents Chemother*. **48**, 2379–2387.

Vascular Dysfunction in Diabetic Vasculopathy and Atherosclerosis. *Circ Res*. **84,** 489-497.

Vesce, S. *et al.* (2007) Glutamate release from astrocytes in physiological conditions and in neurodegenerative disorders characterized by neuroinflammation. *Int Rev Neurobiol*. **82**, 57–71.

Vetreno, R.P. (2013) Increased receptor for advanced glycation end product expression in the human alcoholic prefrontal cortex is linked to adolescent drinking. *Neurobiol Dis.* **59**, 52–62.

Viana, S. D. *et al.* (2016) Regulation of striatal astrocytic receptor for advanced glycation end-products variants in na early stage of experimental Parkinson´s disease. *J Neurochem.* 1-11

Viana, S. D. (2016) Modulation of Receptors for advanced glycation end products network in Parkinson's Disease. (Doctoral Thesis) University of Coimbra, Portugal.

Viana, S. D. (2016) Presymptomatic MPTP Mice Show Neurotrophic S100B/mRAGE Striatal Levels. *CNS Neurosci Ther*. **22**, 396-403.

Villarreal, A. *et al*. (2014) S100B protein activates a RAGE-dependent autocrine loop in astrocytes: implications for its role in the propagation of reactive gliosis. *J Neurochem.***131,** 190-205.

Vissing, H. *et al.* (1994) Localization of the human gene for advanced glycosylation end product-specific receptor (AGER) to chromosome 6p21.3. *Genomics.* **24,** 606-608.

Volkow, N.D. *et al.* (2001a) Loss of dopamine transporters in methamphetamine abusers recovers with protracted abstinence. *J Neurosci.* **21,** 9414–9418.

Volkow, N.D. *et al.* (2001b) Association of dopamine transporter reduction with psychomotor impairment in methamphetamine abusers. *Am J Psychiatry.* **158**, 377–382.

Volkow, N.D. *et al.* (2007) Dopamine in drug abuse and addiction: results of imaging studies and treatment implications. *Arch Neurol* **64**, 1575–1579.

Wagner, G.C. *et al.* (1980) Long-lasting depletions of striatal dopamine and loss of dopamine uptake sites following repeated administration of methamphetamine. *Brain Res.* **181**, 151–160.

Wang, L. *et al.* (2008) Receptor for advan-ced glycation end products (RAGE) mediates neuronal differ-entiation and neurite outgrowth. *J Neurosci Res.* **86**, 1254–1266.

Watterson, L.R. *et al.* (**2014)** Potent rewarding and reinforcing effects of the synthetic cathinone 3,4-methylenedioxypyrovalerone (MDPV).*Addict Biol.* **19**, 165-74.

Winningham-Major, F. (1989) Neurite extension and neuronal survival activities of recombinant S100 beta proteins that differ in the content and position of cysteine residues. *J Cell Biol.* **109**, 3063-71.

Winstock, A.R. *et al.* (2011) Mephedrone, new kid for the chop? *Addiction.* **106**, 154-61.

Wise, R.A. & Bozarth, M.A.(1987) A psychomotor stimulant theory of addiction. *Psychol Rev.* **94**, 469–492.

Wise, R.A. (2004) Dopamine, learning and motivation. *Nat Rev.* **5**,483–494.

Wise, R.A. (2005) Forebrain substrates of reward and motivation. *J Comp Neurol.* **493**, 115–121.

Wolkoff, D.A. (1997) Methamphetamine abuse: an overview for health care professionals. *Hawaii Med J.* **56**, 34-36.

Yan, S.D. et al. (1996) RAGE and amyloid-beta peptide neurotoxicity in Alzheimer's disease. *Nat.* **382**, 685-91.

Yim, C.Y. & Mogenson, G.J. (1980) Electrophysiological studies of neurons in the ventral tegmental area of Tsai. *Brain Res.* **181**, 301–313.

Zang, S. *et al.* (2014) Methamphetamine modulates glutamatergic synaptic transmission in rat primary cultured hippocampal neurons. *Brain Res.* **1582**, 1-11.

Zhang, X. *et al*. (2006) Methamphetamine induces long-term changes in GABAA receptor alpha2 subunit and GAD67 expression. *Bioch Biophys Res Commun.* **351**, 300-305.